ÉCOLE DOCTORALE MSII (269)
LABORATOIRE ICUBE UMR 7375

Machine-learning-based predictive maintenance for Lithium-Ion batteries in electric vehicles

Thèse présentée par :
Inès JORGE

Soutenue le 24 novembre 2023

Pour obtenir le grade de : **Docteur de l'université de Strasbourg**

Discipline/ Spécialité : Informatique

Composition du jury

Directeur	Romuald Boné	Professeur, INSA Strasbourg
Encadrant	Tedjani Mesbahi	Maître de conférences HdR, INSA Strasbourg
Encadrant	Ahmed Samet	Maître de conférences, INSA Strasbourg
Rapporteur	Hubert Cardot	Professeur, Université de Tours
Rapporteur	Jean-Michel Vinassa	Professeur, Bordeaux INP
Examinatrice	Ouafae El Ganaoui-Mourlan	Maître de conférences, IFPEN
Examinateur	Pascal Venet	Professeur, Université Claude Bernard Lyon I
Examinatrice	Djamila Aouada	Professeur assistant, Université du Luxembourg
Invitée	Charlotte Alliod	PhD, Capgemini Engineering
Invitée	Asmae El Mejdoubi	PhD, Tiamat Energy

Abstract

In the case of hybrid vehicles, and even more so in the case of all-electric power-trains, the on-board energy storage system remains the weak link: very expensive, limited in driving range, slow to recharge, main causes of over-costs,... The challenge for any car manufacturer wishing to develop a clean vehicle is therefore not only to optimise the electric power-train, both in terms of cost and range, but also to bring the battery into line with the life of the vehicle. Battery lifetime is therefore a crucial element for the development of electric vehicles under acceptable cost conditions. In this context, the failure of battery could lead to serious inconvenience, performance deterioration, accelerated ageing and costly maintenance.

For that, the predictive maintenance of on-board energy storage system aims at predicting the Remaining Useful Life (RUL) of a Lithium-Ion (Li-Ion) and to perform necessary maintenance services, using past and current operating information. A reliable predictive maintenance model should be able to accurately predict the future state of the battery such that the maintenance service could be scheduled in advance.

The aim of this thesis is to combine the extension of battery life and the analysis of battery ageing with Machine Learning (ML) techniques. The challenge is therefore to use ageing data of Li-Ion batteries in order to extract knowledge on the State Of Health (SOH) of the batteries. Most ageing data come from papers from research institutes such as the NASA Prognostics Centre of Excellence (PCoE) [SGC09, BKD14] or the department of chemical engineering of the Massachusetts Institute of Technology [SAJ+19] that publicly made available the results of different ageing tests on several batteries. We propose several approaches to take operating data such as time series of current, voltage and temperature coming from battery cells to build ageing models. The developed models can either predict the Remaining Useful Life (RUL) of a battery or the evolution of its SOH.

Keys words: *Lithium-Ion batteries; Electric Vehicles; Predictive Maintenance; Machine Learning; Time Series; SOH; RUL*

Résumé

Dans le cas des véhicules hybrides, et plus encore dans celui des chaînes de traction tout électriques, le système de stockage d'énergie embarqué reste le maillon faible : très coûteux, limité en autonomie, lent à recharger, cause principale de surcoûts,... Le défi pour tout constructeur automobile souhaitant développer un véhicule propre est donc non seulement d'optimiser la chaîne de traction électrique, tant en termes de coût que d'autonomie, mais aussi d'adapter la batterie à la durée de vie du véhicule. La durée de vie de la batterie est donc un élément crucial pour le développement de véhicules électriques dans des conditions de coût acceptables. Dans ce contexte, la défaillance d'une batterie peut entraîner de graves inconvénients, une détérioration des performances, un vieillissement accéléré et une maintenance coûteuse.

Pour cette raison, la maintenance prévisionnelle des systèmes de stockage d'énergie embarqués vise à prédire la durée de vie utile restante (RUL) d'une batterie Lithium-Ion (Li-Ion) et à effectuer les services de maintenance nécessaires, en utilisant les données d'utilisation passées et présentes. Un modèle de maintenance prévisionnelle fiable doit être capable de prédire avec précision l'évolution de l'état de la batterie de manière à ce que les opérations de maintenance puissent être programmées à l'avance.

L'objectif de cette thèse est de combiner l'extension de la durée de vie de la batterie et l'analyse du vieillissement de la batterie avec des techniques d'apprentissage automatique. Le défi consiste donc à utiliser les données de vieillissement des batteries Li-Ion afin d'extraire des connaissances sur l'état de santé (SOH) des batteries. La plupart des données de vieillissement proviennent d'articles d'instituts de recherche tels que le NASA Prognostics Centre of Excellence (PCoE) [SGC09, BKD14] ou le département de génie chimique du Massachusetts Institute of Technology [SAJ+19] qui ont rendu publics les résultats de différents tests de vieillissement sur plusieurs batteries. Nous proposons plusieurs approches pour utiliser les données de fonctionnement telles que les séries temporelles de courant, de tension et de température provenant des cellules de batterie pour construire des modèles de vieillissement. Les modèles développés peuvent prédire le RUL d'une batterie ou l'évolution de son SOH.

Mots clef: *Batteries lithium-ion; Véhicules Électriques; Maintenance Prévisionnelle; Apprentissage Automatique; Séries Temporelles; SOH ; RUL*

Remerciements

Malgré des capacités de synthèse avérées [1], je n'ai pu faire tenir en une page ces remerciements, tant il me semble important de mentionner chaque personne ayant contribué à cette aventure.

Parmi toutes les personnes qui m'ont aidée à aller au bout de cette thèse, je tiens en premier lieu à remercier mon directeur, Romuald Boné. Je n'aurais jamais espéré pouvoir bénéficier de tant d'attention, d'empathie et de conseils scientifiques aussi pertinents. Merci pour cette disponibilité malgré la charge de travail qu'implique la position de directeur au sein de l'INSA.

Je remercie mes encadrants, Tedjani Mesbahi et Ahmed Samet de m'avoir fait confiance il y a plus de quatre ans en me proposant ce sujet de thèse. Il y a eu des hauts et des bas, mais leur soutien était immanquablement au rendez-vous.

Merci à Hubert Cardot et Jean-Michel Vinassa d'avoir accepté de rapporter ma thèse. Depuis mon premier comité de suivi, Hubert Cardot et Ouafae El Ganaoui-Mourlan ont participé à l'amélioration continue de mes travaux, par leur écoute, leurs questions et leurs remarques constructives. Merci à Ouafae d'être maintenant examinatrice, aux côtés de Pascal Venet et Djamila Aouada. Je tiens également à remercier Charlotte Alliod et Asmae El Mejdoubi d'avoir accepté cette invitation.

Commencer sa thèse en septembre 2019 rime avec de longs mois de confinement loin des collègues, mais cela ne m'a pas empêchée de tisser des liens hors du commun. Merci à toutes les personnes qui ont partagé avec moi le (tant convoité..!) bureau C219 : Jorge, Yasser, Paul, puis évidemment Théo et Franco, le bureau des légendes. Sans pouvoir les nommer de manière exhaustive, merci à tou·te·s les doctorant·e·s de l'INSA pour la bienveillance et le partage au quotidien. Je me dois de remercier l'ensemble de mes étudiant·e·s, auprès de qui j'ai tant appris. À tous les collègues pour leurs précieux conseils et encouragements, un immense merci.

Je pense également à toutes les personnes que j'ai croisées chaque jour à l'INSA, en les saluant poliment et en les remerciant intérieurement pour leur travail essentiel, l'accueil, le secrétariat, la comptabilité, les dépannages informatiques, mais aussi le ménage, les travaux, le réglage des thermostats et puis les sourires et la bonne humeur.

Si j'ai tenu jusqu'au bout, c'est aussi grâce aux rencontres que j'ai faites à Strasbourg, en dehors et au sein de l'INSA il y a de ça sept ans. Je ne saurais décrire tout ce que je dois à l'Orchestre Universitaire de Strasbourg, pour tout ce que j'y ai appris musicalement et humainement, pour toutes celles et ceux que j'y ai rencontrés et qui sont maintenant une deuxième famille. Merci *viel mols* à Lionel et sa famille,

[1] Résumer sa thèse en trois minutes était visiblement plus simple !
France 3 Grand Est, "Strasbourg - Ma Thèse en 180 secondes : Inès Jorge l'emporte en nous parlant des batteries de voitures électriques"

aux CoolOUS, aux B****OUS, à mes co-pupitres contrebassistes... Je garderai toujours le souvenir ému de chaque concert et de cette musique qui nous rassemble ! Pour le travail acharné jusqu'au diplôme d'ingénieur et tous les moments qui suivent depuis, merci aux insassien·ne·s Mathieu, Maxence, Ophélie, Sébastien, Vitto, Toon, la Furi... Sans vous, ces dernières années auraient été bien fades ! Enfin, à mes ami·e·s dijonnais·e·s de longue date, depuis le conservatoire, le collège, le lycée, la prépa, merci à Zélie, Martin, Alice, Ariana, Laura, Pauline et Mathilde... Quel bonheur de grandir et de m'épanouir à vos côtés !

Pour terminer, que dire de ma famille, source inépuisable d'amour et de soutien... Un merci tout particulier à ma grande sœur Anita, qui depuis ce message du 6 juin 2019 (*Si tu fais une thèse, un conseil, ne la fais pas durer six ans*) a enduré la relecture de nombreux articles et de l'intégralité de cette thèse. Merci à mon grand frère Lucien pour les éclats de rire et à mes parents Nino et Nicole pour tout ce qu'il et elle m'ont apporté. Je vous dois tout. Merci infiniment à tout le reste de ma famille, ma marraine Marianne, mon parrain Olli, ma tante Genny, ma grand-mère Josette, mes cousin·e·s, mon petit cousin (et celui qui arrive bientôt !!) et à deux petits bonheurs, Chinedu et Chimamanda. À mon grand-père Robert, que je porte dans mon cœur comme un grand soleil.

Contents

List of Figures

List of Tables

List of Abbreviations

ANN	**A**rtificial **N**eural **N**etwork
BoL	**B**eginning **o**f **L**ife
BSFS	**B**ackward **S**equential **F**eature **S**election
CC	**C**arbon **C**opy
CNN	**C**onvolutional **N**eural **N**etwork
DHI	**D**irect **H**ealth **I**ndicators
EIS	**E**lectrochemical **I**mpedance **S**pectroscopy
EoL	**E**nd **o**f **L**ife
EV	**E**lectric **V**ehicles
FNN	**F**eedforward **N**eural **N**etwork
FSFS	**F**orward **S**equential **F**eature **S**election
HEV	**H**ybrid **E**lectric **V**ehicles
HI	**H**ealth **I**ndicator
IR	**I**nternal **R**esistance
LAM	**L**oss of **A**ctive **M**aterial
LFP	**L**ithium **F**er **P**hosphate
Li-Ion	**Li**thium-**Ion**
LLI	**L**oss of **L**ithium **I**nventory
LSTM	**L**ong **S**hort **T**erm **M**emory
MSA	**M**ulti **S**teps **A**head
NMC	**N**ickel **M**anganese **C**obalt
OSA	**O**ne **S**tep **A**head
PHM	**P**rognostics and **H**ealth **M**anagement
RHI	**R**efined **H**ealth **I**ndicators
RNN	**R**ecurrent **N**eural **N**etwork
RUL	**R**emaining **U**seful **L**ife
SFS	**S**equential **F**eature **S**election
SOH	**S**tate **O**f **H**ealth
T°	**Temperature**
TCO	**T**otal **C**ost of **O**wnership
V	**Voltage**
$\mathbf{X_C}$	X during **C**harge
$\mathbf{X_D}$	X during **D**ischarge

Introduction

Context

In France as in many other countries in the world, a vast majority of journeys are made by individual motorised vehicles, either cars or two-wheeled vehicles. The transportation field is responsible for 15% of green house gas emissions worldwide, and 30% in France [Big20]. The impact of our mobility over climate change and air pollution is no longer a matter of debate, and the necessity to reduce our carbon footprint has become clear. The European Parliament has reaffirmed its position concerning the zero emission goal for the transportation field by the year 2035 [Eur21]. Among other measures, a text was adopted to forbid the commercialisation of new combustion engine vehicles by this date. Studies have shown that implementing a proactive policy in favour of electric vehicles (EVs) would contribute to reduce the global emissions of CO2 from the transportation field. Up to today, the only serious alternative to combustion vehicles are battery powered vehicles. The most widespread batteries in EVs are Lithium-Ion (Li-Ion) batteries, which have recently emerged as a topic of both interest and concern. Awareness has been raised about the resources needed to built EVs and more especially Li-Ion batteries.

The use of such batteries is one of the main reasons why the spread of EVs is slowed down. They account for the majority of the price of an EV, and although research in the transportation field has brought EVs in line with the performances of thermal vehicles, one of the most often cited arguments against EVs is their lack of driving range.

Electrifying the transportation field will only prove efficient in the global context of the ecological transition under certain conditions. Considering this, EVs could become a key link in the chain of sustainable mobility.

There are two main lines of improvement for EVs. The first one consists in working on the batteries themselves, and the second one concerns the way batteries and EVs are used. Li-Ion batteries are electro-chemical devices built to store electricity under a chemical form. Although a great variety of battery exists, Li-Ion is the dominant technology in the field of EVs due to its superior energy density. One concern about Li-Ion batteries comes from the materials that are necessary to build them, mainly metals such as lithium, nickel and cobalt. Although lithium resources on earth should not be a limiting factor for the spread of EVs [GMK+11], some battery manufacturers have started investing in new technologies that could be a good complement to li-ion batteries. For example, the world leader battery manufacturer CATL has been working for several years on sodium batteries (batteries that use sodium in-stead of lithium). Tesla, among other car manufacturers, are investing in a type of Li-Ion batteries that is free of cobalt, nickel and manganese and rather

uses Iron and Phosphate (LFP batteries). Using a more diverse range of battery types could alleviate the tensions on raw materials.

The other axis of improvement for EVs is to work on the typology of the vehicles themselves and on the energy management both inside vehicles and from a user point. One of the best ways to alleviate the tension on raw materials is to develop vehicles that are optimally sized to meet the real needs of users and to reduce as much as possible the carbon emissions linked to the conception of vehicles and batteries. Sober mobilities should be explored, with smaller and lighter vehicles and smaller batteries. More recently, the company CATL has been working on condensed batteries[2], which could allow batteries twice smaller than current ones to carry the same amount of energy. Focusing on a French battery manufacturer, the company Tiamat has been working on sodium-ion batteries for mobility and stationary energy storage [3]. This technology of batteries offers a higher power density than Li-Ion batteries (from 1 to 5 kW/kg for sodium-ion batteries compared to 0.5 to 1 kW/kg for Li-Ion batteries) and higher cycle life (up to 8000 cycles for sodium-ion batteries).

Vehicles and batteries that are designed to be reparable and recyclable, with a reasonable driving range for daily journeys, and an efficient energy management system are the key points to make electric vehicles truly clean. The energy management on the other hand consists in making the best possible use of the battery. On the vehicle side, it could mean balancing the cells in a battery pack, limiting the current peaks, warming up the battery before charging, cooling it down during driving... On the user side, a very important point is to identify which are the most damaging behaviours for the battery. This way, a feedback could be made in order to avoid hazardous situations and help users develop an eco-driving.

Motivation

Among all the solutions mentioned to enable EVs to become a truly sustainable part of tomorrow's mobility, this thesis focuses on one aspect in particular of the management of batteries. It is known that the storage capacity of a Li-Ion battery degrades throughout its life. The degradation comes from several factors and is quite hard to model considering the complexity of such devices. Several motivations have guided this work. The global objective of this thesis is to establish a predictive maintenance strategy to make the best possible use of a battery inside a vehicle. This strategy must include several aspects:

- the battery needs to be studied in its global operating environment
- the best modelling approach needs to be selected (either from physics or from data, with what type of models...)
- the predictive model should be able to identify the main causes of degradation

[2] "CATL launches condensed battery with an energy density of up to 500 Wh/kg, enables electrification of passenger aircrafts", 19 Apr 2023.

[3] « Nous voulons créer en France un Tesla de la batterie sodium-ion », affirme Laurent Hubard, directeur de Tiamat Energy (Accessed in September 2023)

- the approach should be reliable and applicable to real-life situations.

Structure of the thesis

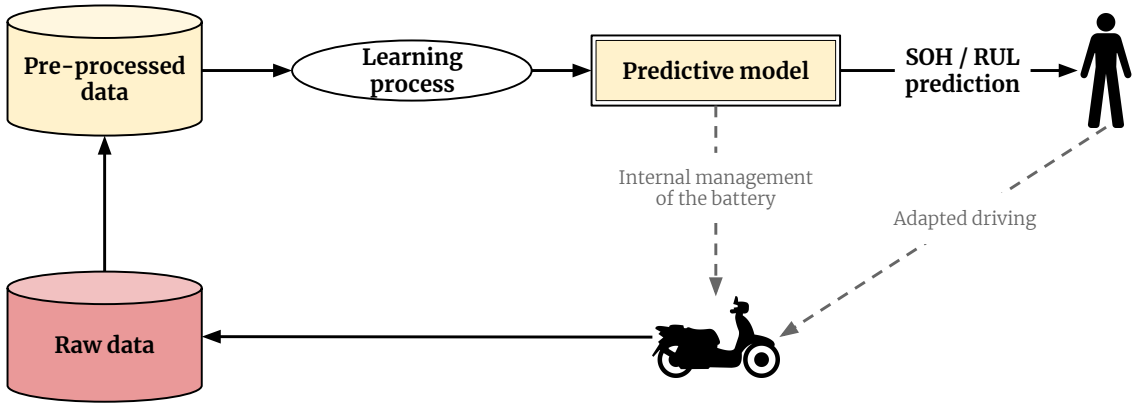

Figure 1: Global framework of the thesis

The global context of this thesis is illustrated in figure 1. This work was carried out as part of the VEHICLE project[4], funded by INTERREG V A Upper Rhine Programme, FEDER and Franco-German regional funds (Bade-Wurtemberg, Rhénanie-Palatinat and Grand Est). The global ambition of this project was to improve the Total Cost of Ownership (TCO) of electric vehicles. This can be achieved, among other things, by improving the cycle life and performances of Li-Ion batteries. In the scope of this thesis, the improvement of battery performances was investigated by focusing on finding raw operation data from Li-Ion batteries, making it usable in a Machine Learning algorithms and building predictive models. In all following chapters, several models will be presented, with a strong focus on data. Information is given on the type of data that is used and on what is extracted from raw data in order to train machine learning models. The aim of the three contributions that will be detailed is to find a way to link the way a battery is being used to its ageing stage and to identify the impact of a certain usage over the storage capacity in advance.

Chapter 1 - State of the Art. Before diving into contributions, the first chapter of this thesis aims as giving a broad vision of the context and tools that are used in all following works. The fundamentals of machine learning and time series are given, as well as basics about the functioning of Li-Ion batteries. The first chapter also contains an extensive review of the literature about predictive prognostics for Li-Ion batteries. The conclusion on the literature review justifies the choices of architecture and exploited data to build the models.

Chapter 2 - RUL prediction from historical features. The first contribution of this thesis is related to the prediction of Remaining Useful Life (RUL) of a battery by exploiting historical data contained in a dataset published by the MIT. Predicting the

[4] https://www.vehicle-project.org/

RUL of a system is a common task in predictive prognostics in order to anticipate the End of Life (EoL) and avoid reaching this point by settling maintenance operations in advance.

Chapter 3 - SOH prediction from time series. As a complement to the prediction of RUL, another approach was developed for predicting the evolution of SOH according to operating data. Different models are exploited in order to make the best possible use of the information contained in time series of current, voltage and temperature. In this chapter, a strong emphasis is put on how to extract features from operating data and structure them for a use in Recurrent Neural Networks (RNN).

Chapter 4 - Seq2Seq for SOH prediction. The last modelling contribution of this thesis is an extension of the SOH prediction from time series chapter. The same data and features are used but a long term prediction of the SOH is made through the use of a more complex models referred to as Sequence to Sequence (Seq2Seq).

Chapter 5 - Experimental setup. This last short chapter is a description of the experimental setup that was developed in the years since the beginning of this thesis. The aim is to study the ageing of batteries by cycling them (*ie.* charging and discharging them continuously) with a specific device and by fixing custom test conditions. The acquired data should be used to train new models or to test the performances of the previously developed models.

Finally, an overall assessment of the work that was done in the scope of this thesis is made in conclusion, as well as a presentation of future works.

Chapter 1

State of the art

Contents

1.1 Theoretical Background

1.1.1 General information on data

In 2020, the amount of data generated each day was equivalent to $2,5.10^{18}$ bytes (10^{18} = **one quintillion**). It was estimated that 94% of all data in the world is stored in digital format, and that 90% of all data ever produced by humans has been made in the past two years [Ade15, Dom21]. Digital data can be of any nature and any quality, and concern any field from data generated by smart sensors to the latest images released by the James Webb telescope. [VR16]

Big data is a recent concept that was born according to the explosion of the amount of data. With concepts such as digitisation, anticipation and controlled processes, a new industrial revolution is underway, known as "Industry 4.0". The transportation field is also being revolutionised with the development of smart, autonomous and cleaner vehicles. Not only should smart factory adapt to the consumer trend, it should also avoid downtime maintenance and optimise the use and lifetime of all the components in a production chain, or of any connected object. The problematic is similar in the transportation field, with a strong focus on electric vehicles that are meant to replace thermal vehicles within a few years.

This is what predictive maintenance is about: avoiding downtime maintenance by observing in real time the behaviour of a system so that replacement or repairing operation can be scheduled in advance, when minimum damage has occurred. Due to the increasing complexity of systems, whether part of a production chain or a vehicle, and the complexity of the interaction between systems, predictive maintenance has reached a critical importance [ZdCd+20].

Predictive maintenance strategies can be developed through data-based models and domain knowledge. In the scope of this thesis, only data-based strategies will be studied. Data-based models rely on the acquisition of data from a given system, through the use of different types of sensors. Data can be of different nature, but an important part of it is generated under the form of time series.

This section aims at giving a definition of time series and reviewing the common operations related to time series.

1.1.2 General information on time series

Time series are a specific type of sequential data, where time is taken into account. A global definition of sequential data could be an ordered list of consecutive k items, picked from a given finite ensemble A. For example, the word "sequence" can be seen as a sequence itself, where each item of the sequence are the letters (S,E,Q,U,E,N,C,E).

In time series, the position of each item in a sequence is related to time. A time series X_t corresponds to a set of observations where each observed value is associated with a corresponding time : $X_t = \{x_1, x_2, \ldots, x_T\}$, with a number of T values. Time series can be continuous or discrete.

In the case of continuous time series, observations are recorded continuously, and related time values are continuous in a given interval (for example $t \in [0, 1]$,

where time can take any possible value between 0 and 1). Continuous time series can be generated by analog sensors for example.

In the case of discrete time series, the set of time values is a discrete set and observations can be made at fixed or irregular time intervals. The time unit related to measurements can be of different natures. A commonly used time unit is the second (SI unit), but sometimes, traditional units such as minute, hour, month, or year can be found. In some specific cases, other custom units related to time can be found. For example, in the case of batteries, some ageing criteria are measured at each charge or discharge cycle and thus evolve chronologically according to the number of cycles. Typical examples of time series are weather data (temperature, wind speed, humidity...), electronic health records (heart rate, blood pressure...) [ROC+18] or data related to industrial devices (levels of vibrations, rotation speed of a motor...).

In the scope of this thesis, a strong focus will be placed on discrete time series since it is this type of data that will be used to build predictive models.

Time series can either be uni-variate or multi-variate. Uni-variate time series refer to time series where a unique variable is observed at each time step. Multivariate time series corresponds to an ensemble of time series relative to different observations [CTPK09]. The several components of a multi variate time series can be synchronous or asynchronous. In this case, X_t includes multiple time series.

Types of operations on time series

The work on time series is not new: very early papers were written in 1906 by Arthur Schuster [Sch06], and major works on Time Series, Forecasting and Control were written by Box & Jenkins in 1970. Still, the recent and phenomenal increase of the amount of collected data each day, correlated with the improvement of the computing power [OHL+08], has opened the way to new challenges. Several common operations on time series are listed here, mostly related to data driven algorithms.

Classification

Time series can be associated with a label according to its characteristics. In a dataset D where each time series $X_{t,N}$ is associated with its corresponding class y_N, $D = \{(X_{t,1}, y_1), \ldots, (X_{t,N}, y_N)\}$, the classification task consists in training a classifier on dataset D so that it can map a given input to its corresponding class. [IFW+19]

Clustering

Some time series can have similarities although there is no clear knowledge about a label, unlike in the classification problem. Clustering time series consists in automatically gathering similar data into homogeneous groups. The classification process can help identifying structures in a dataset. [ASY15]

Prediction

Prediction can be of different nature according to the type of time series (either uni-variate or multi-variate).

Considering a uni-variate time series X with a known number of T time steps

$$X_t = x_i, x_2, \ldots, x_T$$

following unknown values

$$x_{T+1}, x_{T+2}, \ldots, x_{T+N}$$

of X can be predicted.

In the case of a multi-variate time series, predictions can either be endogenous or exogenous. Considering a multi-variate time series X with a known number of T time steps and k variables,

$$X_{i,t} = x_{1,1}, x_{1,2}, \ldots, x_{1,T}, ..., x_{k,1}, x_{k,2}, \ldots, x_{k,T}$$

an endogenous prediction would consist in predicting the following values of one of the k sub series, or all of them.

An exogenous prediction, on the contrary, would consist in predicting the following steps of another time series (either uni-variate or multi-variate) from one or more of the k sub series.

Feature selection

Generated data can sometimes reach such volumes that it becomes impossible to use it directly as input to algorithms. Recent work on time series shows that data needs to be treated in a specific way, by selecting the most useful part of it and getting rid of irrelevant information [CKLF16, GBMP13]. Feature selection aims at focusing on the part of information that is relevant for solving a given problem. For example in multi-variate time series, some acquired signals could bring redundant or useless information for the prediction problem. Feature selection helps keeping only useful signal in the prediction process.

Feature extraction

Feature extraction is another dimension reduction technique. As feature selection selects useful information from the original set of data, feature extraction rather creates a new set of data by transforming the information contained in original data. Transformation of data should result in a lower dimensional space while preserving most of the relevant information [KKN14]. Feature extraction can be combined with feature selection when a great number of new features is created from the original data. It often happens that not all new features are useful, and the best subset of features is therefore identified with feature selection techniques.

1.1.3 Acquiring data

All of the above-mentioned operations are data-driven, which means that before applying any data pre-processing technique (feature extraction or selection) or building any model (whether it is for clustering, classifying or predicting time series), data needs to be acquired and stored. The quality of any data-driven model relies on the quality of data, and no amount of data pre-processing can fully make up for poor data quality.

Discrete time series are acquired through digital sensors. Data sensing is therefore a crucial step in any time series manipulation. Industry 4.0 relies partly on data acquisition, and sensors have evolved into embedded and smart devices. [JHS+21]

Most of the time series that are studied in the scope of this thesis are physical signals related to the functioning of batteries, or their operating environment. Sensors involved in the acquisition of such signals operate in the thermal, electrical and mechanical domains. The physical quantities measured by sensors are referred to as "measurand" and vary according to the domain. [MK19]

Table 1.1: Examples of measurands according to the sensor domain

Domain	**Measurand**
Thermal	Temperature ($T°$)
Electrical	Current (I), Voltage (V), Resistance (R), Internal resistance (IR), Power (P)
Mechanical	Speed, Acceleration, Pressure

Sensors dedicated to prognostics and health management of a system should include memory and/or data transmission abilities.

Through sensors and real-time acquisition of data, especially time series, the functioning of any system in its environment can be observed. In order to increase product reliability, availability and affordability, predictive maintenance appears as a key strategy. Its aim is to take advantage of operating data by turning it into predictive models that can anticipate the evolution of a system and its potential failures [MK19]. In this scope, Machine Learning (ML) appears as the most efficient tool to extract knowledge and build models from data. Most predictive prognostics models are based on ML algorithms, whose fundamentals are described in the following section.

1.1.4 The learning process

ML is a sub-field of Artificial Intelligence (AI) and can be defined as a field of study that gives computers the ability to learn without being explicitly programmed [Sam00]. In more explicit terms, ML is based on algorithms that can extract knowledge from data. Unlike the classical programming paradigm, where models are based on knowledge on a given topic, ML uses a dataset as input and creates models that can perform tasks and allow decision making.

To do so, algorithms are built to learn functions from a set of examples. The set of examples is referred to as the dataset, there is one specific dataset for each application. All ML algorithms follow the same procedure for analysing the dataset and identifying patterns in the data, called the learning process, described in figure 1.1. The aim of the learning process is to find a mathematical function that can map the input data to a corresponding output. The mathematical function that results of the training process is what is called the model, and that will be used to make decisions.

The learning process can vary according to the application and to the type of data. The implied mathematical functions can also vary according to the complexity of the application.

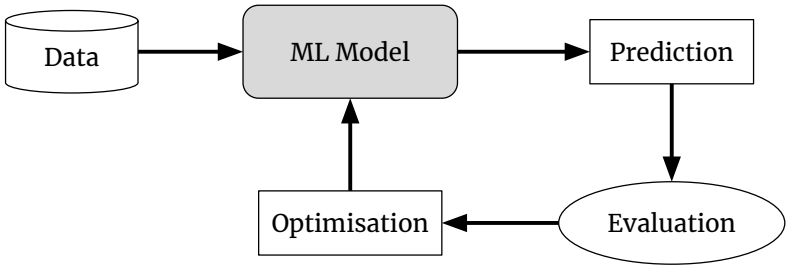

Figure 1.1: Learning process of a Machine learning algorithm

Table 1.2: A (theoretical) dataset for the classification of Li-Ion batteries according to their initial characteristics, through supervised learning

	Features		Label
Batt. ID	Initial capacity (Ah)	Initial IR (mΩ)	(performance)
b1c0	1.0710	16.7424	1
b1c42	1.0803	16.7679	2
b2c30	1.0670	17.7890	3
b3c45	1.0692	15.7420	1

1.1.5 Supervised and unsupervised learning

The nature of the dataset on which a machine learning model is based determines the choice of the learning process.

Supervised learning can be applied when training data is available under the form of input-output pairs, which means that each input sample X_i has a corresponding label y_i.

Table 1.3: A dataset for the prediction of the RUL of Li-Ion batteries through supervised learning

	Features			Label (RUL)
Cycle ID	IR (mΩ)	Charge time (min)	Capacity (Ah)	(cycles)
0	16.7423	13.34	1.0710	1851
50	16.5933	13.43	1.0766	1801
500	16.7248	13.34	1.0619	1351
1000	17.0227	13.43	1.0389	851

The example datasets represented in table 1.2 and 1.3 are divided into features and labels.

In table 1.2, each input sample (each line) corresponds to one battery, and each battery is described by two features. The features characterise the initial performances of a brand new battery (its initial capacity and internal resistance). The corresponding label of each sample is a number between 1 and 3 which indicates the level of performance of the battery (1 means the battery cycle life is between 1000 and 1500 cycles, 2 means the cycle life is between 500 and 1000 cycles, and 3 means the cycme life is lower than 500 cycles).

In table 1.3, each input sample corresponds to one cycle in the life of a battery, and is described by several features (the internal resistance, charge time and capacity). The corresponding output of each sample is the Remaining Useful Life (RUL) of the battery at this precise cycle.

Both datasets could be used for supervised learning, but for different tasks. The type of label in dataset 1.2 are numerical values that correspond to a level of performance. In this case, labels can only take three possible values, and samples are classified according to their labels. Classification is a typical task of supervised learning. On the contrary, labels in dataset 1.3 are numerical values that corresponds to the RUL of the battery in terms of cycles. That label can take any positive value. Therefore, the learning process will result in a model that can make a regression on a numerical value.

Unsupervised learning can be applied when only input features are available, without labels. The learning process will thus aim at building a model that can recognise recurrent patterns in data and use them for different tasks. A very common process in unsupervised learning is clustering, where similar time series are gathered into homogeneous groups. Unsupervised learning can also be used to operate dimension reduction tasks such as Principal Component Analysis (PCA) to reduce the number of features [KP11] or outlier detection to remove abnormal samples.

1.1.6 Artificial Neural Networks

Artificial Neural Networks (ANN) have been become very popular for sequence data and time series treatment since the late 1980s. With the advances in computing abilities and data availability, ANN have been outperforming any other approach since 2009, including in time series related problems. ANN are mathematical models used for ML based on non-linear mathematical functions, giving them the ability to identify complex relationships in data. They have been proven to have universal approximation capabilities, provided there is enough data for training [Puy01].

The most basic form of ANN, and one of the most important ones, is called *Feedforward Neural Networks (FNN)*.

The learning principle mentioned above is achieved thanks to a specific structure that takes data as input and applies non linear transformations to it. The global functioning of ANN involve several mathematical operations at different stages of the learning process. The following sections will describe the mathematical building blocks of ANN. The association of these mathematical building blocks, which creates the global model in the end, is referred to as the architecture of the model.

The neuron

Artificial Neurons that compose ANN were inspired biological neurons. Neurons receive, transform and flow information in one direction. The operation a that takes place in a neuron j is characterised by its weights $w_{i,j}$, bias $w_{j,0}$ and activation function ϕ as represented in figure 1.2. The output of a neuron is computed according to equation 1.1

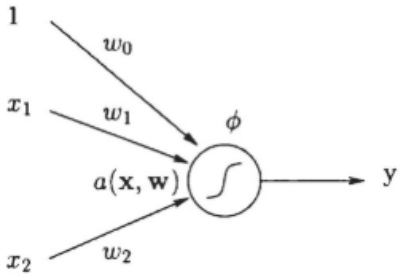

Figure 1.2: Basic form of an artificial neuron, used in ANN [Bou04]

$$y = a_j(x, w) = \phi(\sum_i w_{ij} x_i + w_{j0}) \tag{1.1}$$

Activation functions

Activation functions are generally non-linear functions. Without the activation function, the mathematical behaviour of a neuron would just result in a linear transformation of the input data. Adding a non-linear operation after the neuron is necessary to be able to learn complex relationships in data. Popular activation functions are :

- sigmoid : $\sigma(x) = \frac{1}{1+e^{-x}}$
- Rectified Linear Unit (ReLU) : $R(x) = max(0, x)$
- hyberbolic tangent : $tanh(x) = \frac{2}{1+e^{-2x}}$

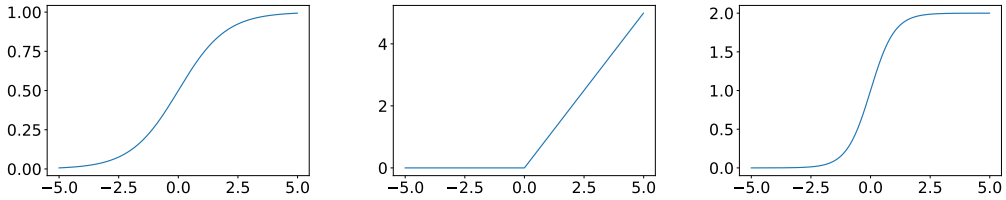

(a) Sigmoid (b) ReLU (c) Tanh

Figure 1.3: Activation functions

Activation functions are systematically associated with neurons. When several neurons are associated together, it creates what is called a *layer*. Layers can be stacked to add depth to the model.

The use and choice of activation function inside each neuron depends on the place of the layer inside the network, the type of data used and the type of prediction.

Loss function

The aim of a ML model, and in this case of an ANN, is to establish relationships between a given input and the corresponding output. In order to make sure the right relationship is established and that it is reliable, a quantitative measure of the performance of the model is needed. The loss function is an error function that is used to evaluate the model during training. According to the number of outputs, the model might have several loss functions, but the results of those functions is averaged so that one unique value of loss is taken into account during the learning process. The quality of the model depends on the choice of loss function, and this choice is guided by the type of prediction that is made. This thesis only focuses on supervised learning models for regression tasks. The Mean Square Error (MSE) is a commonly used loss function for regression. Considering a real output Y and the value predicted by an ANN $\hat{Y}$, the MSE is expressed as shown in equation 1.2:

$$MSE = \frac{1}{n}\sum_{i=1}^{n}(Y_i - \hat{Y}_i)^2 \tag{1.2}$$

Gradient Descent

The learning process described in 1.1.4 includes an optimisation step, and that truly is what gives ML algorithms the ability to learn.

The weights of an ANN are initialised with random values, with a specific distribution and range according to the architecture of the network [TF95, SHK+14]. The model filled with random weights, or *untrained* model, can be used to make predictions from the input dataset, but the result would be meaningless. The output of the untrained model is systematically compared with the expected output, and weights and biases are gradually updated according to the error. This gradual updating of the weights of a network is what is called *training*. After training, thanks to the optimisation, the error between the predicted and expected output should be as low as possible.

In mathematical terms, the optimisation of a ML algorithm is about finding the parameters that minimise the loss function. The optimisation is based on the concept of *gradient descent*.

The loss function of a ML model is a differentiable function, whose global minimum can be determined by calculation in theory. The loss value is computed for each of the input data and depends on the weights of the model, as represented in figure 1.4.

In the case of ANNs, finding the global minimum of the loss function can become very complicated, considering that ANNs often have tens of thousands of parameters. Rather than computing the minimum of the loss function by determining the point where its derivative equals 0, *stochastic gradient descent* is applied.

The gradient is the slope of a curve at a given point. More precisely, it is the derivative of a function that takes a vector as input (thus, a multidimensional input). Considering a given set of weights $w = (w_1, w_2, \ldots, w_n)$, the derivative of the loss function for this set of weights is :

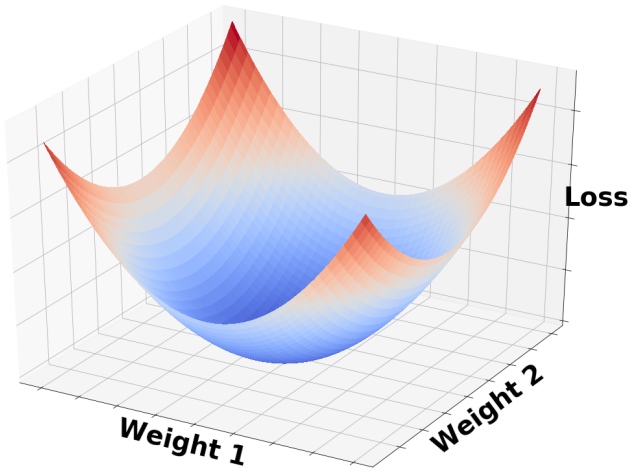

Figure 1.4: Evolution of the loss function according to the weights

$$\nabla f(w) = \begin{bmatrix} \frac{\partial f}{\partial x_1}(w) \\ \frac{\partial f}{\partial x_2}(w) \\ \vdots \\ \frac{\partial f}{\partial x_n}(w) \end{bmatrix} \tag{1.3}$$

For each step of the learning process, the same operation is made. *(i)* The output of the network is computed according to the set of weights. *(ii)* The loss between the predicted and expected output is computed. *(iii)* The gradient of the loss function according to the set of weights is computed. *(iv)* The weights are updated in the opposite direction of the gradient, in order to minimise the loss function.

Backpropagation

Backpropagation is the process through which the gradient of the loss function is computed for each layer of the ANN, from the output layer and backwards to the input layer.

The depth of an ANN

Artificial Neural Networks are built by stacking layers of artificial neurons. The more neurons per layers and the more layers stacked, the deeper the network.

In Feedforward Neural Networks (FNN), the information flows in one direction. Each neuron in an FNN is fully connected to all the following ones in the network, which means the output of a neuron is used as input to the following ones. FNN

are usually used to perform tasks such as clustering, classification and regression on numerical or categorical data. The depth of a network depends on the number of stacked layers. Each additional layer in a model is meant to add a different and increasingly meaningful representation of the input data.

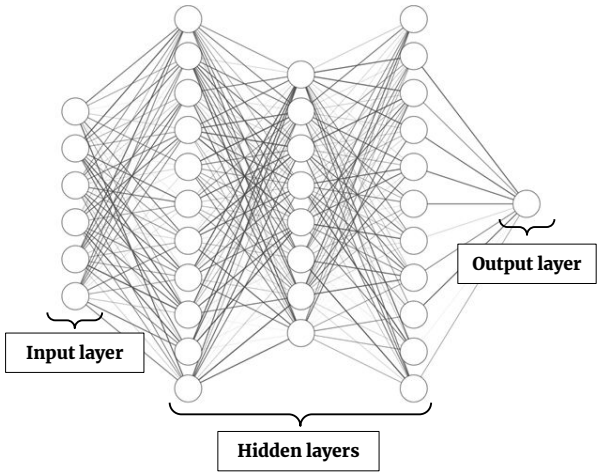

Figure 1.5: A multi-layer ANN

FNN can be combined to other types of networks when complex representations are involved, typically for pattern recognition or time series treatment. In this case, models belong to the category of Deep Neural Networks.

1.1.7 Deep Neural Networks for time series

Convolutional Neural Networks

Convolutional Neural Networks (CNN) are a special type of neural networks that are built to process data in one or two dimensions, in a grid-like topology, typically the pixels of an image [GBC16, Sch15].

Although CNN have been very popular in practical applications such as image recognition, they have been used for speech processing and time series in 1995 by LeCun and Bengio [LB98]. Uni-variate time series can be thought of as 1D images, and multi-variate time series as 2D images. CNN are built to learn translation invariant patterns in data, which means they can automatically isolate relevant local patterns in a time series and recognise them somewhere else in the signal. This process can be seen as automatic feature extraction.

However, when dealing with time series, CNN are mostly used to perform classification tasks, and not prediction. CNN is the most successful architecture on a 2D image topology, but to process sequential data, recurrent neural networks are preferred.

Recurrent Neural Networks

Recurrent Neural Networks (RNN) have become very popular in time series related problems. RNN, unlike FNN or CNN, have the ability to process data sequences by

keeping track of their past elements. They have a memory that can carry information on the history of all the past elements of the input signal, and they use the past states as input to predict the next or future states.

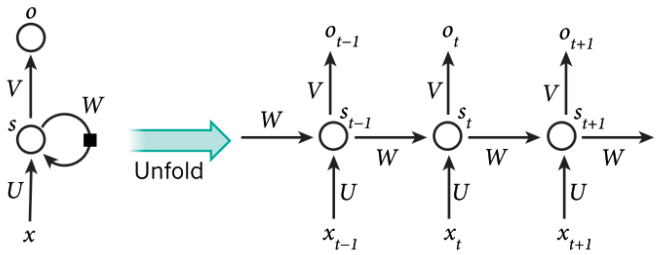

Figure 1.6: Working principle of the cell of an RNN unfolded in time [LBH15]

In figure 1.6, the working principle of an RNN is explained. Each output o_t of the network depends on the input x_t and all the previous input values. U, V and W are weight matrices that do not change with time unroll. The same weight matrices are used at each time step.

The first RNN that were developed were theoretically able to carry information throughout any sequence, but suffered from a vanishing gradient problem when dealing with very long sequences. Simple RNN can therefore not learn long term dependencies.

Several advances in the architecture and the training process of RNN made it possible to overcome this problem. Long Short Term Memory networks (LSTM) is a type of RNN which comprises three gates, making it easier to carry past data over long sequences and therefore resolve the vanishing gradient problem.

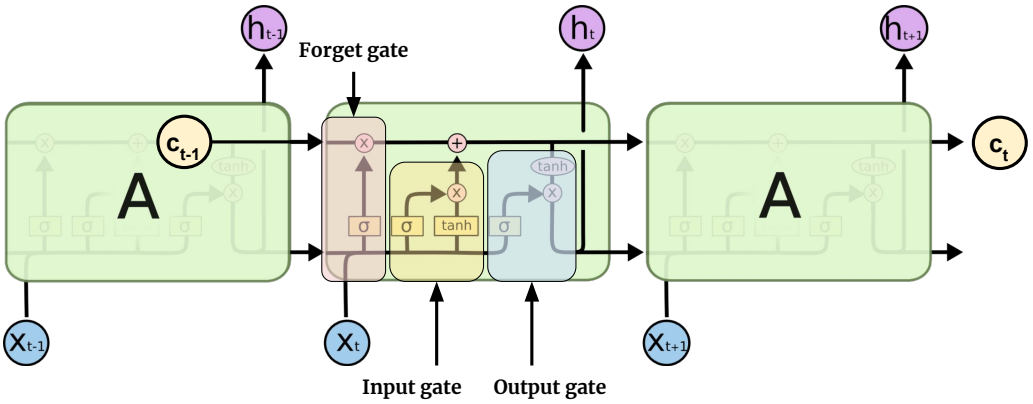

Figure 1.7: Structure of a Long Short Term Memory network

As shown in figure 1.7, an LSTM comprises three gates called the "input", "forget" and "output" gate. For each time step, the *hidden state* of the LSTM is updated, as well as the *cell state*. In the following equations, f_t is the forget gate, i_t is the input gate, o_t is the output gate, c_t is the cell state and h_t is the hidden state. Two different activation functions are used, σ_g for the Sigmoid and σ_c for the hyperbolic tangent.

$$f_t = \sigma_g(W_f * x_t + U_f * h_{t-1} + b_f) \tag{1.4}$$

The forget gate aims at deciding which part of the information should be kept in memory or not. It takes into account the input of the cell at time t, x_t, and the output of the previous layer, h_t, in order to modify the cell state from time $t-1$, c_{t-1}. The cell state carries information along the entire chain of an LSTM.

$$i_t = \sigma_g(W_i * x_t + U_i * h_{t-1} + b_i) \tag{1.5}$$

$$c'_t = \sigma_c(W_c * x_t + U_c * h_{t-1} + b_c) \tag{1.6}$$

$$c_t = f_t \cdot c_{t-1} + i_t \cdot c'_t \tag{1.7}$$

The input gate determines what information should be added to the cell state. The cell state is updated according to the output of the forget and input gates, and of the result of c'_t.

$$o_t = \sigma_g(W_o * x_t + U_o * h_{t-1} + b_o) \tag{1.8}$$

$$h_t = o_t \cdot \sigma_c c_t \tag{1.9}$$

The output of an LSTM cell is computed as a function of the cell state c_t, the input of the cell x_t and the previous output h_t.

A possible variant of the LSTM is the bidirectional-LSTM (bi-LSTM). Bi-LSTM are composed of the same gates as the LSTM but can flow the information forward and backwards at the same time.

Transformers & Attention modules

Transformers are a class of deep learning models that have revolutionised various fields, especially natural language processing [VSP+17]. At the heart of a Transformer lies its attention mechanism, which is often referred to as attention modules. These attention modules enable the model to analyse and weigh the importance of different parts of an input sequence, allowing it to capture complex relationships and dependencies within the data. Unlike traditional RNN or CNN, Transformers excel at handling long-range dependencies and are highly parallelisable, making them well-suited for a wide range of sequential data tasks, from language translation to image generation and beyond.

1.1.8 Parameters and hyper parameters tuning

The learning done by machine learning is finding the parameters (or weights) of a model using a dataset. [Kel19]

The principle of learning algorithms is to find a function f that can map a set of inputs to a set of outputs by minimising some expected loss. Most often the learning process is done by optimising a set of parameters, regarding a training criterion.

Considering a model A (*ie.* a mathematical function), its parameters Θ , a loss function L and samples x from a given distribution G_x, the principle of optimisation resides in solving equation 1.10:

$$Min(L(x; A_\Theta)) \tag{1.10}$$

In the case of ANN, the optimisation consists in setting the right weights and biases to the different layers of neurons.

However, there is another set of parameters to be considered and which cannot be optimised automatically during the training process described above. These are called hyper-parameters, and the actual learning algorithm A is the one obtained after appropriately choosing them.
Regarding neural networks, one should consider the number of layers, and units per layer but also the learning rate, momentum, dropout ...

The problem of identifying the right hyper-parameters can then be considered as an upper layer of optimisation. It consists in finding the best set of hyper parameters λ, in order to minimise the generalisation error of algorithm A, defined as:

$$E_{x\sim G_x}[L(x; A_\lambda(X^{(train)}))] \tag{1.11}$$

There can be a great variety of hyper parameters to consider, and the most critical part is to choose the right way to combine them. The most common way to identify the best hyper parameters λ is to iterate through various combinations of hyper parameters.

While grid search offers an exhaustive way of testing all possible configurations, this method is rather ineffective and can be thought of as a "brute force" method. Depending on the complexity of the model, testing each possible configuration of hyper parameters can be a very long process. The number of possible combinations grows exponentially with the number of hyper-parameters [Bel15].

Random Search however is a more efficient way to go through several possible hyper parameter configurations. Random search produces a set of trials by drawing hyper parameters from a uniform distribution space [BB12].

The work described in [BB12] shows that Random Search has statistically more chances to find a good enough combination of parameters by going through fewer iterations.

Figure 1.8 illustrates a space of nine hyper parameters, whose distribution has important dimensions and less important dimensions. Grid search only tests the important dimension in three distinct places, whereas Random Search explores it at nine distinct places.

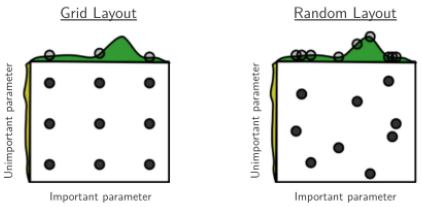

Figure 1.8: Random search vs grid search [BB12]

1.2 Li-Ion Batteries

1.2.1 A brief history of Li-Ion batteries & electric vehicles

At the beginning of the 20th century, thermal cars represented a minority of vehicles on the road [1]. Due to the lack of charging infrastructure and obvious inconvenients in terms of driving range and speed (no more than 65 km, and no faster than 32 km/h), the popularity of electric vehicles declined progressively from 1920.

The environmental impact of thermal cars however has brought attention again on electric vehicles from the late 1990s. The need for better energy storage solutions and alternatives to lead-acid batteries and nickel–cadmium (Ni–Cd) gave way to extensive research in the field of Li-Ion batteries. The first Li-Ion battery was commercialised by Sony in 1991, after the works of Yoshio Nishi [JW98, Mas09]. Thanks to their remarkable performances (higher energy density, longer cycle life, and reduced weight) compared to other battery chemistries used at that time, mainly lead-acid, nickel–cadmium (Ni–Cd) or nickel-hydrid (Ni–MH), Li-Ion batteries were adopted very quickly in all portables devices. Their use started in mobile phones and computers, and now all kinds of vehicles and power tools are running on Li-Ion batteries. In 2019, Stanley Whittingham, John B. Goodenough and Akira Yoshino received the Nobel Prize of chemistry for their joint works on Li-Ion batteries.

1.2.2 Working principle of Li-Ion batteries

Li-Ion batteries, and batteries in general, are electrical energy storage devices. They are electrochemical devices that convert chemical energy into electricity back and forth. All batteries, no matter the chemistry, are composed of an *anode* (negative electrode) and a *cathode* (positive electrode). Both electrodes are floating in an *electrolyte*, and they are separated by a membrane called the *separator*. In Li-Ion batteries, the cathode is protected from direct contact with the electrolyte by a filter called the *Solid Electrolyte Interface* (SEI).

During discharge, the energy contained in the battery under a chemical form is converted to electricity by connecting the anode and the cathode through an external circuit. Electrons flow from the cathode (which has the lower potential) to the anode (which has the higher potential), which creates current. As batteries are reversible conversion devices, the reaction can be reversed by the addition of an

[1] Britannica, Early electric automobiles (Accessed in September 2023)

external electrical energy source. Then, electricity is converted back to chemical energy.

The chemical reactions that take place inside batteries are oxido-reductions. When electrons move from one electrode to the other through an external circuit, positive ions Li^+ flow in the opposite direction from one electrode to the other through the electrolyte, the separator and the SEI. Electrons and cations can go from one cathode to the other according to the oxido-reduction reaction that occurs (either during charge or discharge).

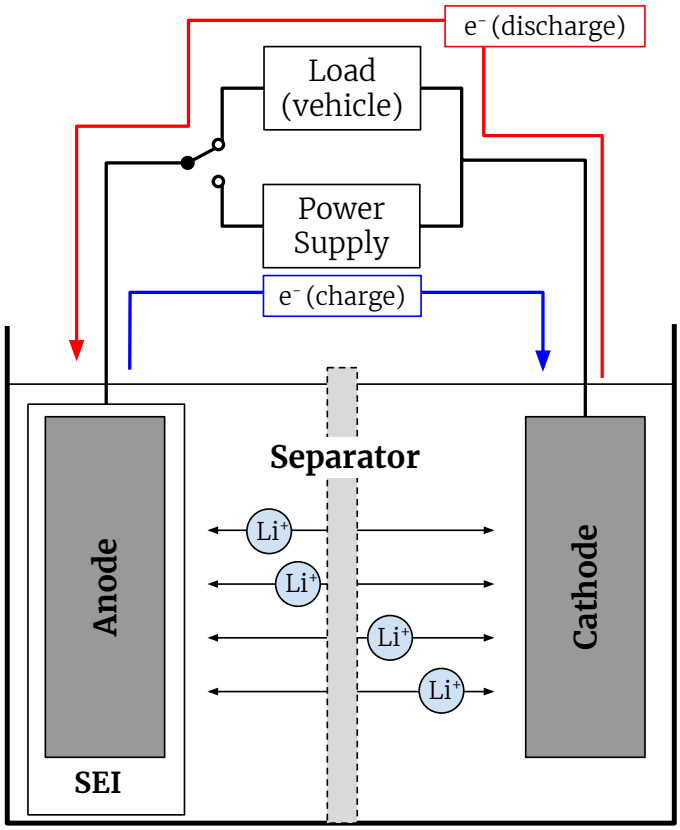

Figure 1.9: Operating diagram of a Li-Ion battery

Cell chemistries

There are three main technologies of Li-Ion batteries on the market at the moment: Nickel-manganese-cobalt (NMC), Nickel-cobalt-aluminium (NCA) and Lithium-Iron-Phosphate (LFP) cells. The differences between those chemistries are the materials used for the electrodes and electrolyte. Depending on the materials used, batteries have different advantages and disadvantages that make them more or less suitable for each application. Battery chemistries can be classified according to six criteria: cost, specific energy, specific power, safety performance and life span [The10]. The most widespread battery chemistry on EVs for the moment is NMC cells because they have a higher energy density (which means a higher driving range) and wider operating temperature range. NCA have a shorter life cycle than NMC batteries

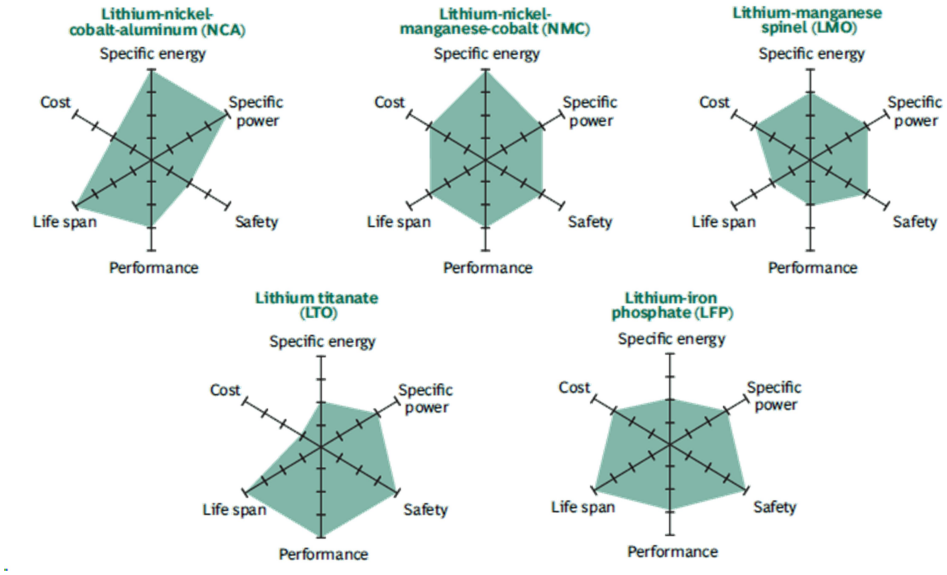

Figure 1.10: Comparison of different cell chemistries according to six criteria [The10]

and are not used in so many cars nowadays. LFP cells on the contrary have a lower energy density but better cycle life, and increased security (less thermal runaway risk). All those characteristics are summarised in figure 1.10.

All the dataset described in the section make use of one or more of these chemistries, with cells that have a cylindrical shape.

Cell architectures

There are three main types of packaging for batteries: cylindrical, prismatic and pouch. They also have consequences over the performances of the batteries [SAS17].

Cylindrical batteries are easy to manufacture and are mechanically stable. They prevent batteries from swelling. They benefit from longevity and their cost is quite low. However, the cylindrical shape leads to a lower space efficiency. They are extensively used in portable applications such as laptops, but also in electric vehicles. The most commonly found dimensions for cylindrical batteries are 18650 and 21700.

The advantage of prismatic batteries, on the contrary, lies in their thin shape. They allow a better space management and flexibility. However, they have a shorter lifespan and they are more expensive to build.

Pouch batteries are an alternative to cylindrical and prismatic batteries. The principle is to weld foil tabs to the electrodes and to bring them outside in a fully sealed way. They are light and cost effective but an important swelling has to be

taken into account. As the metal enclosure is eliminated, the weight is reduced but the cells need allowance to expand in the battery compartment.

1.2.3 Ageing mechanisms in Li-Ion batteries

The ageing phenomenon in a Li-Ion battery can come from many external and internal factors. Physical mechanisms such as thermal or mechanical stress can influence the degradation (for example with high external temperature, vibrations due to the state of the road etc ...). Chemical mechanisms occur inside the battery and can be divided into two main degradation modes : Loss of Lithium Inventory (LLI), which is caused by consumption of lithium ions through side reactions and Loss of Active Material (LAM), which results in a loss of storage capacity. LLI is mainly caused by SEI film formation and decomposition, electrolyte decomposition, and lithium plating. All degradation mechanisms are detailed in references [Chr17a] and [HXLP20].

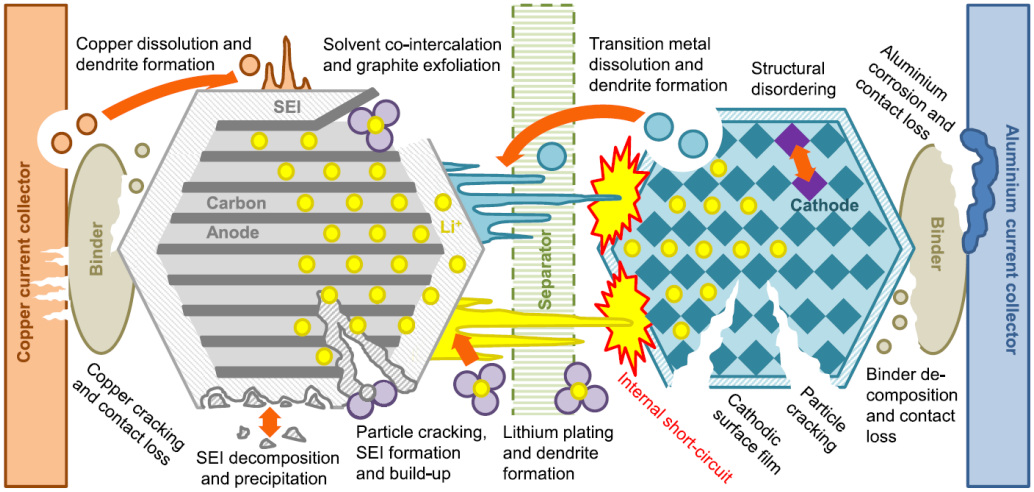

Figure 1.11: Degradation mechanisms in Li-Ion cells [BRM+17]

1.2.4 Battery Ageing Data

Li-Ion batteries are quite recent as explained earlier, and the spread of electric vehicles is only starting. Operating data of Li-Ion batteries inside vehicles is very difficult to obtain due to the challenges linked to battery performances. Car manufacturers are most likely to keep all information about batteries and battery management private in order to be competitive and gain market share in the automotive sector. Therefore, most of the publicly available data comes from laboratories that have led research on the performances of Li-ion batteries in different contexts, with different objectives. Acquiring ageing data from Li-Ion batteries can take a very long time and requires lots of resources because they are so efficient that a large number of cycles is needed to observe any deterioration. Moreover, test devices are very costly, even more so with extreme test conditions (such as high or low controlled temperature in climate chambers). In order to reduce the costs and required

power for battery testing, it is almost systematic to use battery cells and not full battery packs. Indeed, the power required to fully charge or discharge real vehicle battery packs is much higher than with isolated cells.

In this section, several of the most useful publicly available datasets are presented. Most of them have been used at some point in this thesis, either to get information about battery ageing in general or to built predictive models that will be described in the three contribution chapters. Information that is provided here mainly comes from references [HHHK19], [HXLP20] and [dRSYL21]. Several of those datasets can be downloaded from the online platform Battery Archive [2]. Table 1.4 gives a summary of the presented datasets, with their names, institutes, the years over which tests were conducted, and optional remarks. A detailed review of each of the datasets in this table is given in the next paragraphs.

Table 1.4: Main Public Ageing Datasets

Dataset Name	**Institute**	**Number of Cells**	**Year**	**Remarks**
PCoE Battery Dataset	NASA Ames	34	2008-2010	
Cycle Life Prediction Dataset	MIT - Stanford University	124	2017-2018	
Short-Term Cycling Performance Dataset	Sandia National Laboratories	24	2017	Different chemistries and temperatures
Long-Term Degradation Dataset	Sandia National Laboratories	86	2018-2020	Different chemistries, temperatures, and depths of discharge
Oxford Battery Degradation Dataset	Oxford University	8	2015	Driving profiles

NASA PCoE Dataset

The NASA PCoE dataset is known as a reference benchmark since it was the first public dataset on battery ageing [3]. This dataset contains 34 cells divided into 6 groups. The cycling experiment was segmented into three parts: charging, discharging and impedance spectroscopy. The charging protocol is the same for all tests, a constant-current/constant-voltage (CC-CV) charging protocol with 1.5A rate and a 4.2V charging voltage threshold. Various discharging currents were used. Cells were cycled at different ambient temperatures, which influences the ageing

[2] batteryarchive.org

[3] Accessed in 2021 at https://ti.arc.nasa.gov/tech/dash/groups/pcoe/prognostic-data-repository/

speed. After each cycle, the impedance of battery cells is measured through an electrochemical impedance spectroscopy (EIS) with a frequency sweep from 0.1Hz to 5kHz.

MIT - Stanford Dataset

The MIT dataset was elaborated in collaboration with Toyota engineering and with the Department of Materials Science and Engineering of Stanford University in 2019[4] [SAJ+19]. It is the largest available dataset regarding Li-Ion battery ageing. The cells used for testing are Li-Ion Iron Phosphate (LFP) / graphite cells from A123 manufacturer, model APR18650M1A. These cells have a 3.3 V nominal voltage and a 1.1 Ah nominal capacity. They can provide discharge currents up to 30 A. The cells were tested in a 30°C climate chamber. The batteries are always discharged at a constant current of 4.4 A (4 C) (see section about health indicators for an explanation about the C-rate 1.3.1). The most important factor in the tests is the charging policy. Batteries are charged following a multi-step CC-CV policy which makes it possible to reduce the charging time. A complete overview of the 124 different battery cells and their associated charge protocol is given in table 1.6, and all charge protocols are detailed in table 1.7 (there are 69 different charge protocols for 124 battery cells).

The cells were divided into three batches. Each batch shows some irregularities which are detailed on the dataset's web page. The temperature measurements were made using a thermocouple attached to the surface of battery cells with thermal paste and adhesive tape. Internal resistance is measured during charging at 80% SOC, using an average of ten 30ms or 33ms pulses of $\pm$3.6C.

Table 1.5: Characteristics of the battery cells tested in the MIT dataset

N_{cells}	Type	Manufacturer	V_{nom} (V)	C_{nom} (Ah)	T (C°)
124	LFP	A123	3.6V	1.1Ah	30° C

Short-Term Cycling Performance Dataset SNL

The Sandia National Laboratory dataset [5] is described in [BFCF17]. This interesting dataset contains data from multiple types of batteries tested at different temperatures, as summarised in table 1.8.

Temperature measurements are obtained using a thermocouple attached to the body of the batteries, and the chamber used for testing has a temperature range of -73 °C to 200 °C. The experiment is segmented into two main parts : cycling tests and abuse tests. Cycling test protocols go as follows. First, 3 batteries of each type are entirely discharged. They are then placed in a climate chamber and left to rest for 12 hours to reach the desired temperature. The charging protocol is the same for every test, and consists in a 1C CC-CV charge. Between each charge and discharge, a 10-minute rest period is implemented. EIS is then performed on the cells, before

[4] Accessed in 2019 at https://data.matr.io/1/projects/5c48dd2bc625d700019f3204

[5] Accessed in 2020 at https://www.sandia.gov/energystoragesafety-ssl/research-development/research-data-repository/

Table 1.6: MIT dataset : all tested batteries and their associated charge protocol

Cell	Cycle life	Protocol	Cell	Cycle life	Protocol	Cell	Cycle life	Protocol
b1c0	1852	0	b2c0	300	22	b3c0	1009	61
b1c1	2160	0	b2c1	148	23	b3c1	1063	62
b1c2	2237	0	b2c2	438	24	b3c3	1115	63
b1c3	1434	1	b2c3	335	25	b3c4	1048	64
b1c4	1709	1	b2c4	444	26	b3c5	828	63
b1c5	1074	2	b2c5	480	27	b3c6	667	65
b1c6	636	3	b2c6	511	28	b3c7	1836	66
b1c7	870	3	b2c10	561	29	b3c8	828	61
b1c9	1054	4	b2c11	477	30	b3c9	1039	62
b1c11	788	5	b2c12	458	31	b3c10	1078	66
b1c14	880	6	b2c13	483	32	b3c11	817	64
b1c15	719	6	b2c14	485	33	b3c12	932	63
b1c16	862	7	b2c17	494	34	b3c13	816	64
b1c17	857	7	b2c18	487	35	b3c14	858	63
b1c18	691	8	b2c19	461	36	b3c15	876	67
b1c19	788	8	b2c20	502	37	b3c16	1638	66
b1c20	534	9	b2c21	489	38	b3c17	1315	62
b1c21	559	9	b2c22	513	39	b3c18	1146	64
b1c23	1014	10	b2c23	527	40	b3c19	1155	63
b1c24	1017	11	b2c24	495	3	b3c20	813	61
b1c25	854	11	b2c25	461	3	b3c21	772	65
b1c26	870	12	b2c26	471	3	b3c22	1002	68
b1c27	842	12	b2c27	468	41	b3c24	825	61
b1c28	860	13	b2c28	509	42	b3c25	989	62
b1c29	917	13	b2c29	498	43	b3c26	1028	64
b1c30	709	14	b2c30	481	44	b3c27	850	63
b1c31	876	14	b2c31	492	45	b3c28	541	65
b1c32	731	15	b2c32	519	46	b3c29	858	67
b1c33	757	15	b2c33	520	47	b3c30	935	62
b1c34	742	16	b2c34	499	48	b3c31	731	68
b1c35	703	16	b2c35	463	49	b3c33	1284	61
b1c36	704	17	b2c36	535	50	b3c34	1158	62
b1c37	648	17	b2c37	478	51	b3c35	1093	64
b1c38	617	18	b2c38	465	52	b3c36	923	63
b1c39	625	18	b2c39	459	53	b3c40	796	64
b1c40	966	19	b2c40	499	54	b3c41	786	63
b1c41	1051	19	b2c41	429	55	b3c42	1642	66
b1c42	702	20	b2c42	466	56	b3c43	1046	61
b1c43	651	20	b2c43	462	57	b3c44	940	62
b1c44	616	21	b2c44	457	58	b3c45	1801	66
b1c45	599	21	b2c45	487	59			
			b2c46	429	60			
			b2c47	713	15			

Table 1.7: All charge cycles in the MIT dataset

#	Protocol	#	Protocol	#	Protocol
0	3.6C(80%)-3.6C	23	2C(10%)-6C	46	5.2C(50%)-4.25C
1	4C(80%)-4C	24	2C(2%)-5C	47	5.2C(58%)-4C
2	4.4C(80%)-4.4C	25	2C(7%)-5.5C	48	5.2C(66%)-3.5C
3	4.8C(80%)-4.8C	26	3.6C(22%)-5.5C	49	5.2C(71%)-3C
4	5.4C(40%)-3.6C	27	3.6C(2%)-4.85C	50	5.6C(25%)-4.5C
5	5.4C(50%)-3C	28	3.6C(30%)-6C	51	5.6C(38%)-4.25C
6	5.4C(60%)-3C	29	3.6C(9%)-5C	52	5.6C(47%)-4C
7	5.4C(60%)-3.6C	30	4C(13%)-5C	53	5.6C(58%)-3.5C
8	5.4C(70%)-3C	31	4C(31%)-5	54	5.6C(5%)-4.75C
9	5.4C(80%)-5.4C	32	4C(40%)-6C	55	5.6C(65%)-3C
10	6C(30%)-3.6C	33	4C(4%)-4.85C	56	6C(20%)-4.5C
11	6C(40%)-3C	34	4.4C(24%)-5C	57	6C(31%)-4.25C
12	6C(40%)-3.6C	35	4.4C(47%)-5.5C	58	6C(40%)-4C
13	6C(50%)-3C	36	4.4C(55%)-6C	59	6C(4%)-4.75C
14	6C(50%)-3.6C	37	4.4C(8%)-4.85C	60	6C(52%)-3.5C
15	6C(60%)-3C	38	4.65C(19%)-4.85C	61	5C(67%)-4C-newstructure
16	7C(30%)-3.6C	39	4.65C(44%)-5C	62	5.3C(54%)-4C-newstructure
17	7C(40%)-3C	40	4.65C(69%)-6C	63	5.6C(36%)-4.3C-newstructure
18	7C(40%)-3.6C	41	4.9C(27%)-4.75C	64	5.6C(19%)-4.6C-newstructure
19	8C(15%)-3.6C	42	4.9C(61%)-4.5C	65	3.7C(31%)-5.9C-newstructure
20	8C(25%)-3.6C	43	4.9C(69%)-4.25C	66	4.8C(80%)-4.8C-newstructure
21	8C(35%)-3.6C	44	5.2C(10%)-4.75C	67	5.9C(15%)-4.6C-newstructure
22	1C(4%)-6C	45	5.2C(37%)-4.5C	68	5.9C(60%)-3.1C-newstructure

Table 1.8: SNL dataset : tested batteries and test conditions

N_{cells}	Type	V_{nom} (V)	C_{nom} (Ah)	T (C°)	I_{max} (A)
6	LFP	3.3V	1.1Ah	5,15,25,35,45°C	30A
6	LCO	3.6V	2.5Ah	5,15,25,35,45°C	20A
6	NCA	3.6V	2.9Ah	5,15,25,35,45°C	6A
6	NMC	3.6V	3Ah	5,15,25,35,45°C	20A

the cycling starts. Cycling consists of a discharge rate of 1C, which changes every 5 cycles and takes the values from 5A to 30A or until reaching the manufacturer's limit. When using high load currents, the maximum recommended temperature can be attained, and in this case the discharge procedure becomes segmented to allow the experiment to continue. This cycle is repeated for every temperature value. Note that when reaching 25° C, another EIS test is conducted and a 1C cycling is performed. The second part of the experiment is the abuse tests, which uses the same protocol as the cycling test but allows the battery to reach temperatures beyond the manufacturer's recommendations.

Long-Term Degradation Dataset SNL

This dataset[6] is described in [PBF+20]. The aim of this dataset is to study the effect of depth of discharge (DoD), load current and temperature on battery degradation. 86 cells of three different chemistries were considered in this study.

Table 1.9: SNL dataset: tested batteries

Type	V_{nom} (V)	V_{low} (V)	V_{high} (V)	C_{nom} (Ah)	I_{max} (A)
LFP	3.3V	2V	3.6V	1.1Ah	30A
NCA	3.6V	2.5V	4.2V	3.2Ah	6A
NMC	3.6V	2	4.2V	3Ah	20A

The experiments are conducted in a climate chamber and the body temperatures of the batteries are measured using a thermocouple. First of all, cells are placed in thermal chambers for a day to reach the desired temperature. The cells are then discharged to 0% SOC. A round of cycling consists here of a capacity measurement, a certain number of cycles and another capacity measurement. Capacity measurement in this study consisted of 3 charge and discharge cycles at 0.5C with a DoD of a 100%. The number of cycles defining a round varies between 125 and 1000 cycles. The number of cycles of the next round is halved if a 5% capacity loss is measured. EIS is performed every 3% capacity loss. Tests are conducted beyond 80% SOH. The tests can be aborted if the voltage or temperature limits of the cells is reached. The following table shows the different combinations of parameters used in this experiment. The charging of all cells was done at 0.5C, and the NCA cells were not discharged at 3C since it would be destructive.

Table 1.10: SNL dataset: test conditions

Discharge rate	Conditions 1	Conditions 2	Conditions 3
0.5C	40%-60%, 25°C	20%-80%, 25°C	0%-100%, 25°C
1C	0%-100%, 15°C	0%-100%, 25°C	0%-100%, 35°C
2C	0%-100%, 15°C	0%-100%, 25°C	0%-100%, 35°C
3C	40%-60%, 25°C	20%-80%, 25°C	0%-100%, 25°C

[6] Accessed in 2020 at https://www.batteryarchive.org/snl_study.html

Oxford Battery Degradation Dataset Oxford

This dataset[7] is used in [Chr17b]. Ageing data is collected from 8 pouch battery cells. The batteries were tested with a CC-CV charging profile and a driving discharging profile based on the urban Artemis profile. The Artemis cycle is a standardised speed profile used to asses the performances of vehicles. For more information, see chapter 5. Every 100 cycles, characterisation cycles were made. The available data is comprised of two files, the first *ExampleDC_C1.mat*, only contains the data from the first cycle with a 2C charging profile and a variable discharge profile. The other, *Oxford_Battery_Degradation_Dataset_1.mat* contains the results of each characterisation test made every 100 cycles, until the EoL of the batteries.

Table 1.11: Oxford dataset : tested batteries and test conditions

N_{cells}	Type	C_{nom} (Ah)	T°C	N_{cycles}
8	NMC	740mAh	40°C	End of life

1.2.5 Choice of ageing data

Five different datasets were presented in the previous sections, but not all of them had the same utility in the contributions that are described in the next chapters. Only three datasets out of all of them were used to build models. The preferred dataset is the one published by the MIT because it contains significant ageing data coming from 124 similar battery cells. The LFP technology is used in more and more vehicles due to the increased safety and cycle life as mentioned earlier. The high quality of the dataset in terms of amount of data and provided signals makes it more suitable for model training. The NASA dataset was also employed for model training as it is a reference in the field of predictive prognostics for Li-Ion batteries. Indeed, it was the first publicly available dataset and a great number of approaches are based on it, as will be described in the next section. Finally, the SNL dataset was used in one of the models described in chapter 3 for the variety of battery chemistries and test conditions.

1.3 Related work

1.3.1 Prognostics and Health management of Li-Ion batteries

Predictive prognostics

Predictive maintenance was officially defined in a European and French norm (NF EN 13306 [AFN19]) as a *"condition-based maintenance carried out following a forecast derived from repeated analysis or known characteristics and evaluation of the significant parameters of the degradation of the item"*. According to this definition, predictive maintenance includes aspects such as :

[7] Accessed in 2020 at https://ora.ox.ac.uk/objects/uuid:03ba4b01-cfed-46d3-9b1a-7d4a7bdf6fac

- **condition monitoring** : an activity carried out manually or automatically, designed to measure at predetermined intervals the characteristics and parameters of the actual physical state of an element
- **default diagnostics** : actions taken to identify faults, locate them and determine their causes
- **prognostics of failure** : actions taken to predict a future state (of reliability) on the basis of current and historical conditions, or to estimate the Remaining Useful Life (RUL) of items

There are two main approaches for battery predictive prognostics (and predictive prognostics in general) : physical-model-based and data-driven approaches. Physical-model-based techniques were the first ones to be developed, before data acquisition linked to the industry 4.0 exploded. Both methods have their advantages and drawbacks but we believe that their different aspects are complementary.

A model-based approach for the PHM of a system relies on the establishment of a simulation model according to physical rules and modelling equations. The aim is to understand and reproduce the behaviour of a system in order to obtain data that could be exploited, in particular with the introduction of disturbances. It implies a complete understanding of the system and gives a global representation of the different answers to sollicitations. There are several types of physic-based models for the predictive prognostics of Li-Ion batteries, including mechanistic, equivalent circuit, empirical or fused approaches. References [HXLP20] and [HXGL12] have established comparisons between the different battery models that have been developed in literature. However, the main drawback of physic-based models is that they require many resources to model often very complex physical rules. Most of the time, the problem has to be simplified due to computational cost [TR15].

In data-driven approaches, no deep physical understanding of the model is required. A "black box" model is established instead of a fully representative model for simulations. Rules are built from data : this kind of approach requires to have historical data on the system in order to predict future degradation trends. Data-driven approaches have reached very promising results due to the increasing amount of data collected from batteries. Although there is a great variety of possible data-driven approaches thanks to statistical models or machine learning algorithms, PHM of batteries relies on the same three global steps in all cases: *(i)* data acquisition, *(ii)* data processing, and *(iii)* decision making.

Health Indicators (HI)

Predictive prognostics of Li-Ion batteries aims at determining in advance when a failure could occur. The physical manifestations of degradation in a battery were described in the previous section 1.2.3, however, in real life applications such as in an EV, it is impossible to settle sensors that would be able to catch physical phenomenon such as dendrite formations or any degradation of the electrodes for example. Defining a predictive prognostics strategy for Li-Ion batteries requires to observe other signals that can either be acquired with non-intrusive sensors, or to compute other Health Indicators (HI) from those originally acquired signals. Some

of those HI directly reflect the physical battery degradation, and are therefore referred to as Direct Health Indicators (DHI). Although DHI are the best tools to quantify the degradation stage of a battery, they might be difficult to observe or compute directly from a vehicle, which is why other HI are considered in the contributions of this thesis. Signals that can easily be acquired in EV are current, voltage and temperature. Many Refined Health Indicators (RHI) can be computed from them such as the mean, minimum or range of those easily acquired signals. In the following paragraphs, DHI are described.

Capacity A battery is an electrochemical component built to store electrical energy under the form of chemical energy. The capacity of a battery is the quantity of electrical energy, measured in ampere-hours (Ah), that a battery can deliver during one discharge [PS16]. Capacity is computed by integrating the current over a whole cycle. The current rate (C-rate) when using a battery is often given according to its capacity. For example, discharging a 1.1Ah battery cell at a current rate of 1C means the battery is discharged with a 1.1A current.

State of Health (SOH) SOH is a global term to define the available storage ability of a battery in use. The *State of Health* (SOH) of a battery is defined as the ratio between the storage capacity of the battery at any time ($Q(t)$) and its initial capacity (Q_{nom}). Trivially, the higher the SOH, the better the performance.

$$SOH(t) = \frac{Q(t)}{Q_{nom}} \quad and \quad SOH(t)\% = \frac{Q(t)}{Q_{nom}} * 100 \tag{1.12}$$

Usually, the SOH of a Li-Ion battery degrades very slowly in the early cycles of its life and the curve is almost linear with a very gentle slope, and after a certain time, there is an inflection point from which the curve starts decreasing much faster.

End of Life (EoL) and Remaining Useful Life (RUL) Monitoring the SOH of a battery is essential, considering that it decreases throughout its life. Concerning electric vehicle applications, a battery is considered out of use when it has lost 20% of its initial capacity [HXLP20, LZWD19]. The EoL of a battery corresponds to the time (often expressed as a number of charge and discharge cycles) when a battery reaches this threshold.
It is to be noted that EoL for EV application does not mean the battery is completely out of use. After reaching 80% of its initial capacity, a battery is considered unsuitable for EV applications but not for domestic use where they can be offered a second life. Considering this definition, the Remaining Useful Life (RUL) of a battery corresponds to the number of charge and discharge cycles it can go through before reaching its EoL.

Internal Resistance (IR) The Internal Resistance (IR) of a battery encompasses the notion of resistance, capacitance and inductance in one model. The IR of a battery highly affects its performances. Indeed, a high IR causes the battery to heat up due

to current restrictions, and also causes voltage drops. IR can be measured with different methods such as current pulses to study the voltage drops or Electrochemical Impedance Spectroscopy (EIS).

1.3.2 Existing approaches for Prognostics and Health Management for Li-Ion batteries

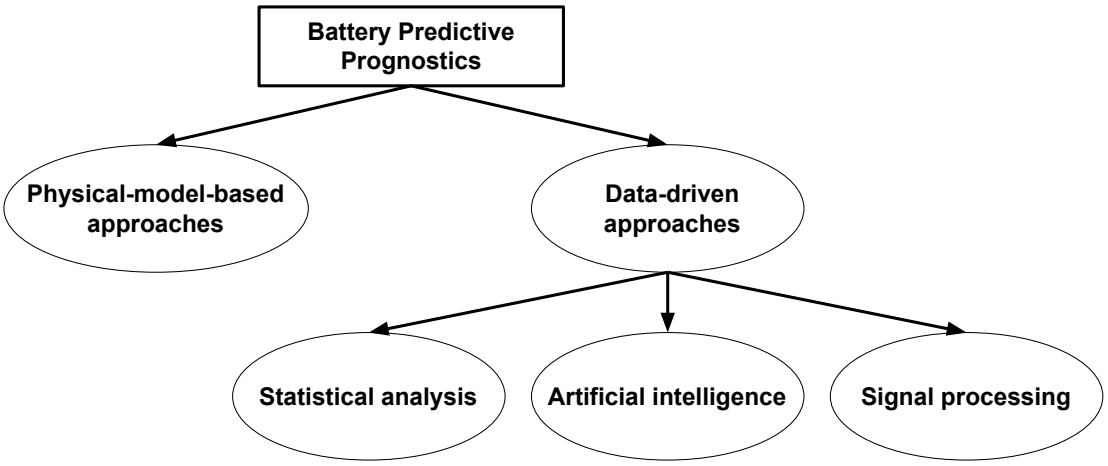

Figure 1.12: Global classification of models for predictive prognostics of Li-Ion batteries

As described in the previous sections and illustrated in figure 1.12, the first distinction in battery predictive prognostics models is made between model based and data driven approaches. This section will not go into detail about physical-model-based approaches, but will focus extensively on data-driven approaches. Data driven approaches can themselves be divided into three sub-categories, namely **statistical analysis**, **artificial intelligence** and **signal processing**.

Signal processing based Predictive prognostics

Signal processing approaches can have several interests. Concerning predictive prognostics, identifying degradation patterns thanks to frequency decomposition can help predicting the shape of the degradation curve knowing the evolution of SOH during the first cycles in the life of a battery. However, signal processing is more widely used for data cleaning and pre-processing. Several treatments can be applied to raw data in order to remove noise in collected signals, and decomposed signals can be used as extracted features in input of other types of models.

Statistical analysis

Statistical approaches aim at predicting the future degradation trend of a health indicator by comparing historical variations with known signals [MSV+20].

Artificial intelligence based

Artificial intelligence approaches have proved very efficient in the field of predictive prognostics due to their ability to approximate complex phenomenon without need for expert knowledge. The major topic in predictive prognostics for Li-Ion batteries is to predict the evolution of one of the HI mentioned above, according to different inputs. Considering that the desired output is known in advance, mainly supervised learning models are developed. Therefore, supervised learning is the only type of learning that will be described in the scope of this thesis. The predictive prognostics strategies built on artificial intelligence are often classified according to the implemented algorithm. A first distinction in the category of artificial intelligence based approaches can be made according to the complexity of the employed model. Not all artificial intelligence models require the same training process, amount of data or computation complexity. The following paragraphs aim at describing several approaches that were encountered in the literature based on the type of model and their applications.

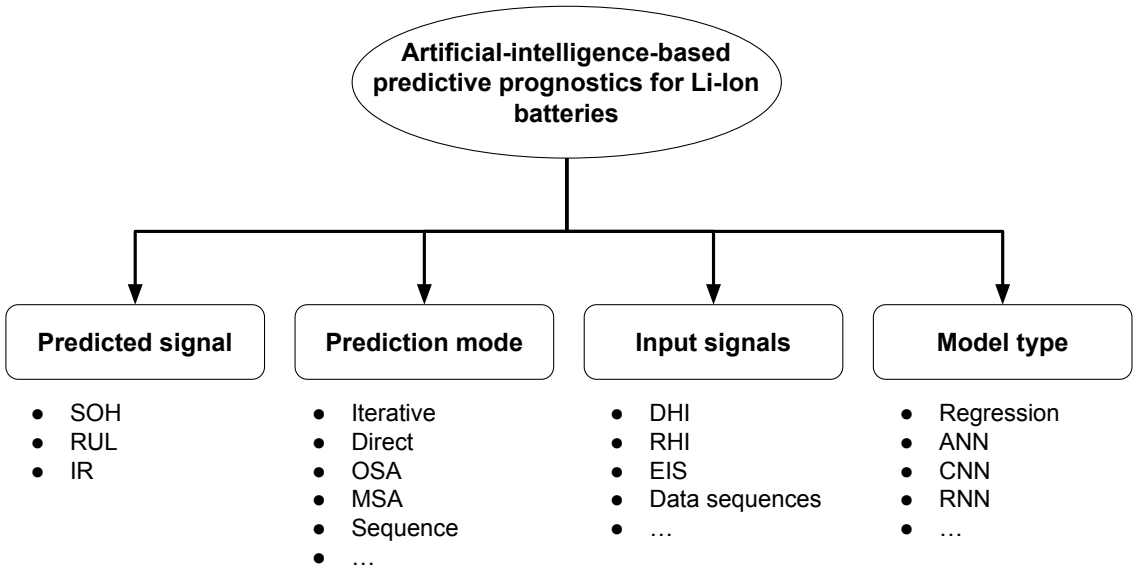

Figure 1.13: Different ways to classify the AI-based predictive prognostics models for Li-Ion batteries

Gaussian process regression (GPR) Gaussian process regression aims at mapping input features to a given output through a non-parametric regression. In [ZTZ+20], Zhang *et al.* have developed a model that is both able to predict SOH and RUL from Electrochemical Impedance Spectroscopy (EIS) measurements. EIS and capacity measurement that compose the training dataset are generated in their laboratory with custom operating conditions, and point predictions of capacity and RUL are made according to one single EIS measurement. GPR was also employed in [zKYZ+21] by Kong *et al.*, who have extracted features from voltage and temperature curves to predict SOH and RUL. The employed data for training comes from the MIT dataset. Their model takes as input several consecutive charge and

discharge cycles (up to 400 hundred cycles) and outputs point predictions of SOH or RUL.

Linear regression Some approaches in the literature have found linear relationships between computed features and SOH or cycle life. Along with the dataset published by the MIT, a linear model completed with an elastic net for regularisation was studied to link computed features from early cycles with the global cycle life of the batteries. Studied features are derived from the difference between capacity curves at cycle 1 and 100, but also from a linear interpolation of the capacity fade curve between cycles 91 and 100, and from other HI such as the IR, charge time and temperature. The aim of their model is not to make an online prediction of the RUL of a battery, but rather to identify its global cycle life from early cycles, which is to say before degradation signs appear. Another reference mentions the use of a linear model that uses raw voltage curves and V', a computed feature called the unit time voltage drop to predict both SOH and SOC [HTL+17]. The SOH depends on V' and on the estimated SOC at each cycle, and can be estimated at each cycle with a good accuracy (RMSE < 0.04).

Artificial Neural Networks Among artificial-intelligence-based approaches for predictive prognostics of Li-Ion batteries, some models stand out by their effectiveness and popularity. It is the case for Artificial Neural Networks (ANN), which have been used in countless articles in the literature, whatever the architecture. The present paragraph and following ones aim at describing the most relevant existing approaches according to the type of ANN.

FNN is the most basic form of ANN, and some approaches have been exploiting their performances with different types of input features and for different types of predictions.

An Extreme Learning Machine (ELM) model was developed by Razavi-Far *et al.* to predict RUL of a battery from capacity data [RFCS+18]. They built their model on the NASA dataset and developed several strategies for One-Step-Ahead (OSA) and Multi-Step-Ahead (MSA) predictions of SOH. Up to 60% of the historical degradation curve of SOH is kept for training and a variable number of predictions according to the strategy is made in order to determine the RUL of the battery.

You *et al.* [YPO17] have developed a method to cluster current, voltage and temperature distributions over the whole life of a battery in order to distinguish similar patterns according to the degradation stage of a battery. The aim of their model is to use the information contained in a sample of current, voltage and temperature data coming from a portion of charge or discharge cycle to predict the actual SOH of the battery. Raw values of current, voltage and temperature are used as input to an ANN that outputs one single value of SOH. Their model is trained "offline" with available data, and prediction can be made "online" with newly collected data.

Data of current, voltage, temperature have also been employed in approaches by Kumprom *et al.* and Choi *et al.* [KY19, CRPK19] as input to an ANN that predicts either RUL and SOH or simply capacity. Both approaches have employed battery ageing data from NASA. Kumprom *et al.* have also added capacity measurement as input feature to their predictive model and have compared the performances of a

deep ANN (an ANN with multiple hidden layers) with other models such as linear regression, support vector machine and shallower ANN (i.e. an ANN with only one hidden layer) with a clear advantage for the deeper ANN. Choi *et al.* on the other hand have compared the performances of the ANN with more complex models such as RNN and CNN, with an advantage for the RNN model. Such structures are presented in the next paragraph.

Recurrent Neural Networks One can understand why ANN have been so widely employed for the predictive prognostics of Li-Ion batteries. The ageing phenomenon of Li-Ion batteries depends on intrinsic characteristics of the batteries, but also on a great number of external parameters and mainly the operating conditions of an electric vehicle. The type of data that is manipulated when building a data-driven predictive prognostics model for Li-Ion batteries is time series. Whether they describe the long term evolution of SOH (over the whole cycle life of a battery) or the short term variations of current, voltage or temperature during one use cycle, all battery-related signals refer to a time unit. RNN have been described in detail in the previous part of this chapter (see Theoretical background 1.1.7), and were proved to be particularly adapted to the study of time series, especially in prediction tasks. This explains why so many articles in the literature are based on this type of model. Although a great number of models have in common the use of RNN, some specific feature extraction techniques, input signals or prediction modes make it possible to distinguish several approaches.

The first observation that can be made is that the vast majority of RNN-based predictive prognostics models use capacity (or SOH) as single input signal to predict the future trend of capacity (or SOH). Non linear models (such as ANN) that use past values of a given signal to predict the future values of the same signal are referred to as **Non linear Auto-Regressive models** (NAR). The principle of NAR models is summed up in equation 1.13

$$y(t+1) = f\{y(t), y(t-1), ..., y(t-d)\}. \tag{1.13}$$

where d is the size of the input time window and t is the time stamp.

Liu *et al.* [LZP19] have developed a RUL prediction model based on a mix of Bayesian Moving average and LSTM. A notion of uncertainty is introduced in their results and the accuracy of the prediction is guaranteed with the development of multiple LSTM sub-models based on different divisions of the initial training dataset. All the sub-models are trained on capacity data only, focusing on a small window of consecutive capacity values (39 cycles). The prediction corresponds to the value of SOH at the 40^{th} cycle. To the best of their performances, with a RUL prediction made after 500 full cycles, the error between the actual RUL and the predicted one is of 9 cycles.

Zhang *et al.* [ZXHL17] have also based their model on an LSTM that predicts RUL according to historical values of SOH. Two models are developed according to the amount of capacity degradation data that is kept to train the model. The first one used 50% of SOH data and the second up to 70% of the whole curve. With those two models, they reach an average error of -3 cycles and 15 cycles respectively.

Li *et al.* [LZWD19] and Qu *et al.* [QLMF19] have developed similar approaches in that an LSTM is used to predict SOH from historical data of SOH. In both approaches, historical data of SOH is decomposed into several sub-signals following an Empirical Mode Decomposition (EMD), each corresponding to a given frequency. Those several signals are used as input features to an LSTM, combined with Elman Neural Networks in the first case and particle swarm attention mechanisms in the second case. Models are trained on the beginning of the degradation curve of a battery (up to 70% of the whole curve). Li *et al.* have obtained a 2.99% MAPE on the prediction of RUL of one of the batteries in their test dataset. Qu *et al.* have obtained an RMSE of 0.0119 on the prediction of SOH for one of the batteries in their dataset, by using 30% of the degradation curve for training.

More recently, Liu *et al.* [LSOW21] have employed this same decomposition method combined with an LSTM to iteratively predict the SOH. The uncertainty of the prediction is given with a Gaussian process regression sub-process. GPR also aims at capturing short term regeneration phenomena when the LSTM focuses more on the long term dependencies. The combination of the two models gives the prediction of future capacity data. SOH is either predicted on the short term (6 steps ahead) or long term (24 steps ahead). Predictions are made using an iterative technique : the previously predicted capacity value is used as input for next prediction and so on. In their approach, the first 80 cycles are kept for training the model, and the rest of capacity data is used as validation. For long term predictions, they reach an RMSE of 0.0041 on one of the batteries in their dataset.

Fewer approaches have exploited the alternative of using only current, voltage and temperature data to predict SOH or RUL. Non linear models that use past values of one or several signals to predict the future values of one or several other signals are referred to as **Non linear Regressive models with exogenous inputs** (NRX). The principle of NRX models is summed up in equation 1.14

$$\begin{aligned} y(t+1) = f\{&x_1(t), x_1(t-1), ..., x_1(t-d_1), \\ &\dots, \\ &x_n(t), x_n(t-1), ..., x_n(t-d_n)\} \end{aligned} \quad (1.14)$$

where y is the target time series, x_n are exogenous variables, t is the timestamp and d is the size of the input window.

In an article by You *et al.* [YPO17], a focus is made on capacity fade curves. Their approach consists in improving the history-based methods for capacity forecasting, based on the global observation of current and voltage curves. They develop a "snapshot based" approach that can adapt to atypical changes in current and voltage discharge curves and brings more flexibility to the predicting model. Their model is based on an LSTM, mixed with a pooling layer that merges the output of the LSTM layer, and a regression layer at the end. To build their model, they gathered custom ageing data from 70 battery cells and managed to get an average error of 2.46% on the SOH prediction.

The paper [RDW+21] describes an innovative model for RUL prediction, based

on Auto-CNN-LSTM. Their strategy aims at improving three different points : offline training should be made possible by including information from adjacent charge and discharge cycles, cleaned from any noise. Their prediction of the RUL should be continuous and not a single point value. To do so, they implement a model based on auto encoder CNN and LSTM, and a post smoothing method to solve the discontinuity in the prediction results. All the tests are conducted on NASA PCoE data. Features are extracted from temporal curves of voltage, temperature and current at every cycle with measurements such as the largest measured voltage during charging etc. All the data is normalised in a [0,1] range before being used in any model. Tests are conducted on two batteries of the NASA PCoE dataset.

Sequence to Sequence In a recent approach, an extensive use of LSTM is made, with the development of a sequence to sequence model for the prediction of SOH by Li *et al.* [LSD+21]. Their goal is to predict in one shot the whole SOH degradation curve at any moment in the life of a battery, including before degradation signs appear. The model takes as input the past SOH curve only (NAR model). They start making prediction after 100 cycles, and add data to the input sequence of the model as the battery ages. This is made possible by the use of Seq2Seq recurrent neural network that are particularly adapted to sequence prediction problems with variable length. The structure of the model is built to take sequences of variable length as input, and to output sequences of variable length also. The first sequence to be taken as input for a given battery corresponds to the first 100 cycles. As the battery gets older, ageing data is concatenated to the initial vector and thus, the input vector grows. Training is done on all available data, which makes an online prediction possible. If the model is trained to predict the future SOH curve at any time, any input vector can be given as input and the prediction can be made. The ultimate goal of their model is to be implemented in an on board BMS. The performances of the model are evaluated with the Mean Absolute Percentage Error (MAPE). Five random battery cells are kept aside for validation. As can be expected, their model shows a lower accuracy when the prediction is made at the Beginning of Life (BoL). The more data taken as input, the better the accuracy. Error metrics are given according to several criteria. The model is built to predict either the 80EoL, 65EoL or the knee point (the moment when SOH starts to drop after the plateau). They reach a MAPE of 1.78% relatively to the SOH prediction.

Convolutional neural networks Although CNN are traditionally used in image recognition problems, their ability to automatically extract features from data has brought attention to them, including in the field of time series prediction. Shen *et al.* [SSL+20] have developed a model based on several CNN models for the prediction of capacity, coupled with transfer learning and ensemble learning to improve the prediction and combine the results of the several models. They have based their study on two different datasets, a first custom dataset to train the models, and the NASA dataset for transfer learning and testing. The aim of their study is to predict the capacity of a battery at each cycle according to partial curves of current, voltage and capacity.

1.3.3 Literature discussion

The previous sections aimed at describing in detail the different types of models based on artificial intelligence and more particularly neural networks. Three types of models clearly appear as dominating the predictive prognostics approaches for Li-Ion batteries : ANN (feed forward type), RNN (either LSTM or Sequence to Sequence) and CNN (mainly for feature extraction from time series). In table 1.12, a comparative summary of the existing approaches is made. What is interesting to note is that other connections between models can be made, not only based on the type of model that is used but rather on the type of prediction and on the input features that are employed.

In the paragraph on RNN, a distinction is made between NAR and NRX models, depending on whether or not they take SOH as an input when predicting SOH. Based on the description of several articles of the literature, and on the summary that is made in table 1.12, it appears that NAR models are the most popular models in the field of predictive prognostics for Li-Ion batteries. This can be explained by the nature and the shape of the degradation curve of SOH. As presented in section 1.2.4 and again in the definition of the SOH that is given earlier, the degradation curve of Li-Ion batteries is similar from one battery to another if the use conditions remain the same. Using past SOH values to predict future ones, and especially at very short term (as is the case for most approaches) seams logical considering that SOH varies very little from one cycle to the next. Very accurate predictions of future SOH values from past ones can be reached, especially with models that are dedicated to time series prediction such as LSTM. Although NAR models are very efficient, those results should be interpreted in a specific context. The data that was described earlier and that is used in all state-of-the-art articles corresponds to lab tests of batteries that are cycled following pre-defined protocols. The use conditions of batteries generally remains the same from the beginning to the end of life, which is why the degradation process is very stable, without recovery or accelerated ageing phases. In this context, the only use of past SOH values to predict future ones is very efficient, because all SOH degradation curves follow the same pattern. However, in a more realistic context, it is very unlikely that two batteries will degrade in the same way in an electric vehicle. If the operating condition of a battery changes completely during its life (for example if the user changes, if the vehicle is used in a different region with higher or lower temperatures, with different roads . . .), predicting SOH looking only at its past values might not be sufficient to take into account all the external parameters. Therefore, in all the contributions that were developed in the scope of this thesis, only NRX models were developed, either to predict SOH or RUL. Moreover, the ultimate goal of a predictive prognostics strategy for Li-Ion batteries in an EV is to be directly implementable on board a vehicle. This implies that the features used as inputs to the predictive models can be retrieved directly from the battery in the vehicle. This criterion has motivated the choice to use exclusively current, voltage, and temperature data in our SOH predictive models.

In addition to the classification of models according to their input features, there is also a difference between models that can predict SOH at very short terms or long terms. It appears clearly in table 3.9 that very few approaches are able to

give a long term estimation of the evolution of SOH with one single prediction. In most approaches, and no matter the type of inputs (NAR or NRX models), it is the current SOH value that is estimated (direct prediction) or the value of SOH One-Step-Ahead (OSA prediction), without long-term projections in the future. In some NAR approaches, predictions are used as new inputs to the models in order to iteratively predict further values of SOH, which is a way of making long term predictions. Only two state-of-the-art articles intended to predict the SOH several time steps ahead directly, with one prediction. In ref [LSOW21], the SOH is predicted multi steps ahead (MSA prediction), but the maximum horizon is of 24 cycles only. In [LSD+21], the developed model is an NAR model. This statement has brought another goal to the models developed in the scope of this thesis, which is to obtain a reliable and long term prediction of SOH according to the operating data, without using iterative predictions.

The last distinction that can be made between state-of-the-art article relies in their ability to make online predictions or not. The term "online" here means that SOH predictions (either at short term or long term) can be made at any time in the life of a battery, depending on the amount of data that is taken as input by the predictive model. Some approaches use up to half of the SOH curve to train the model and can only make predictions on the rest of the curve. Our goal is to build models that take a limited amount of data as input and that are able to make predictions on unseen data even at the very beginning of the life of a battery.

Table 1.12: Summary of existing artificial intelligence based approaches for the predictive prognostics of Li-Ion batteries

Reference	Type of model	Complementary model	Type of input features	Online prediction	Long term SOH prediction	Employed dataset
[SAJ+19]	LR	Elastic net	NRX	No	No	MIT
[wYPO16]	ANN	KNN	NRX	Yes	No	Custom
[KY19]	ANN	None	NARX	Yes	No	NASA
[WFG16]	ANN	Importance Sampling	NRX	Yes	No	Custom
[YPO17]	LSTM	Pooling	NRX	Yes	No	Custom
[RDW+21]	LSTM	CNN	NRX	Yes	No	NASA
[LZP19]	LSTM	BMA	NAR	No	No	CALCE
[QLMF19]	LSTM	Particle swarm + attention mechanisms	NAR	No	No	NASA
[LZWD19]	LSTM	Elman networks	NAR	No	No	CALCE
[ZXHL17]	LSTM	None	NAR	No	No	Custom
[LSOW21]	LSTM	GPR	NAR	No	Yes	NASA + CALCE
[SSL+20]	CNN	None	NARX	Yes	No	Custom + NASA
[LSD+21]	Seq2Seq	None	NAR	Yes	Yes	RWTH

Chapter 2

RUL prediction from historical features

Contents

2.1 Introduction - The challenge of predicting battery life

Previous chapters have shown why Li-Ion batteries are so widespread in EV and HEV. In comparison with other battery chemistries, their characteristics in terms of energy density, operating temperature range, lifetime, voltage levels ... make them the most suitable technology for the transportation field, or any type of portable device.

However, Li-Ion batteries are the subject of many expectations from the consumers regarding the driving range, cycle life and safety. The performances of Li-Ion batteries are highly impacted by their operating environment, and each period of driving or storage has a direct impact on battery health. Calendar ageing is linked to storage conditions of a battery and is completely uncorrelated with the way a battery is used. Cyclic ageing on the other hand depends mostly on the operating conditions of a vehicle and on the behaviour of users. Many factors have already been identified as hazardous for the battery, but it is of crucial importance to monitor the evolution of the SOH of a battery and understand the ageing mechanisms that are at stake. In addition, even though operating conditions play a major role in the evolution of battery performance, not all batteries have the same basic characteristics and some may degrade more rapidly than others.

One of the aims of PHM is to search for reliable health indicators in order to build models that help monitoring and predicting the evolution of the performances of a battery.

This chapter describes the work that has been done regarding both an early and offline estimation of the global cycle life of Li-Ion batteries and an online prediction of the RUL of a battery. First, an analysis of the data provided by the MIT is made. The reason why this study is based on the MIT dataset is given in chapter 1 as a conclusion of the description of all available datasets. Several health indicators are extracted from raw operating data. Depending on the type of prediction (*offline* cycle life prediction or *online* RUL prediction), two models are designed and evaluated, built on different data structures and health indicators. This approach makes a direct link between battery operating data and its cycle life.

2.2 Data analysis

In the MIT dataset, information is provided on two bases: per cycle and according to time. In the per cycle base, for example, the value of internal resistance for each cycle is stored, which makes it possible to evaluate the evolution of the factor on the whole cycle life of the battery cell. All quantities related to the ageing of batteries and whose evolution can be traced over the entire life of a battery are referred to as historical features. For each cycle, one single value of each historical feature is stored. In figures 2.1a and 2.1b, the evolution of two historical features, the SOH and the internal resistance, is represented for several different batteries. Each curve represents one battery, and the longer the life cycle of the cell, the darker the curve.

In the time base, data about the cell temperature, voltage, current and capacity are collected at a given frequency during each operating step (charge, discharge or pause) of each cycle according to the time. The sampling rate is variable depending on the test step, but on average data is collected every 5 seconds.

Figures 2.2a and 2.2b show the temporal evolution of operating data for several different cycles of one given battery (time series of I_C and V_C) The color of the curve depends on the cycle number.

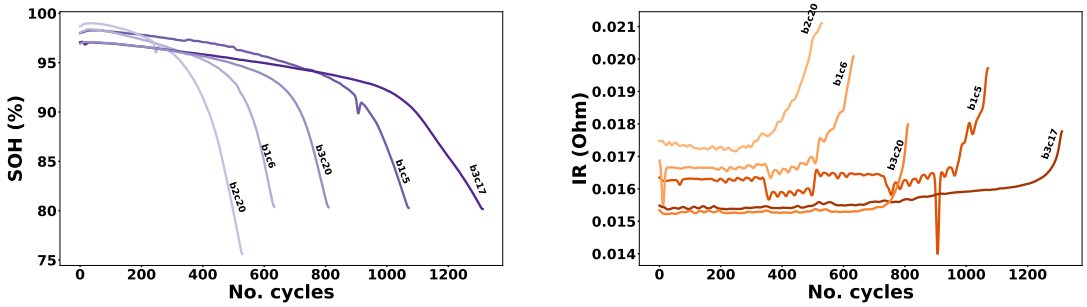

(a) Evolution of SOH over a cycle life

(b) Evolution of IR over a cycle life

Figure 2.1: Historical data for five different battery cells

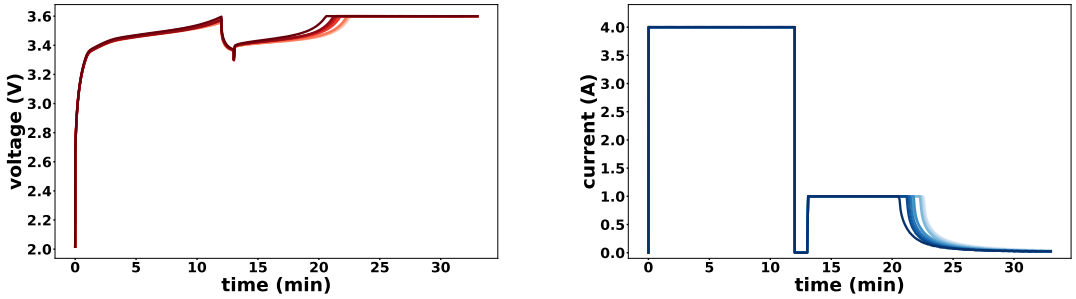

(a) Charge voltage (several cycles)

(b) Charge current (several cycles)

Figure 2.2: Operating data of battery cell b1c4

Each battery in the MIT dataset was cycled from beginning to end of life, that is until each battery reaches 80 % of its initial storage capacity. The study lead by the MIT intentionally aimed at observing the effects of fast charging on battery cycle life. According to figures 2.3a and 2.3b, the influence of operating conditions is clearly identifiable. The whole dataset gathers operating data from 124 different battery cells which are evenly separated into three batches. Each batch is defined by the date when the tests were started. The first two batches were tested from May and June 2017 respectively, and the last one was tested from April 2018. There are minute differences in the use conditions of the battery cells between the first two batches and the last one, mainly regarding the length of the pauses during the charge phase and the IR measurement method. Globally, the charge time varies between 9 and 14 minutes and comprises pauses of variable length, and the cycle life of the tested battery cells ranges from 300 to 2237 cycles. Figure 2.3b also shows

that two batteries that are cycled at the same moment, in the same conditions and with the same charge protocol can have a cycle life gap of up to 1000 cycles. In both figures, each dot represents one cell. Some charge protocols were used for several batteries which is represented by the colour of the vertical lines on which dots are placed. The more batteries per charge protocol, the darker the vertical line. Each charge protocol is represented by a number, and detailed information are given in the first chapter, in table 1.7.

Those simple observations highlight the fact that two batteries (and therefore two vehicles) with the same characteristics but different use conditions can have very different cycle lives, and that even batteries with same characteristics and same use conditions can have variable performances. Based on these observations, the need to develop models to estimate the cycle life of a battery is clear. The aim of such tools is to determine which batteries perform best from the very first cycles of use, which could make it possible to use only the best performing batteries in vehicles, and to monitor the evolution of a battery's performance in order to identify any failures as far in advance as possible.

2.3 From a global life cycle estimation to an online prediction of the Remaining Useful Life

We previously illustrated the importance of developing cycle life prediction strategies. The confidence of drivers and the Total Cost of Ownership (TCO) of EVs depend on the performances of the battery and on its global life span. Therefore, an early cycle life prediction strategy could make it possible to select only the best performing batteries to be used in EVs, leaving batteries with lower performances for stationary applications. The goal is to estimate the global cycle life of a battery before any degradation signs appear. A common strategy is to take advantage of the information contained in historical operating data and to build an estimation model based on the offline computation of health indicators, which will be detailed in the following sections.

The early degradation of the cycle life of a battery can be combined to an online prediction of its RUL. An embedded approach where data is acquired continuously while the battery is used makes it possible to continuously predict and update the ageing stage of a battery and its RUL. The following sections describe the different strategies that were developed for the early offline prediction of the global cycle life of a battery and the online prediction of the RUL of a battery.

2.3.1 Offline strategy for global cycle life estimation

A great variety of approaches in the literature tackles the problem of predicting battery life with an *offline strategy*. As described in the last paragraph, predicting the global cycle life of a battery before capacity degradation is a key point in the management of an electric vehicle and in the understanding of early ageing mechanisms of batteries.

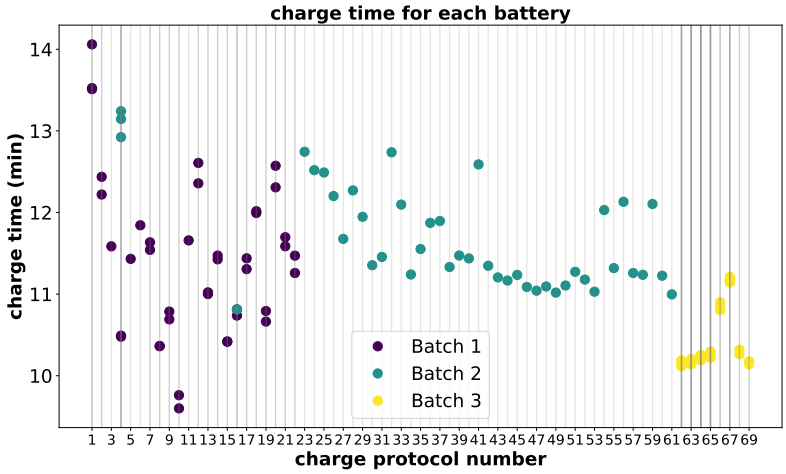

(a) Charge time

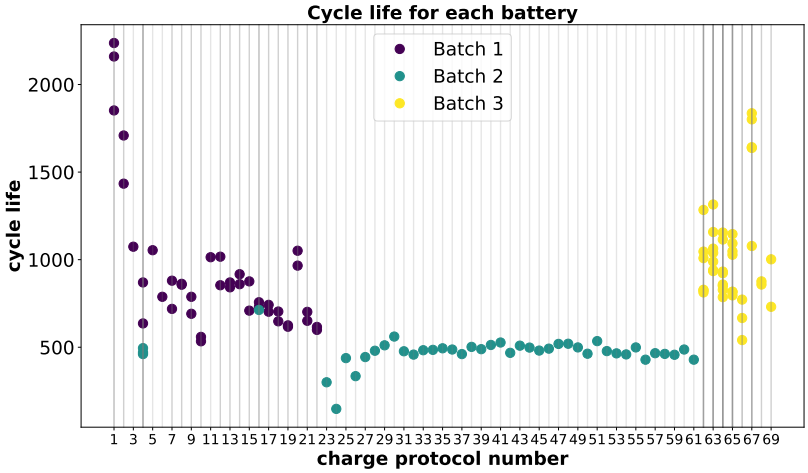

(b) Cycle life

Figure 2.3: Influence of the charge protocol over the cycle life and charge time of all cells in the MIT dataset

The *offline strategy* for global cycle life estimation described in this chapter consists in comparing the state of a brand new battery that has not been through any charge or discharge phases with the state of the same battery after 100 full operating cycles (successive complete charges and discharges) as it was done in the study by [SAJ+]. Li-Ion batteries being very efficient, and the use of batteries being identical from BoL to EoL in the MIT dataset, minimal damage is observed between cycle 0 and cycle 100. Nevertheless, even the slightest change of the battery performance after 100 use cycles can be exploited to estimate its global cycle life.

An estimation model is built by learning how to link minute degradation signs between cycle 1 and 100 to the global cycle life of the battery. This means that for each battery, a single prediction of its global cycle life is made after 100 cycles, considering observed data at cycles 1 and 100.

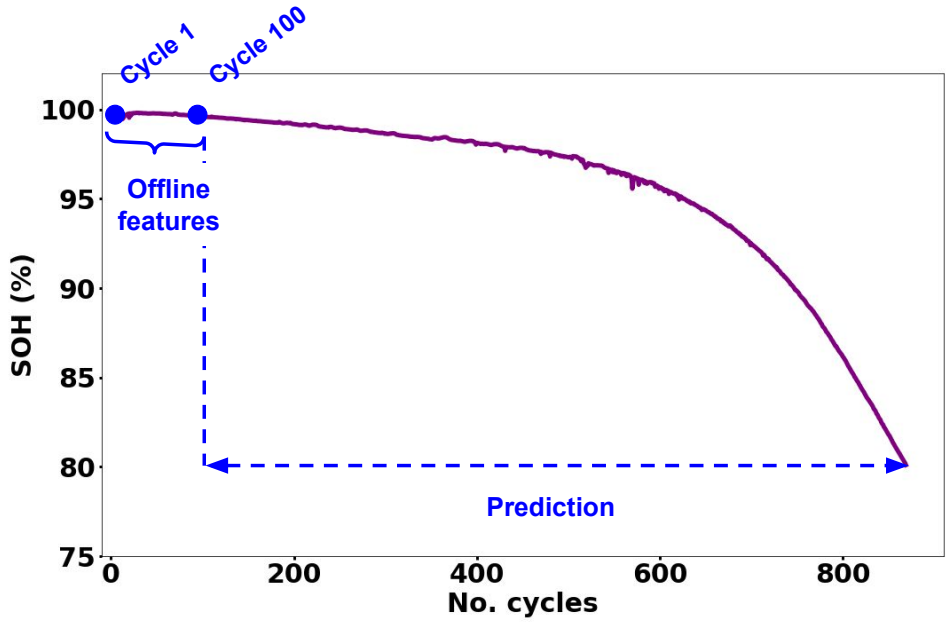

Figure 2.4: Offline strategy for global cycle life prediction

In the following section, a description of the ageing indicators that are computed after 100 cycles of use is given.

2.3.2 Offline health indicators for global cycle life estimation

As described in section 2.2, the MIT dataset contains several types of information. Whether it is on the per cycle basis or the temporal basis, raw data signals are provided, without pre-processing or feature engineering. All this raw data contains information about the RUL and the ageing stage of the battery at a given time, but it needs to be pre-processed and combined in order to highlight the factors that most represent the evolution of life cycle.
In references [SAJ+19, WFG16, RZH+18] to cite a few, features are computed from geometrical properties of charge and discharge curves (Voltage, Current, Internal Resistance, Temperature, ...). Those features are meant to be independent of the length of the time series, because not all cells charge and discharge at the same speed. Therefore, features such as the time when the battery terminal voltage reaches its maximum value, or the moment when the output current of the battery starts to drop are used.

In the predicting approach developed in [SAJ+19], the geometrically computed features are combined with scalar features from the aforementioned per-cycle data.

In the offline strategy for global cycle life prediction, several features are computed from the early cycles of a cell (from cycle 4 to 100). Each cell is represented by several offline health indicators defined by [SAJ+], and that take into account the performances of the battery during the early cycles of its life. All the formulas that are given regarding offline features are taken from [SAJ+]. For a great number

of those features, the difference between the capacity computed during cycle 1 and capacity computed during cycle 100 is used. Considering that the charge and discharge time varies from one cycle to another, the time series of capacity at each cycle has a different length. In order to subtract the two vectors (capacity at cycle 1 and 100), they need to be the same length. To do so, a linear interpolation is made on capacity curves and the are evenly re-sampled over 200 points. Computed features are the following:

Features computed from the difference of capacity Q between cycles 100 and 10 ΔQ_{100-10} (in all formulas, p is the length of the resulting vector after subtraction)

- Minimum: $min\Delta Q_{100-10} = log(|min(\Delta Q)|)$
- Variance: $var(\Delta Q_{100-10}) = log\left(\left|\frac{1}{p-1}\sum_{i=1}^{p}(\Delta Q_i - \overline{\Delta Q_i})\right|\right)$
- Skewness: $skew(\Delta Q_{100-10}) = log\left(\left|\frac{\frac{1}{p}\sum_{i=1}^{p}(\Delta Q_i - \overline{\Delta Q_i})^3}{\left(\sqrt{\sum_{i=1}^{p}(\Delta Q_i - \overline{\Delta Q_i})^2}\right)^3}\right|\right)$
- Kurtosis: $kurt(\Delta Q_{100-10}) = log\left(\left|\frac{\frac{1}{p}\sum_{i=1}^{p}(\Delta Q_i - \overline{\Delta Q_i})^4}{\left(\frac{1}{p}\sum_{i=1}^{p}(\Delta Q_i - \overline{\Delta Q_i})^2\right)^2}\right|\right)$

Features computed from the difference of capacity between cycles 4 and 5 (ΔQ_{5-4})

- Minimum: $min\Delta Q_{5-4} = log(|min(\Delta Q)|)$
- Variance: $var(\Delta Q_{5-4}) = log\left(\left|\frac{1}{p-1}\sum_{i=1}^{p}(\Delta Q_i - \overline{\Delta Q_i})\right|\right)$

Features computed from the capacity during cycle 2

- Q_{D_2}: The value of discharge capacity at cycle 2
- $\Delta Q_{D_{(max-2)}}$: Difference between the maximum value of discharge capacity between cycles 1 and 100, and Q_{D_2}

Features computed from the linear fit to the capacity fade curve

A linear model is computed to best fit the evolution of several consecutive discharge capacity values, as a function of the cycle number. The target of the linear model is to find the appropriate weight vector **b*** (slope and intercept) to bring the predicted values $\hat{q}$ as close as possible to the real capacity values Q.

$$\mathbf{b^*} = argmin_b \frac{1}{d}\|q - Xb\| \tag{2.1}$$

In this formula, d corresponds to the number of cycles used in the prediction. In this scope, two features are used, which are:

- the slope of the linear fit to the capacity fade curve between cycles 2 and 100

- the intercept of the linear fit to the capacity fade curve between cycles 2 and 100

Other offline features computed from the time series of temperature

- $T°_{max_{100-2}}$: The maximum value of temperature between cycles 2 and 100
- $T°_{min_{100-2}}$: The minimum value of temperature between cycles 2 and 100

Other offline features computed from historical data

- IR_2: The value of internal resistance at cycle 2
- IR_{min}: The minimal value of IR from cycles 2 to 100
- ΔIR_{100-2}: The difference of IR between cycles 2 and 100
- $\overline{T_C}$: Average charge time

2.3.3 Online strategy for Remaining Useful Life prediction

The true interest of battery cycle life prediction is to be able to update the estimations as a function of the use of the battery at any moment of its life. While various approaches of the literature focus on predicting battery life from early degradation signs, fewer ones focus on an online prediction of the RUL of a battery. The logical complement of the offline strategy is to design an *online* method for estimating the RUL of a battery continuously and not only once after 100 use cycles.

The *online strategy* for RUL prediction described in this chapter consists in observing each operating cycle of a battery and extracting health indicators from it. Those health indicators are used as input to an estimation model that allows an online prediction of the RUL of a battery. This means that for each battery, each use cycle can be used as input to the estimation model, and there can be as many prediction as the number of cycles in the life of a battery.

2.3.4 Online health indicators for Remaining Useful Life prediction

The features that are described in section 2.3.2 correspond to the offline strategy where 100 charge-discharge cycles are necessary to perform a prediction of the global cycle life of a battery cell.

An online prediction of the RUL of a battery requires to use different input features and to shift the approach from a cell-based prediction to a cycle-based prediction. The features that are used to make an online prediction of the RUL are not computed by comparing two cycles between them anymore, but only considering the operating data coming from a cell during one cycle. Each operating cycle is then represented by a combination of features that either come from historical data or time series of temperature. The online features for RUL prediction are the following:

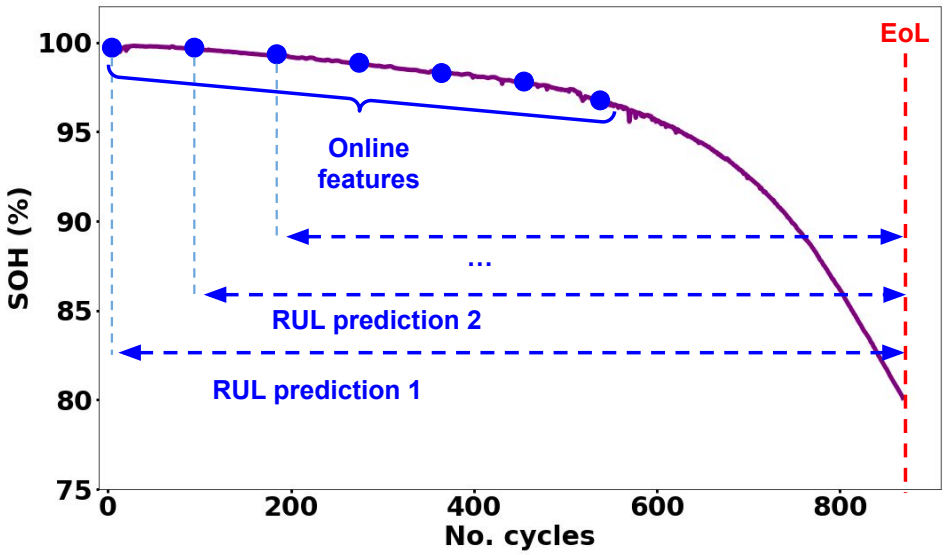

Figure 2.5: Online strategy for RUL prediction

Online features taken from historical data

- IR: The value of internal resistance during one cycle
- Q_C: The value of charge capacity
- Q_D: The value of discharge capacity
- SOH: The SOH of a cell at a given cycle
- T_C: The charge time

Online features computed from time series of temperature

- The average temperature during one cycle: $T_{Avg} = \frac{1}{N}\Sigma_{t=0}^{N} T°_t$ (for a cycle with N time steps)
- $T°_{min}$: The minimal temperature during one cycle
- $T°_{max}$: The maximal temperature during one cycle

2.4 Building training datasets for offline and online cycle life predictions

2.4.1 Offline prediction

Data structure

The dataset that is used for the offline prediction of the global cycle life of battery cells is built as shown in Figure 2.6. This dataset is used to train several algorithms

that are presented in the following sections. The basic dataset contain as many samples as there are batteries provided by the MIT dataset. Each cell is represented by a combination of offline features, computed as detailed in section 2.3.2. In its initial form, this dataset contains 124 samples and 16 features.

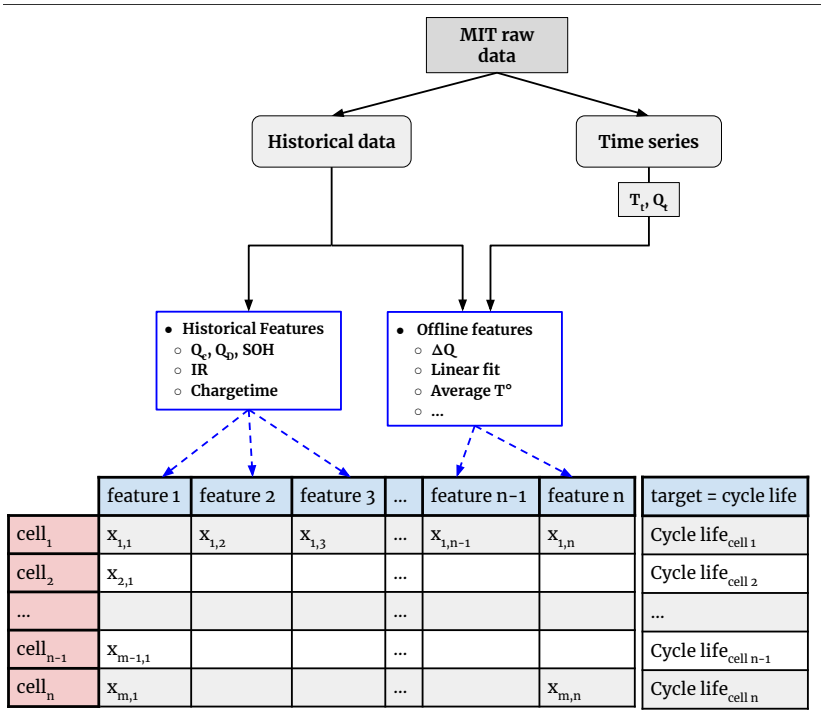

	feature 1	feature 2	feature 3	...	feature n-1	feature n	target = cycle life
$cell_1$	$x_{1,1}$	$x_{1,2}$	$x_{1,3}$	...	$x_{1,n-1}$	$x_{1,n}$	$Cycle\ life_{cell\ 1}$
$cell_2$	$x_{2,1}$			...			$Cycle\ life_{cell\ 2}$
...				...			...
$cell_{n-1}$	$x_{m-1,1}$			...			$Cycle\ life_{cell\ n-1}$
$cell_n$	$x_{m,1}$			...		$x_{m,n}$	$Cycle\ life_{cell\ n}$

Figure 2.6: Cell-based dataset for the offline prediction of the global cycle life

Dimension reduction

Some offline computed features as detailed in the previous section may contain similar or sometimes useless information. Therefore, to figure out which features are the most influential and how to combine them in a model, a common practice is to use data reduction techniques. Two simple dimension reduction techniques were used on the previously detailed dataset: outlier detection and feature selection based on unsupervised and supervised learning.

Outlier detection Outlier detection consists in detecting samples that are far away from the regions where data are most concentrated. The presence of abnormal samples could be caused by measurement errors, experimental errors, data processing, or from abnormal battery cells that could be defective. Deleting these outliers cleans the data and helps to obtain better predicting performances.

The outlier detection process applied in this approach is a tree-based algorithm for anomaly detection called the isolation forest [LTZ12].

Given a dataset X, the aim of the isolation forest is to determine which samples in X are abnormal by isolating them. The isolation forest algorithm "isolates" samples or observations by randomly and recursively splitting a dataset according to a

split value p chosen between the minimum and maximum value of a given feature. Abnormal samples require less partitioning than regular samples, and the lower the number of partitions to isolate a sample, the higher the abnormality.

From the dataset of 124 battery cells, and with a contamination rate of 5%, 7 outliers were spotted and deleted from the dataset. The 5% criterion is an empirical threshold commonly used in the literature. Figure 2.7 represents the cycle life of the 124 cells as a function of one of the computed features, with outlier samples shown in purple.

For the following treatments on dimensionality reduction and more precisely feature selection, several algorithms were applied both on the initial 124 samples dataset, and on the resulting 117 samples without outliers.

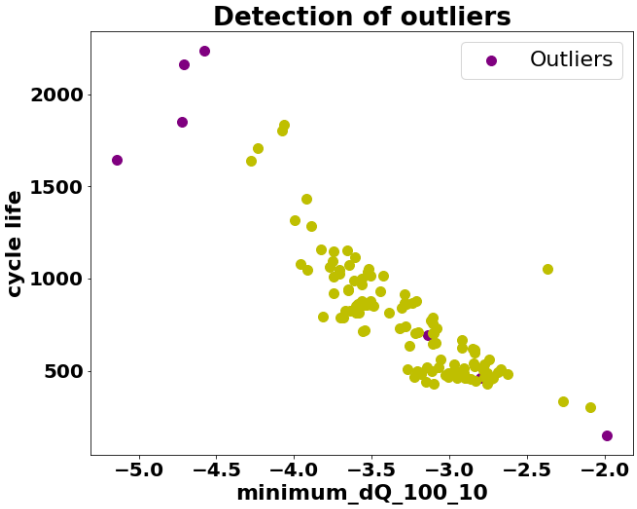

Figure 2.7: Detection of outlier samples

Feature selection Three selectors have been used in order to check which features should be kept according to different criteria. Each feature selection test applied to the initial dataset gives a new dataset to be separated into train, validation and test sets for the predictive prognostics algorithms (an extensive description of the distinction between train, validation and test ensembles is given in the coming section 2.4.3). The three selectors that were chosen are based on variance estimation for each feature (selector 1), dependency test between the features and the target (selector 2), or coefficient estimation based on the development of a theoretical machine learning model (selector 3). The theoretical model that was used for selector 3 is a linear regressor. More details about the feature selection algorithms are given in table 2.1.

The number of features kept by each selector and the name of the resulting dataset are summarised in table 2.2 and figure 2.8. Datasets D1 to D8 are used to build several independent offline predictive models whose performances are described and compared in the rest of the chapter. The number of features kept in each dataset is independent of the number of samples, but the selected features are

Table 2.1: The three feature selection approaches for offline global cycle life prediction

	Selector	Type	Description
1	Variance Threshold	Baseline approach	All features whose variance is lower than a pre-defined threshold are deleted
2	Select K Best	Dependency Tests	The dependence between the target (the global cycle life) and the input features (offline feature) is computed
3	Select from model	Estimator	A theoretical model is trained (either a NN or a linear model) to select the most useful features based on importance weight

different according to whether outlier detection is made or not. According to the accuracy of the different models built after the different datasets, the best subset of features and therefore most efficient dimension reduction technique will be highlighted.

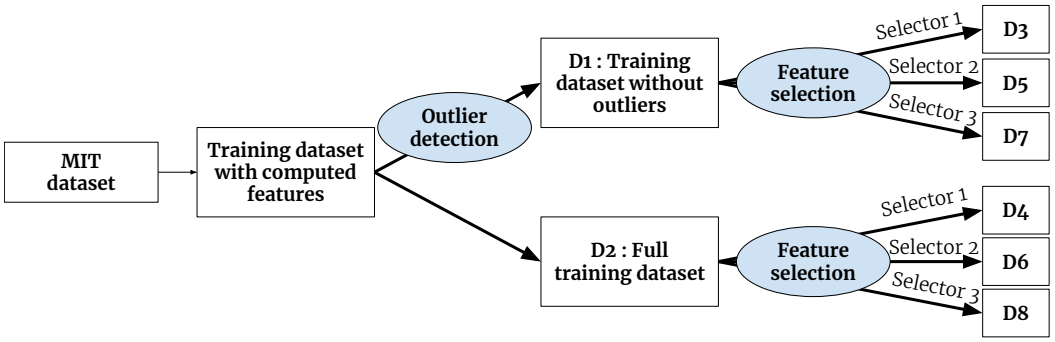

Figure 2.8: Dimension reduction process

Table 2.2: Dataset number according to the number of samples and features

Feature selector	Outlier detection (117 samples)	No outlier detection (124 samples)	# Features
Ø	D1	D2	16
Selector 1	D3	D4	6
Selector 2	D5	D6	7
Selector 3	D7	D8	3

2.4.2 Online prediction

Data structure

An online prediction of the RUL of a battery requires to use different input features and to shift the approach from a cell-based prediction to a cycle-based prediction. That is, each input sample of the online dataset corresponds to one cycle in the life of one cell. Each cycle is represented by several features described earlier in section 2.3.4.

If the model is trained offline with all available data for all cycles, the prediction can be made online starting from any cycle and providing data coming from only one cycle.

The number of samples in the resulting cycle-based dataset is given by the formula:

$$S = \sum_{i=1}^{N} k_i \tag{2.2}$$

where N is the total number of cells in the dataset and k_i is the cycle life of cell number i.

The online RUL prediction approach is based on the complete number of cycles of each battery. The resulting cycle-based dataset provides almost 100,000 training samples. The target prediction is the RUL of the cell, which can be computed for each sample following equation 2.3:

$$RUL = k_i - n \tag{2.3}$$

where k_i is the cycle life of cell number i and n is the observed current cycle of the cell.

The features that are kept in the online dataset are easily obtained and do not require any pre-process, except for SOH that is obtained by comparing the current capacity with the initial one. That means online estimation can be done at a low computational cost once the predicting model is trained offline. This final dataset will be mentioned in the rest of the chapter as *D9*.

2.4.3 Training, validation and tests ensembles

The training principle of an ANN requires to split the original dataset into three ensembles: a training set, a validation set and a test set. The training ensemble is the one used for computing the loss of the model during the weight optimisation phase as explained in section 1.1.4. The validation set is used to evaluate the capacity for generalisation of the model on unseen data during the training process. Once the model is fully developed and trained, the final performance measurements are done on the test set which is completely unknown to the model.

Random split

Random split is the simplest way to divide the data into three sets. If enough data is available, the whole ensemble is randomly separated in three. The train ensemble

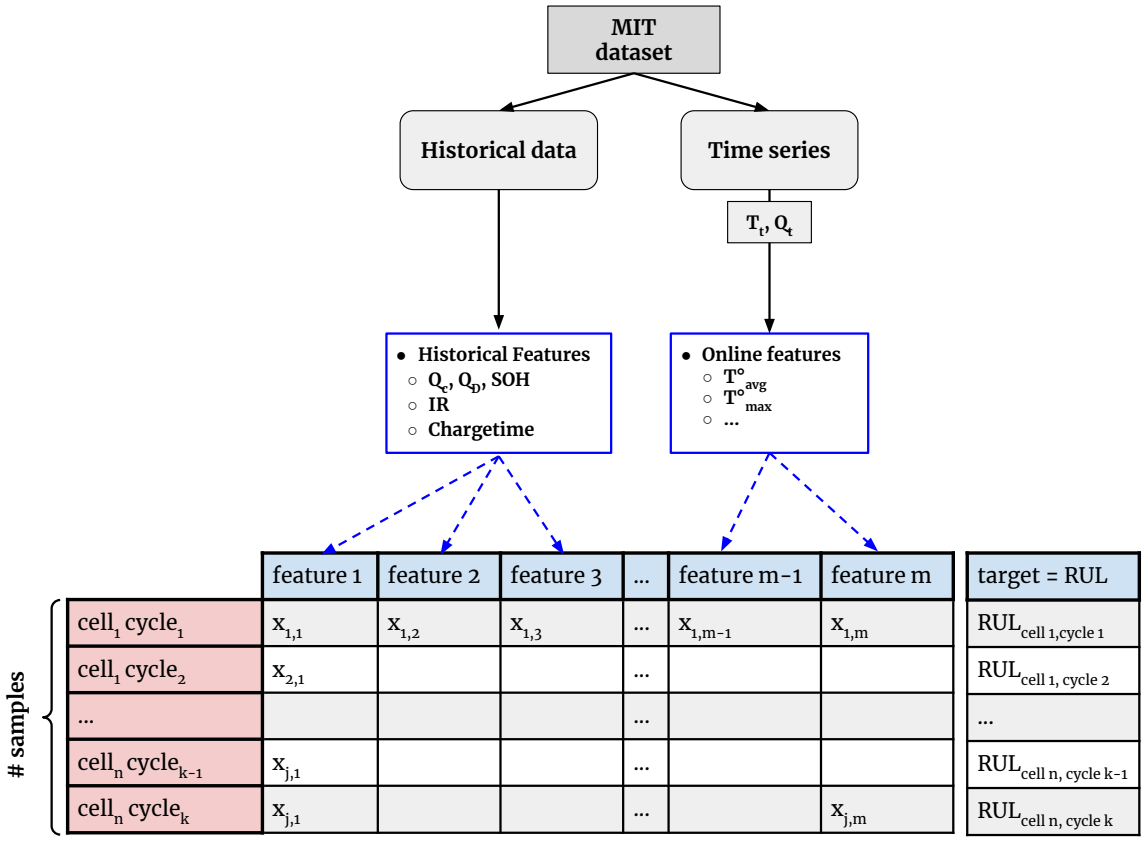

Figure 2.9: 2D dataset with scalar features

generally contains more data than the validation and test ensembles. This approach was employed in this chapter for the online prediction model. The three sets were distributed in the following proportions: first, the global dataset is divided in two, with 80% for training and 20% for validation. The test ensemble is then created by taking 20% of the train ensemble. In the end, 64 % of the data goes to the training set, 20 % to the validation set and the test set is composed of the remaining 16 %.

K-Fold cross-validation

When little data is available in the original dataset, randomly splitting it in three ensembles could lead to inhomogeneous spreads. With a K-fold approach, data is split into K partitions of equal size. For each partition i, a model is trained on the remaining K – 1 partitions, and evaluated on partition i. The final score is then the average of the K scores obtained. This method is helpful when the performance of the model shows significant variance based on the train-test split. Schematically, K-fold cross-validation looks like figure 2.10 [1]. A 10-fold cross validation process was employed for training and defining the hyper-parameters of the offline model.

[1] https://scikit-learn.org/stable/modules/cross_validation.html

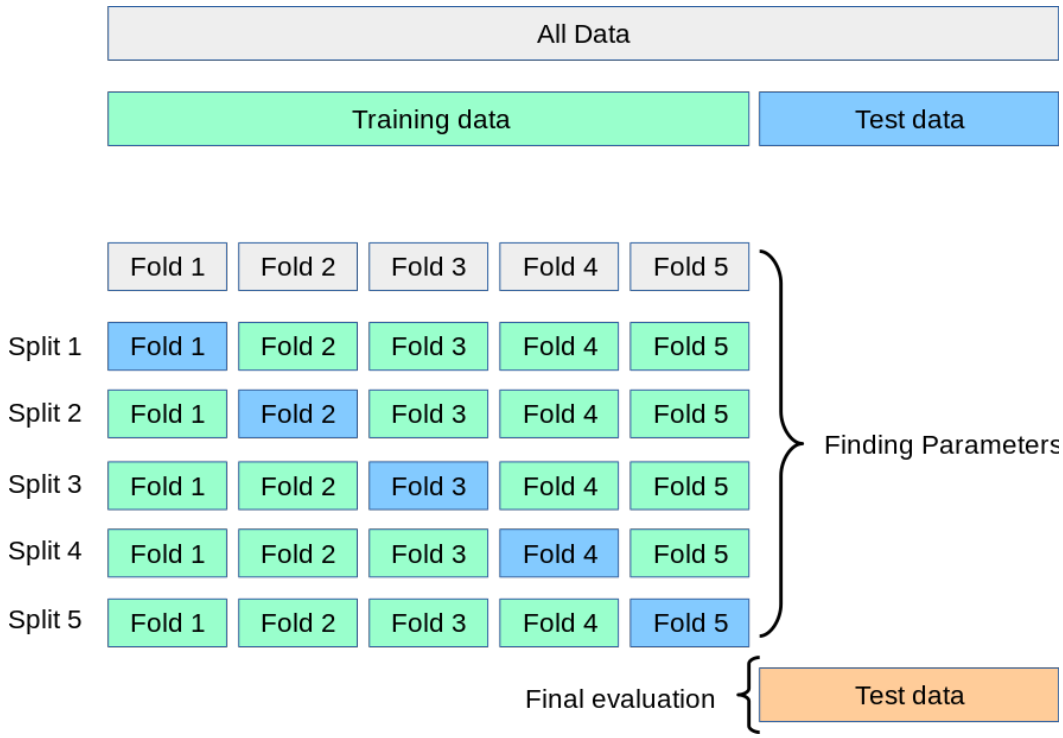

Figure 2.10: K-fold validation process (Sklearn, Cross-validation: evaluating estimator performance)

2.5 Methodology

2.5.1 Two types of predictive models

Linear model

The first and most basic model to perform the global cycle life prediction is a linear model. The linear model maps the input features $X = (X_1, X_2, \ldots, X_n)$ to the corresponding cycle life Y of a cell according to the equation:

$$f(X) = b_0 + \sum_{j=1}^{n} w_j X_j \tag{2.4}$$

The weights of the function $w = (w_1, w_2, \ldots, w_n)$ are determined through an ordinary least square regression in order to minimise the residual sum of squares between the observed cycle life of the cells in the dataset, and the cycle life predicted by the linear approximation.

This model is considered as a baseline approach and mainly aims at providing a reference for the predicting performances of the second offline predictive model, described in the following section.

Feedforward Neural Networks

Although there have been multiple models developed for the prediction of any degradation signs of Li-Ion batteries (RNN [VABA18], auto-regressive models [LXJL13],

LSTM [QLMF19] [ZRFG17], CNN [LDS18]), this contribution only explores the performances of an ANN coupled with various feature selection techniques. ANN are studied for this specific application because they can adapt to a great variety of data types and sizes. Moreover, we based our approach on a prediction of the global cycle life or of the RUL as a scalar value. No sequential prediction of the SOH or other ageing features such as the internal resistance is made. A complete overlook of the functioning of ANN is given in section 1.1.6.

Cell based ANN for global cycle life prediction The models described in this chapter are based on feed-forward neural networks (FNN) for the prediction of a single numerical value, which in the case of the offline prediction, is the global cycle life of a battery cell expressed in number of cycles.

Given that the offline dataset is quite small (124 samples for the 124 battery cells contained in the original dataset), the associated predictive model must be of a limited size in terms of number of layers and number of units per layers. A small network usually avoids over-fitting when only limited training data is available. The offline cell-based model uses a stack of fully connected layers and the last layer only contains one unit and no activation function. This is a classical setup for regression: the last layer is linear, therefore the network can predict the global cycle life in any range. A description of the architecture of the cell based ANN is given in section 2.5.2.

Cycle based ANN For the same reasons as exposed in section 2.5.1, the online prediction of the RUL is performed with an FNN, trained on dataset *D9*. *D9* has fewer features but many more samples than the cell-based dataset, which entails using a deeper model. A description of the architecture of the cycle-based ANN is given in section 2.5.2.

2.5.2 Building the predictive models

Optimisation

Offline prediction model Because there are so few samples in D1 to D8, hyper-parameter tuning of the offline ANN was carried out using a 10-fold cross validation technique. Cross validation helps reducing the biases that could be introduced by the separation of the dataset between train and test sets. Especially with small datasets, the validation dataset used to tune hyper-parameters might be unrepresentative of the training data.

When error is calculated on several partitions of the dataset, the evaluation is more reliable. After several tests with different configurations, it appeared that the best performances were obtained with a single layer perceptron, composed of 64 units and a Rectified Linear Unit activation function. The number of units in the input layer varies according to the number of features in the training dataset (cf table 2.2).

Online prediction model The dataset on which the online-prediction model is based contains many more samples, which makes the use of cross validation for hyper parameter tuning less relevant. However, as the structure of the ANN is more complex, several possibilities for the number of layers, number of units per layer and activation functions for each hidden layer have been tested. In order to test a wide range of configurations and to methodically evaluate all possible association of parameters, a Tree of Parzen Estimators algorithm is implemented. In the end, the selected model consists in a four-layer ANN. The first three layers all have 128 units and a Sigmoid activation function, and the output layer is the same as in the cell-based ANN.

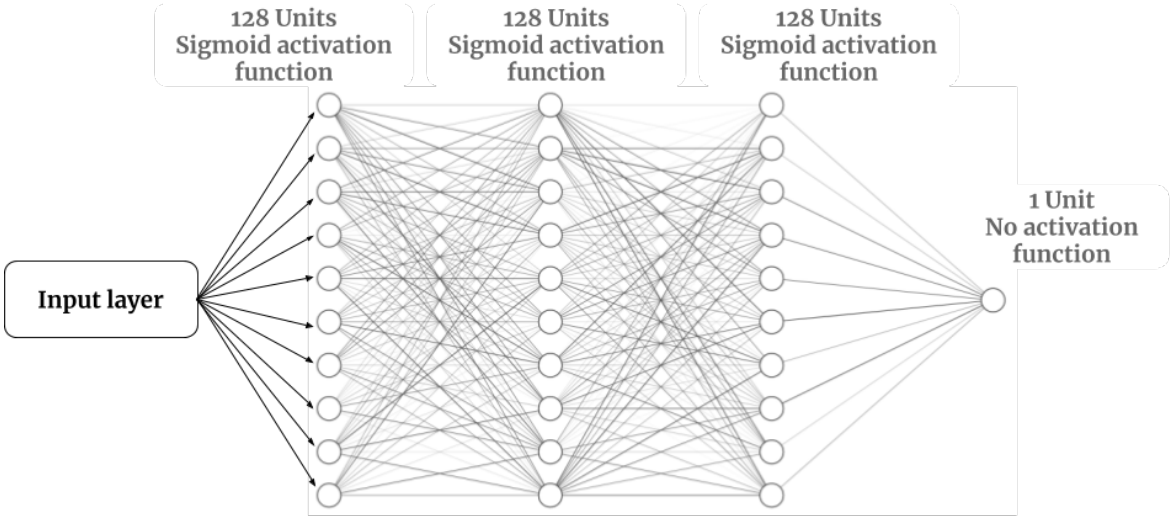

Figure 2.11: Structure of the 2^{nd} ANN

Weight initialisation

Gradient descent and backpropagation aim at modifying the weights of a neural network during training. Nevertheless, the first prediction of the network is performed with initial weights, and the efficiency of the training depends partly on the way the weights are initialised. ANN are generally initially filled with small uniform random values (very close to 0).

For both models, either offline or online, the weight initialisation of the ANN is performed following a Glorot normal initialisation, also called Xavier normal initialisation. This method draws samples from a truncated normal distribution centred on 0 with a standard deviation that depends on the number of input and output units in the weight vector, as described in equation 2.5. Each weight in a layer receives its input from all the nodes in the previous layer (or directly from the input layer itself) and sends its output to all the following nodes in the following layer. With n_j the size of a given layer, and n_{j+1} the size of the following layer, the normalised initialisation is defined by the following equation [GB16]:

$$W \sim U = \left[-\frac{\sqrt{6}}{\sqrt{n_j + n_{j+1}}}, \frac{\sqrt{6}}{\sqrt{n_j + n_{j+1}}} \right] \tag{2.5}$$

Initialising the weights following the Glorot normal initialisation allows a faster convergence.

2.5.3 Training setup

Optimisers

Offline and online models were trained using different optimisers, Root Mean Square propagation (RMSProp) and Adam.

RMSProp RMSProp is a very popular extension of the gradient descent algorithm for training ANN and was first introduced by [TH12]. RMSProp is designed to accelerate the learning process and improve the performances of the resulting model. With this optimiser, the learning rate is not considered fix during training and its value changes over time according to the value of the gradient. The aim is to put a stronger emphasis on recently computed gradients and therefore enable the optimiser to better take into account the local shape of the learning space. This optimiser was used to train the offline-prediction model.

Adam Another optimiser was employed for the training of the online RUL prediction. The online model takes more parameters as input and iterates through a lot more samples during training which makes the use of the Adam optimiser more appropriate according to [KB15].

Adam optimisation is a stochastic gradient descent method that is based on adaptive estimation of first-order and second-order moments of the gradient. The name *Adam* comes itself from adaptive moment estimation. The evolution of the learning rate is close to the one obtained with RMSProp, but it was shown that the Adam optimiser has better performances than the RMSProp algorithm regarding the correction of the bias term in a neural network and leads to better performances with large models in terms of data and parameters.

Initial learning rate

The optimisers that are implied in the learning process and that are described in the previous paragraphs are designed to modify the learning rate directly during the training process. Although there are recommended default settings for the optimisers, the initial value of the learning rate can influence the training time. Therefore, the initial learning rate can be considered as one of the hyper-parameters that are defined during hyper-parameter optimisation. The learning rate is combined with the gradient (computed from the error between the output of the network and the expected output) during the training process. The gradient is computed at each step of the training process and the parameters are modified in the opposite direction of the gradient according to the learning rate. The learning rate plays a very important role in the learning process. Defining the right initial learning rate and modifying its value during the training process should lead to a fast convergence toward the global minimum of the loss function and prevent any divergence.

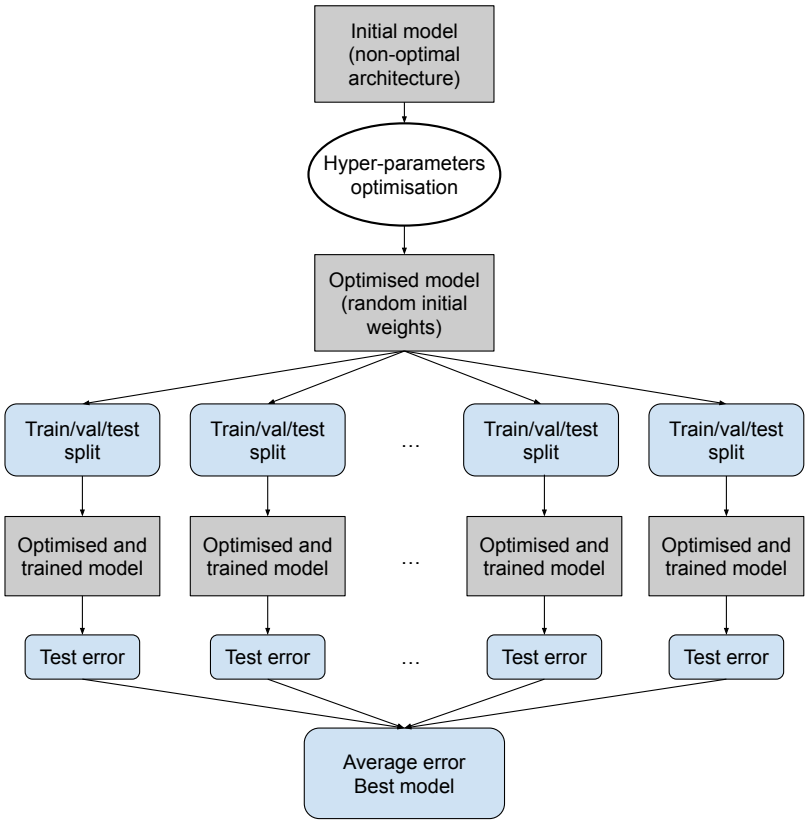

Figure 2.12: Experimental process

The offline model was trained with an initial learning rate of 0.009, and the online model was trained with an initial learning rate of 0.001.

Experimental process

Whether it is with the offline or online prediction model, the experimental process is the same. Both models are initialised with random weights as described in paragraph 2.5.2 and a baseline architecture. The first step is to perform the optimisation of all hyper-parameters in order to define the best possible architecture. Hyper parameters optimisation is described in detail in section 1.1.8. Once the architecture of the learning models is defined, all models are trained and tested on 10 different train, validation and test splits. From those ten different splits, 10 different models are obtained. The performance of the best of them is mentioned as "best", and the performances of the 10 models are also averaged.

2.5.4 Monitoring the training process

During the training phase, two different techniques were employed to avoid overfitting and determine the number of training epochs. The first one is an empirical method which consists in interpreting the evolution of the validation curve in comparison with the training curve after the training. The second one allows an online observation of the validation loss and a better monitoring of the training process.

Graphical visualisation of the validation error

A way to graphically detect overfitting consists in visualising the evolution of the train and validation curves. The validation ensemble aims at evaluating the performances of the model on unseen data at each step of the training process. Thanks to backpropagation, the weights of the model are adjusted in order to minimise the training loss, which decreases through the whole training process. If train and validation set are well defined, the validation loss should follow the same trend as training loss. However, at some point, the validation loss stops decreasing while the training loss keeps decreasing. From the moment when validation and train curve start diverging, the model is overfitting. A simple way to avoid it is to train the model, visualise train and val loss, identify the moment when overfitting appears, and re-train the model from scratch with fewer epochs. This method is mostly applied during the early stages of the development of the model in order to visualise the impact of the hyper-parameters on the performances of the model.

Early stop

Determining the length of the training process by observing the validation vs train curves requires to perform the training at least twice (once for checking the moment when overfitting starts to occur, and another time to perform the training from scratch without overfitting).

A more direct and accurate way to figure out the training length once the architecture is fixed is to observe the evolution of the validation loss in real time during the training process. The goal of the training process is to make the train and validation loss decrease, and the training process should be stopped whenever validation loss stops decreasing. The early stop process consists in computing the validation loss at each step and keeping in memory its minimum value. If after a certain number of epochs the loss value does not improve, the training process terminates and the weights of the best performing model (the ones that gave the minimum loss) are restored.

Training process

After having completed the setup of hyper-parameters for the cell-based ANN and cycle-based ANN, both models are re-trained on a training set without validation data. The initial datasets D1 to D9 are both randomly split into train and test sets. In order to obtain reliable results, the process is repeated several times. The error measure is computed as the average of all obtained measures.

During training, the backpropagation process for weight optimisation is carried out with the Adam optimiser for the cycle-based ANN and with RMSprop for the cell-based ANN. The loss is calculated with Mean Square Error and performance is judged with the Mean Absolute Error metrics [Cho15]. We used mini-batch gradient descent in order to obtain an efficient and relatively short training time combined with an accurate convergence towards the minimum loss.

2.6 Prediction results

In this section the results of the offline prediction models and the online prediction model are presented. Both cell-based ANN and cycle-based ANN are built to predict one single value of global cycle life or RUL. The output can take any possible positive value.

Global cycle life

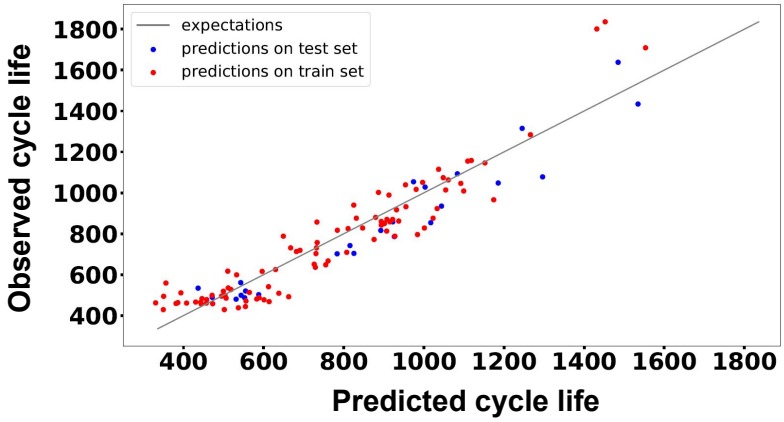

Figure 2.13: Predicting performance of a linear regression on D1

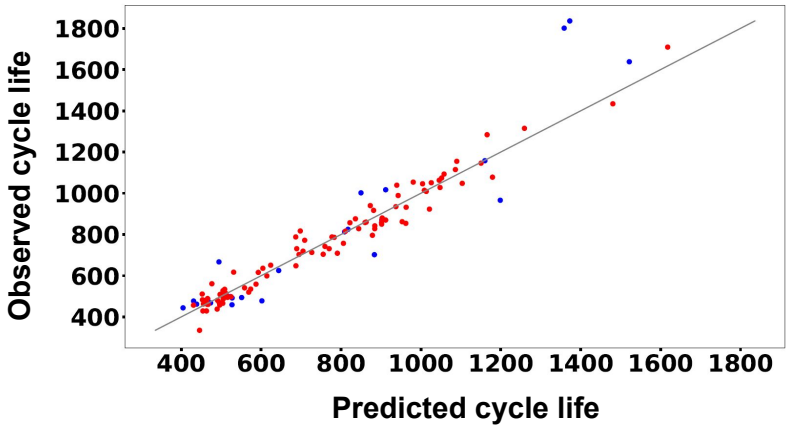

Figure 2.14: Predicting performance of the cell-based ANN on D1

Figures 2.13 to 2.15 represent the predicting performances of the different networks and of the linear regression. The predicted RUL is plotted as a function of the real RUL. Table 2.3 summarises the performances of a linear regression made on datasets D1 to D8.

To the best of its performance, linear regression reaches a 12.97 % error. This performance is reached using dataset D1, where outlier samples have been removed and all features are kept. Looking at the global performances of the regression,

Table 2.3: Linear regression performances

	RMSE	MAE	MAPE
D1	131.17	**96.43**	**12.97 %**
D2	151.86	107.61	18.23 %
D3	137.52	107.64	15.69 %
D4	**125.59**	117.92	18.47 %
D5	127.11	98.53	13.73 %
D6	159.6	117.4	18.04 %
D7	259.63	188.37	25.92 %
D8	202.25	143.35	21.24 %

Table 2.4: Cell based ANN performances

	RMSE	MAE	MAPE
D1	**115.94**	**81.91**	**10.09 %**
D2	158.13	100.3	13.25 %
D3	128.94	94.58	13.4 %
D4	128.95	94.36	13.61 %
D5	119.89	85.96	11.16 %
D6	203.21	132.59	28.37 %
D7	331.96	251.68	3.97 %
D8	1956.9	559.2	71.42 %

datasets with less features give worse prediction performances, but generally, all datasets without outliers give better MAPE performances than their equivalent datasets still containing outliers.

With the use of the cell-based ANN on D1 to D8 datasets, the predicting performances are slightly improved compared to the linear regression. The best error percentage is of 10.09 % and feature selection has the same impact on performances than with linear regression.

The results described in tables 2.3 and 2.4 show that outlier detection on the initial dataset has proved very efficient. For the linear regression, removing outliers helps improving the prediction of about 13 cycles on average, and of about 18 cycles with the cell-based ANN (we excluded the results obtained with D7 and D9 as they clearly are not reliable). On the other hand, we can observe that the best predicting performances are always obtained with D1, which means that the more features, the better the accuracy. All the features used for predictions have a share of representative data that is important to take into account.

RUL prediction

The best predicting performances are by far obtained with the cycle-based ANN. Its performances are summarised in table 2.5. The network was trained and tested 10 times with different train/validation/test splits of D9 and the MAPE obtained is of 4.49 % with a MAE of 5.84 cycles, on average over the 10 different trainings.

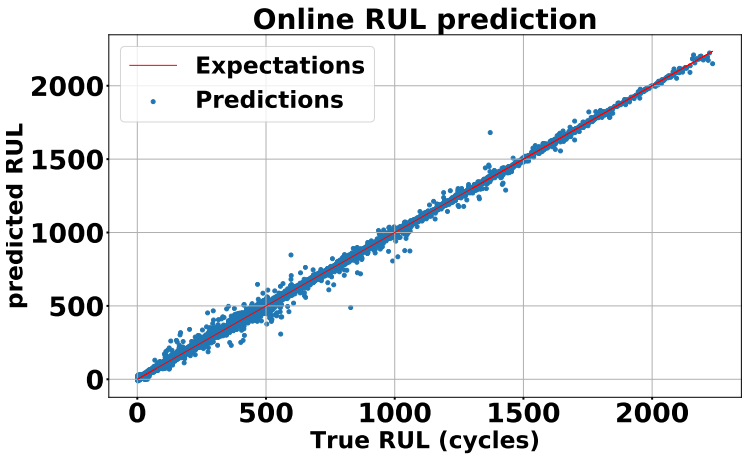

Figure 2.15: Online RUL predictions with the cycle-based ANN

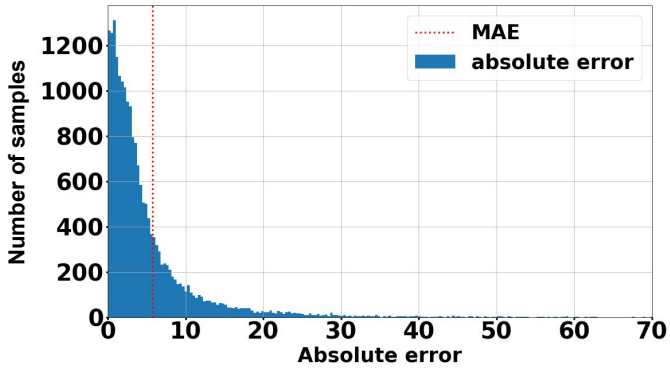

Figure 2.16: Absolute error distribution of the cycle based ANN for RUL prediction

The average standard deviation of the absolute error (σ_{AE}) is also given and is obtained by computing the standard deviation of the MAE for each distribution and averaging the obtained measures.

In table 2.5, the performances of the best model out of the 10 different distribution is also shown. This model reaches a 4.26 % MAPE and a 5.76 MAE. The standard deviation of the absolute error on this distribution is of **10.81** cycles.

Table 2.5: Cycle-based ANN performances, on average and for the best distribution

	MAE	$\overline{\sigma_{AE}}$	σ_{AE}	MAPE (%)	RMSE	NMSE
Average	5.84	12.69		4.49	13.97	$1.34*10^{-3}$
Best	**5.76**		**10.81**	**4.26**	**12.25**	**$1.03*10^{-3}$**

Table 2.6: Comparison of different approaches in the literature

	RMSE	MAE	MAPE
Cycle-based RUL prediction	**12.25**	**5.76**	**4.26 %**
LR from [SAJ+]	173	N/A	8.6 %
CNN from [HK19]	N/A	115	N/A

Comparison and interpretation

Although many papers in the literature mention their performances in the prediction of RUL, the results obtained in the scope of this contribution can only be compared with other approaches that were developed using the same dataset. For now, few papers have based any predictive model on this dataset. The original paper by [SAJ+19] proposed a feature-based approach using a linear combination of the selected features. The only other approach that was found using this dataset was proposed by a research group in an online application designed to predict the RUL and current cycle of any battery [HK19]. They have based their approach on a CNN.

Table 2.6 compares the results obtained by all existing approaches with our best performing model. Although not all the same scoring measures were used in the two previous works, the available scores show that our approach outperforms the prediction performances of the linear model developed by [SAJ+19] and CNN developed by [HK19]. These results illustrate the fact that accurate prediction through machine learning needs a great number of samples. Changing the dataset to a cycle representation of ageing factors is more efficient than building features from early cycles or from a temporal window over several consecutive cycles.

Chapter 3

SOH prediction from time series

Contents

3.1 Introduction - Predicting the SOH of Li-Ion batteries

Currently, a vast majority of approaches make use of past SOH curves only to predict future SOH curves as shown in the description of the literature in chapter 1. Among NAR models, various architectures have been employed with very good results. NAR models in the field of PHM for batteries are very efficient due to the smooth and slow degradation process of Li-Ion batteries in experimental datasets. Indeed, the storage capacity of a battery, represented by its SOH, describes a decreasing curve, with a steady plateau at the beginning and a knee point from which capacity starts dropping. However, building a PHM strategy for Li-Ion batteries should take into account all available information about the use of the battery, and especially current, voltage and temperature curves. Studying only past values of SOH can give very accurate predictions of SOH for the coming cycles only if the use of the battery stays the same. If the use conditions vary, the prediction of SOH will not be impacted consequently when using NAR models.

In chapter 2, a first model for predicting the RUL of a battery according to temperature and historical features of one cycle was described. For the contributions that are described in this chapter and the following one, the emphasis is put on exploiting the information contained in time series of current, voltage and temperature exclusively, considering that they are the simplest signals to acquire on board of an EV. The aim is to link the way a battery is used (through the aforementioned time series) to a future degradation of SOH, possibly at short and long term. This chapter describes the work that has been done concerning feature extraction and feature selection from time series of I, V and T°, and concerning SOH prediction with different types of models based on LSTM.

To begin with, a short preliminary study is delivered in order to justify the choice of working with NRX models rather than NAR models.

3.1.1 Preliminary Study

In order to study the complexity of the SOH degradation curve, we have applied a very simple model to a full SOH degradation curve. We define the Carbon Copy (CC) of the SOH curve as a signal that takes at time t the exact same value as SOH at time $t-1$ [HCR+17], as described in equation 3.1.

$$SOH_{CC}(t) = SOH(t-1) \tag{3.1}$$

Table 3.1: Prediction performances of SOH one step ahead with CC on a battery from the MIT dataset

	Carbon copy
RMSE	**5.4** * 10^{-4}
NMSE	**1.2** * 10^{-4}
MAE	**3.0** * 10^{-4}

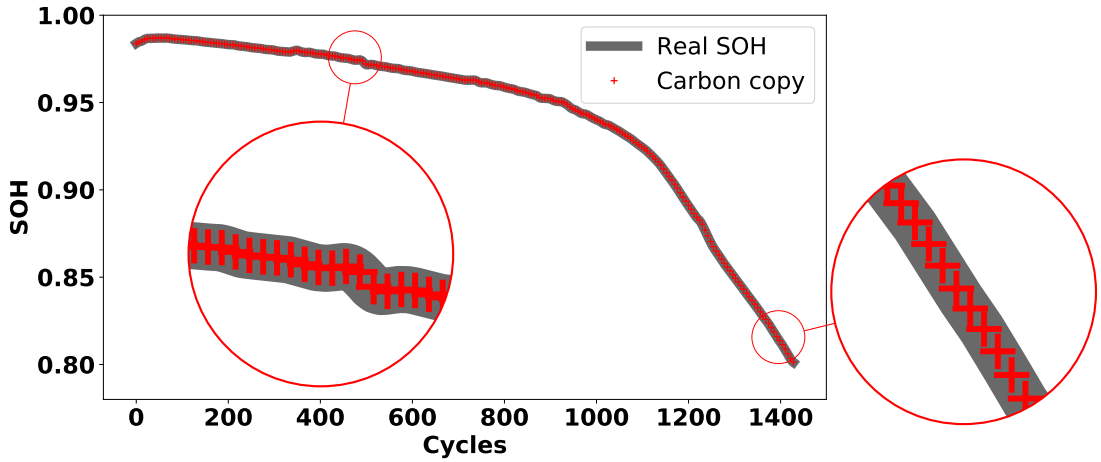

Figure 3.1: Carbon copy and LSTM prediction of the SOH

Figure 3.1 shows a comparison between the real SOH curve and its prediction through CC. The two curves are almost identical. Table 3.1 shows the predicting error of the one-cycle-ahead prediction of SOH by CC. The MAE of the CC of SOH reaches 3.10^{-4}. It appears clearly here that predicting SOH future values from the observation of past ones is quite a trivial process. From one cycle to another, the variation of SOH is very limited, and the shape of the curve facilitates short term predictions.

The very good performances are to be interpreted in a specific context. First of all, the carbon copy is built to predict the next step of a signal. For long term predictions, such simple models could not give accurate results. Moreover, the MIT dataset on which this carbon copy is based contains ageing data from 124 battery cells that were all tested with similar discharge rates. Indeed, all batteries are fully discharged with a constant current of 4A, and although the charge protocol varies from one battery to another, it remains the same for a given battery from the beginning to its end of life. This means that the degradation process is very stable, without recovery or accelerated ageing phases. In this context, the only use of past SOH values to predict future ones is very efficient, because all SOH degradation curves follow the same pattern. However, in a more realistic context, it is very unlikely that two batteries will degrade in the same way in an electric vehicle. Therefore, other parameters should be taken into account as input to a predictive model in order to build a more reliable representation of the ageing phenomenon that takes place inside a battery.

3.2 Taking advantage of operating data

3.2.1 Data analysis

In chapter 2, a detailed analysis of the data is given 2.2, with an emphasis on the differences between historical data (SOH, IR, charge time...) and local time series

(current, voltage, temperature...). Historical data and local time series do not vary on the same scale but both carry information on battery ageing.

For all following contributions, features are computed and extracted from six different temporal curves: charge current, charge voltage, charge temperature, discharge current, discharge voltage and discharge temperature, namely I_C, V_C, T_C, I_D, V_D and T_D.

In this chapter, two different methods are used for feature extraction : Auto-Encoders (AE) extraction or calculation-based extraction. The features that are either extracted by AE or by calculation are used as input to a window-based exogenous LSTM. Several models are designed according to the type of feature exctraction and selection.

The global framework of this contribution is described in figure 3.2, and the following subsections detail the different principles of time series sliding windows, feature extraction, feature selection and window LSTM for SOH prediction.

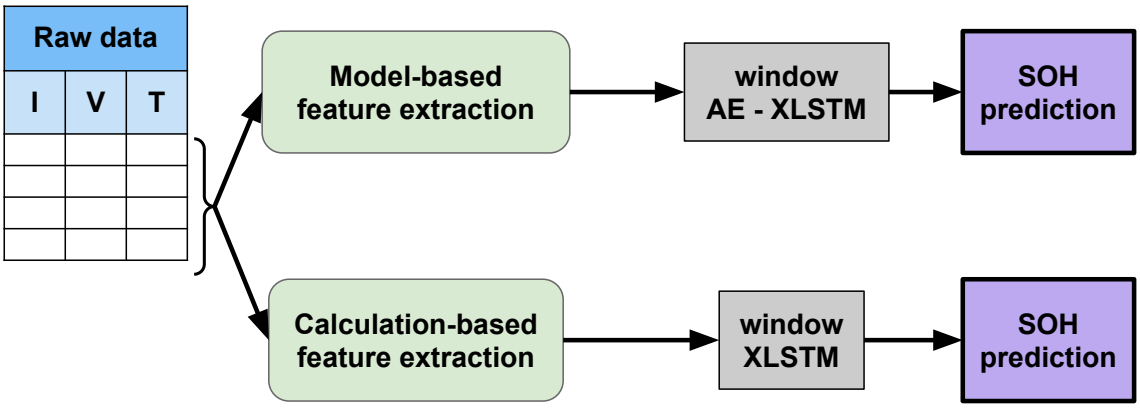

Figure 3.2: SOH point prediction based on the time series of current, voltage and temperature

3.2.2 The principle of sliding windows of time series for SOH prediction

The first contribution, detailed in chapter 2 only made use of historical data and of a limited amount of features extracted from time series of temperature. In the first contribution, those features are computed for each use cycle, and a prediction of the RUL of Li-Ion batteries is made at any moment in the life of a battery. The input of this network consists in a combination of features computed for only one cycle. Therefore, two major aspects of this approach could be completed in order to make the best possible use of all available ageing data acquired during the operation of Li-Ion batteries. The first aspect concerns the type of data that is used as input of a predictive model. Only temperature curves are used for predicting RUL, and information about the use of a battery through current and voltage data is not utilised. By combining the information contained in historical data and temperature curves with the information contained in voltage and current curves, a global representation of the ageing stage and of the operating conditions of a battery can be obtained.

The second aspect concerns the amount of data that is fed to the predictive model in order to obtain a reliable model. Predicting the RUL of a battery from only one use cycle can prove very useful, especially in the beginning of life of a battery when little ageing data is available. However, when predicting the SOH of a battery, it can prove more useful to use a larger window of operating data, for example, several consecutive cycles. The state of health of a battery does not degrade significantly from one cycle to the next, as the preliminary study 3.1.1 of this contribution has proven. That is why a larger window of operating data should be used.

In this contribution, RNN are used in order to take advantage of operating data that are time series. The aim is to observe a window of operating data and to extract features from it in order to predict the impact on the SOH several cycles ahead.

Although RNN and especially LSTM are built to learn long term dependencies in time series, small input windows are used in this contribution. Rather than giving as input the complete time series of current, voltage and temperature coming from a battery since the beginning of its life, a smaller window of several consecutive cycles is considered. This allows more flexibility in the models. There is no need to store large data sequences, and data preprocessing is made simpler because the size of the window is fixed. The window dataset that is built differs from one approach to another, as a function of the feature extraction process. Predictions can be made on a very short scale, or for longer time horizons. The training dataset for SOH prediction in this approach is built in a way that several forecasting horizons are made possible. Future values of SOH are predicted from 25 up to 400 cycles ahead according to the model. In the scope of this contribution, an online prediction of SOH is made. As described in the literature review in chapter 1, most approaches implement very short term predictions, or iterative prediction, which consists in updating the input signal given to the predictive model with the last prediction. The two different approaches described in this chapter are trained with "offline data", and prediction can be made "online", on unseen data corresponding to a window of 25 consecutive cycles at any moment of the cycle life of a battery cell.

Two different feature extraction strategies are studied in the scope of this chapter: model-based feature extraction and computational feature extraction. The aim of feature extraction in this case is to reduce the dimension of the input time series of I, V and T° in order to reduce the amount of data processed by the predictive model.

3.2.3 Model-based feature selection

Automatic feature extraction

In several approaches of the literature, Auto-Encoders Neural Networks (AENN) are used for feature extraction [DLM18, RDW+20]. These models are mainly used for their dimensional reduction [RZH+18] and augmentation [RDW+20] capabilities, but are also used for feature extraction and data fusion [DLM18]. As can be seen in Figure 3.3, they have a symmetrical structure.

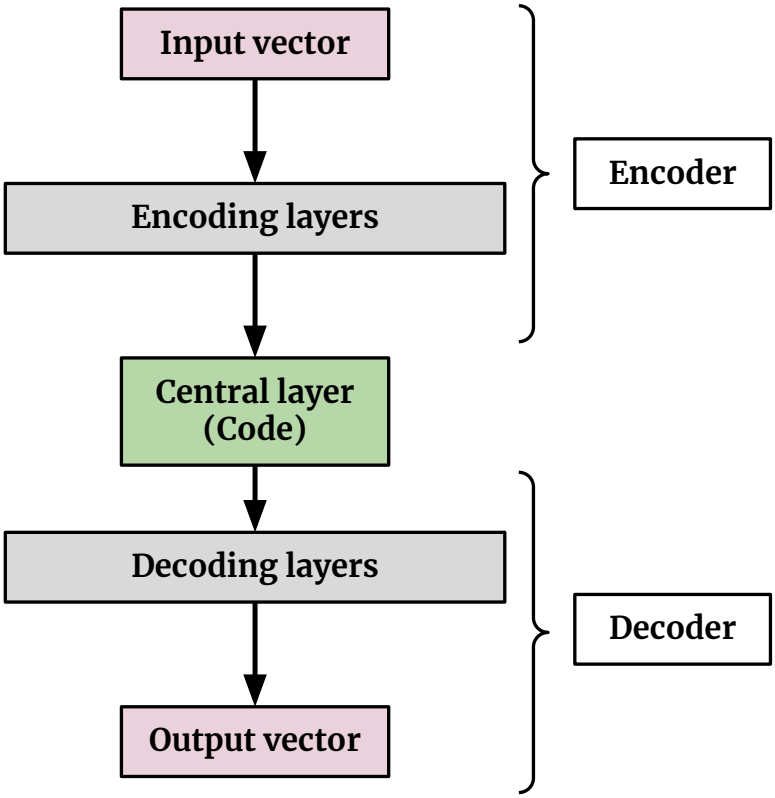

Figure 3.3: Global structure of an Auto-Encoder

The AENN is basically composed of three parts : the input layer (called encoder), the output layer (called the decoder), and the central layer which is the encoded version of the input signal. The global aim of the AENN is to reduce any input signal to a low dimensional vector (the encoded vector) and to decode it back to its original form without losing information. If the decoder is able to accurately reconstruct the input signal, then the encoded version can by used as a condensed representation of the input signal with confidence. Therefore, when AENN are used for dimension reduction, only the encoding part is kept in order to get the encoded vector as an output of the model, and not the decoded vector. Encoding and decoding layers are made of LSTM layers.

Sliding windows of raw time series

As explained in section 3.2.2, the predictive models developed for this contribution are built on small windows of time series of current, voltage and temperature. The encoded signals given by auto-encoders are used directly as input to the predictive models, which means windows of raw time series need to be constructed before being fed to the auto-encoder. The length of the input window is fixed to 25 consecutive cycles. The first window consists of the first 25 cycles of a battery, and each subsequent window moves forward one cycle. The resulting dataset consists in successive sliding and overlapping windows of raw time series that all have a

different length. The six different signals that are taken into account are time series of current, voltage and temperature during charge and discharge separately.

Selection of inputs

In order to determine which of the six studied inputs (voltage, current and temperature, during charge and discharge) have most impact on the SOH prediction, a comparison was made between different combinations of inputs. The aim of the comparison is to select the best possible combination.

Tests are made on the global architecture of the model that uses AE feature extraction. The model is referred to as AE-XLSTM and is described in detail in section 3.3.1. The AE-XLSTM outputs a SOH prediction, and different subsets of input signals are tested with the complete model. The different tested combinations of input signals are shown in table 3.2. Note that tests are not conducted on every possible combination to limit computing time. Tested combinations are those we think are the most relevant, based on expert knowledge. For each combination of signals, three different trainings are conducted, and the average performances of the resulting models on SOH prediction are shown in table 3.3. All trainings are done using the SNL dataset.

Table 3.2: Tested combinations of input features for the AE-XLSTM

Name	**Uc**	**Ud**	**Ic**	**Id**	**Tc**	**Td**
All	X	X	X	X	X	X
Charge	X		X		X	
Discharge		X		X		X
Voltage	X	X				
Current			X	X		
Temperature					X	X
Current / temp.			X	X	X	X

Table 3.3: Predicting performances of the AE-XLSTMwith the different tested combinations of input signals

Name	**MAE**	**RMSE**
All	$\mathbf{0.73.10^{-2}}$	$\mathbf{1.09.10^{-2}}$
Charge	$1.78.10^{-2}$	$2.04.10^{-2}$
Discharge	$2.75.10^{-2}$	$3.21.10^{-2}$
Voltage	$0.99.10^{-2}$	$1.32.10^{-2}$
Current	$1.44.10^{-2}$	$1.81.10^{-2}$
Temperature	$1.20.10^{-2}$	$1.43.10^{-2}$
Current / temp.	$0.99.10^{-2}$	$1.30.10^{-2}$

As can be seen in Table 3.3, the best performing combinations are the one using all available inputs and the one using only current and temperature time series. This could have been expected, as temperature reflects both the battery's environment

and use (even in a climate-controlled chamber), and the current output is directly linked to the strain put on the battery.

3.2.4 Calculation-based feature extraction

As a complement to the model-based feature extraction strategy, another and completely different method was implemented in order to extract features from the same time series of current, voltage and temperature. Rather than using a complex model like the Auto-Encoder, low computational features are defined. For each of the input signals, and at each cycle of the life of each cell, several features are computed in the temporal, statistical and spectral domain. The list of all computed features for each of the aforementioned curves is the following, separated into domains [BFF+20]. In all equations, s represents the time series signal vector, t is the corresponding time vector and N is the length of s.

Temporal domain

- **Total Energy**: $\frac{\sum_{i=1}^{N} s^2}{t_N - t_0}$
- **Area Under the Curve (AUC)**: $\sum_{i=1}^{N} (t_i - t_{i_1}) * \frac{s_i + s_{i-1}}{2}$

Statistical domain

- **Root Mean Square (RMS)**: $\sqrt{\frac{1}{N} \sum_{i=1}^{N} s_i^2}$
- **Maximum** : the largest value in s
- **Minimum** : the smallest value in s

Spectral domain

The Fast Fourier Transform of the signal is computed ($freq, fmag = fft(t, s)$), from which several features are extracted:

- **Fundamental frequency** : the lowest frequency of the Fourier transform
- $\mathbf{F_{max}}$: the maximum frequency of the Fourier transform
- **Power Bandwidth** : the width of the frequency interval in which 95% of the power of the signal is located

By reducing current, voltage and temperature time series to a combination of several scalar features, local time series can then be represented at the same scale as Historical Features (HF), in the form of Time Series Features (TSF). For example, the global evolution of the RMS value of charge current is shown in Figure 3.4, and the AUC of charge voltage is shown in Figure 3.5, both over the whole cycle life of different cells, just as HF can be represented. Every curve corresponds to a different battery, and the darker the curve, the longer the cycle life.

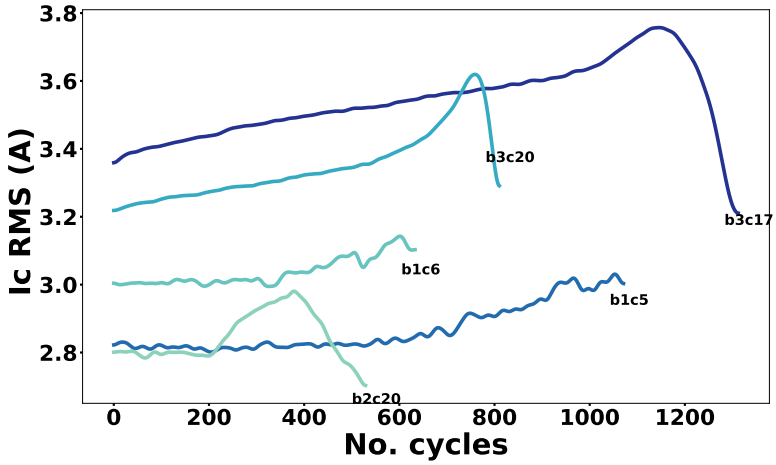

Figure 3.4: I_C RMS

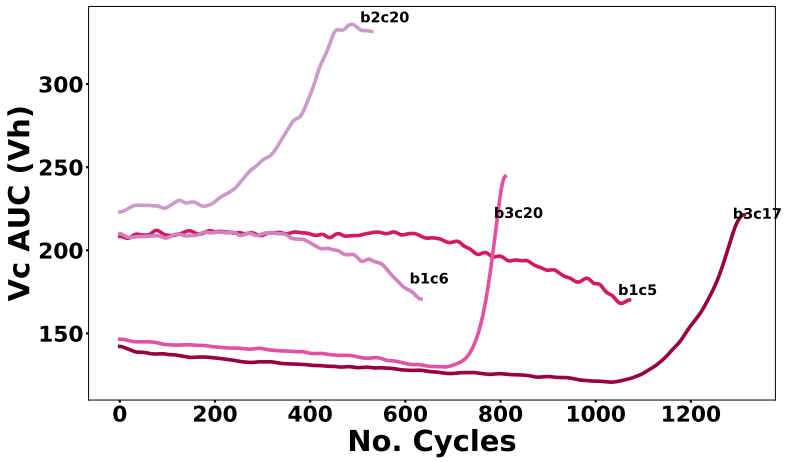

Figure 3.5: V_C Area under the curve

Sliding windows of time series features

Model-based feature extraction implies that time series are sliced in windows before being fed to the auto-encoder. With the computation-based feature extraction, features are first computed for each time series of current, voltage and temperature during charge and discharge, and the input vectors of the predictive models are sliced afterwards.

Given any cycle in the life of a battery, it can be represented by a vector that combines HF and TSF as follows:

$$x_{cycle_i} = \{x_i^1, x_i^2, \ldots, x_i^n\} \tag{3.2}$$

where n corresponds to the number of HF and TSF combined.

As the architecture involves an LSTM that is made to deal with data sequences,

the input of the network is made of several consecutive cycles, as shown in equation 3.3:

$$w_j = \{x_{cycle_i}, x_{cycle_{i+1}}, \ldots, x_{cycle_{i+m}}\} \tag{3.3}$$

where m corresponds to the size of the window.

To each input vector corresponds an output predicted value of SOH y_j. The final dataset is composed of a series of overlapping windows from several batteries. After feeding all the dataset composed of a series of Z windows $\{w_1, w_2, \ldots, w_Z\}$, the LSTM produces an output vector of SOH values $\{y_1, y_2, \ldots, y_Z\}$.

Time Series Feature selection

After computing features from the original time series, each cycle is represented by a vector of features that includes TSF and HF. The architecture that is developed here is based on supervised learning models that use as input vector this combination of TSF and HF to predict future SOH values. Machine learning models have the ability to focus on the most relevant features during the training process. However, the vector that combines HF and TSF has a very high dimensionality, because the same number of features is computed from each of the six time series described earlier. Having a great number of features increases the chances to have irrelevant or less significant information, which can be seen as noise and the training data. Including useless features in the training process of a machine learning model means that the complexity of the model is increased for nothing, with a higher training time and less reliable results. A common practice is to reduce the dimensionality of the input vector of a learning algorithm by selecting a subset of features that best represent the predicting problem. Two common methods to implement feature selection are the Filter method and the Wrapper method.

Filter methods do not depend on the learning model that is used for the prediction problem. Features are chosen independently by an evaluation criterion such as the variance, as implemented in the previous chapter.

The approach described in this contribution uses wrappers for selecting features [KH13, TNN+19, LKRH15]. Wrappers have the advantage of evaluating the relevance of features according to the performance of a predictive model. The wrapper technique for feature selection uses the training process on a given machine learning model to select the best combination of features. The aim is to obtain the best possible performances with a given algorithm by testing iteratively different subsets, numbers and combinations of features. The strategy is to start with an initial set of features and to add or remove several features after each training process in order to study the impact on the performances. This process is called the Sequential Feature Selection (SFS). The selection can either be done forwardly or backwardly. For each working direction, a global number of features should be chosen first, which is the termination criteria p.

With Forward Sequential Feature Selection (FSFS), the model is first tested with each feature isolated and the best performing feature is kept as the first feature of the subset. The model is then trained again with a set of two features composed of

the first selected one, and all the remaining ones iteratively. The process is repeated as many times as needed to reach the termination criteria p.

With Backward Sequential Feature Selection (BSFS), the model is first tested with all available features, and the less relevant feature is removed at each training round until the termination criteria is reached.

For this contribution, FSFS is done using an ANN. 10 features are kept, mainly coming from charge curves. A summary of the selected features is given in table 3.8.

3.3 Two approaches for a point prediction of SOH with XLSTMs

The working principle of a recurrent neural network and especially Long Short Term Memory is described in the first chapter, section 1.1.7. The idea is to make a better use of battery operating data than with a simple FNN by taking into account the sequential aspect in time series of I, V and T°, through the features that are extracted from them.

3.3.1 AE-XLSTM

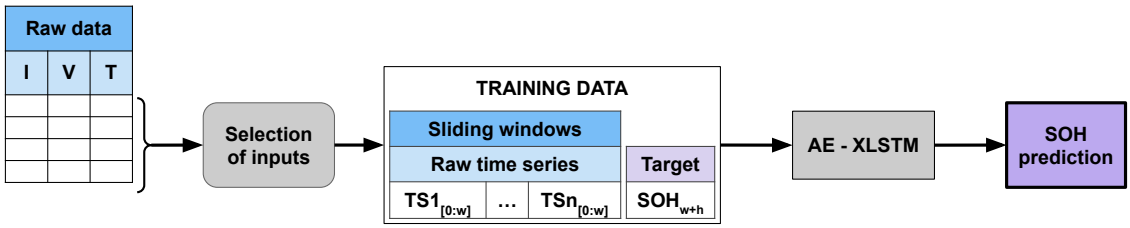

Figure 3.6: Framework of the point prediction of SOH with the AE XLSTM

The global framework of the AE-XLSTM approach is summarised in figure 3.6. Windows of raw time series are used to make an SOH prediction. Each of these time series are identically distributed to two branches. One of them is made of the encoding layers of an AE trained to reconstruct this particular time series as explained in section 3.2.3. This encoder outputs encoded versions of the various input signals. The second branch is composed of LSTM layers.

The complete architecture of the AE-XLSTM is given in figure 3.7. The AE part is made of LSTM layers of the following sizes : [256,16] (looking back at figure 3.3, those two layers belong to the encoding layers). The size of the encoded vector is equal to the size of the layer preceding the Repeat vector layer, which means 16 units. In parallel to the encoding layers, the input time series are distributed towards LSTM layers. These two LSTM layers are of size 256 and 32. The reason why time series are both distributed to an encoder and to LSTM cells is that the encoder branch acts as a static feature extraction method while the second branch

gives more context as it learns from time series of varying lengths. After concatenating the outputs of the different branches, the SOH prediction is made using LSTM layers of sizes [512,256,256,32] and a final dense layer with 1 unit and a linear activation function giving the final output.

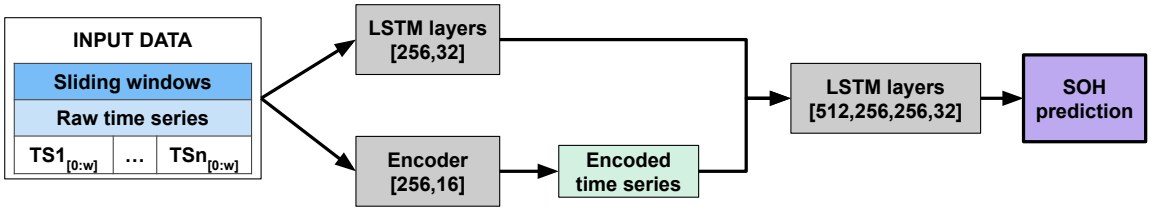

Figure 3.7: Architecture of the AE-XLSTM

Data pre-processing

Contrary to the model described in the first chapter, and to the TSF-XLSTM model, the AE-XLSTM was trained on the dataset published by the SNL. An extensive description of this dataset is given in chapter 1. In this study, only the data measured from the NMC cells tested at a 0-100% depth of discharge is used. A first look at the SNL data showed some spikes in most capacity evolution curves, which had to be dealt with using a simple function which detects these spikes and computes their new value using the neighbour ones. These spikes are artefacts indicated on the dataset download page, and are due to the transitions between normal cycling and capacity checks. After excluding these outliers, the data could be normalised before being used. Min-Max normalisation is applied to the data :

$$MinMax = \frac{data - min(data)}{max(data) - min(data)} \tag{3.4}$$

The output data ranges from 0 to 1. Note that this normalisation process is applied to the input of the models, as the target data is the SOH which is obtained by dividing the capacity values by the nominal capacity of the battery.

Training process

The training process of the model has two steps. First, each auto-encoder is trained to reconstruct a particular time series. For the six time series of charge and discharge voltage, current and temperature, six different AE were trained. Windows of 25 time series with a length of around 750 time steps each are used as input to the AE. The encoders reduce this input and condenses the information contained in each of the time series into a vector of 16 values. Then, the encoding layers of the AE are used inside the general model. The encoders' weights are frozen during the training of the final model. The loss function used in all training sessions is the Mean Square Error. The AE were trained for 500 epochs and the general model for 1000 epochs, both using an initial learning rate of $5 * 10^{-5}$ and the Adam optimiser.

The AE-XLSTM model, unlike the TSF-XLSTM model, was first trained on the SNL dataset (see description in chapter 1). In this study, only the data measured from the NMC cells tested at a 0-100% depth of discharge is used.

The batteries are split as follows : 60% for training, 20% for testing and 20% for validation, which is a common data distribution in ML problems. To evaluate the prediction performance of the proposed architecture, a dozen trainings were executed on the SNL data to evaluate the prediction performance of the model. Each training was done using a different distribution of training, validation and testing data. Tests on the MIT Life cycle dataset are also conducted subsequently in order to study the effect of different charging protocols and to compare the results with the ones of the TSF-XLSTM model. For those tests, 18 batteries are randomly picked from the three batches of the MIT dataset. The 18 batteries are split as for the SNL dataset (60% for training, 20% for validation and 20% for testing), and the whole model is trained anew with the MIT batteries (including the AE for feature extraction).

3.3.2 TSF-XLSTM

Exogenous LSTM

As explained in the preliminary study 3.1.1, the aim of this contribution is to make use of the information contained in local time series of current, voltage and temperature and not only historical data. The features that are extracted are used as input to a multi layer LSTM which has for final goal to predict the SOH multi cycles ahead. Each input sample corresponds to a window of 25 consecutive cycles, and the developed LSTM takes into account the temporal aspect of data from the beginning to the end of the window.

Exogenous bi-directional LSTM

For comparison, another type of RNN was trained with the same structure as our TSF-XLSTM, except that bi-directional LSTM (biLSTM) are used instead of unidirectional LSTM. BiLSTM imply the same data transformations as detailed earlier, but two LSTM are trained on the input sequence : the first one on the original input sequence and the second one on a reversed copy of the input sequence. The comparative architecture involving biLSTM is referred to as TSF-biXLSTM.

Data pre-processing

Each vector representing a cycle gathers features that have different ranges and units. In order to improve the efficiency of the learning process and to give the same importance to all features, a scaling step is necessary. For this work, a feature-wise maximum-absolute normalisation is applied. Each feature is scaled by its maximum absolute value and therefore is shifted to a [-1,1] range or [0,1] if all the values are positive.

Training process

The ability of an ANN to learn relationships between inputs and outputs relies on the training process during which the weights and biases of the network are updated and optimised. However, before optimising the weights and biases of the network, its global structure should be considered and treated as an upper layer of optimisation. The structure of a network is defined by a set of hyper parameters which include the number of layers and number of units per layer, but also the learning rate, momentum and dropout used in each layer. There are different approaches designed to optimise the hyper parameters of a machine learning model. The simplest way, and most exhaustive, is the Grid Search method. All possible configurations of hyper parameters are tested, which can lead to a very long process according to the complexity of the model [Bel15]. Random Search is a more efficient way to go through several possible hyper parameters configurations. Random search produces a set of trials by drawing hyper parameters from a uniform distribution space [BB12]. However, hyper parameters optimisation can be done faster and more efficiently than with grid and random search, with Bayesian optimisation [WCZ+19, SLA12]. The principle of hyper-parameters is explained in detail in section 1.1.8 of chapter 1.

Tuning hyper parameters consists in minimising a given loss function. Bayesian optimisation outperforms grid search and random search by reducing the number of iterations used to minimise this loss function. Following this procedure, the final structure of the model for SOH prediction consists of two LSTM layers with respectively 256 and 32 neurons, and a fully connected output layer of one unit with no activation function as one single value is predicted.

After defining the best set of hyper parameters for the network, the training process is completed through backpropagation, with the Adam optimiser and a learning rate of 0.01.

For each training process, the whole dataset is divided into three parts: a training, a validation and a test set. The training set contains 64% of all available data, the validation set contains 20% of all available data and the test set is composed of the remaining 16%. This distribution was also employed and explained in the previous chapter 2. The three ensembles are distinct and every single battery is used only once. The distribution of batteries between train, validation and test sets is made randomly.

Each measurement showed in the following section is computed as follows: for each model, 10 different random train/validation/test splits are made, and the model is trained from scratch 10 times. For every training process, performance measurements are done on the test set as the average of all errors on all predictions. After completing the 10 consecutive training processes, the final error measurement is computed as the average of all previously computed measures.

3.4 Prediction results

3.4.1 AE-XLSTM

Table 3.4 shows the average of the error metrics computed during twelve different training sessions. The error is computed only for 50-cycles-ahead predictions of SOH. The MAE value of around 0.01 on the SOH prediction reflects an average error of 1% on the capacity loss prediction, which is a good result knowing that the model does not use historical SOH values. As a benchmark, we study a well-performing NAR model based on LSTM layers and historical SOH values only. A window of previously measured SOH values is used as an input to predict a future value of SOH.

Table 3.4: Comparison of predicting performances between the AE-XLSTMand a NAR LSTM on the SNL dataset

	Usage (AE-XLSTM)	History (LSTM)
MAE (10^{-2})	**1.03**	**0.96**
σ_{AE} ($*10^{-2}$)	**0.93**	3.00
RMSE (10^{-2})	**1.32**	**1.24**
MAPE	1.32	1.29
NMSE	0.18	**0.14**

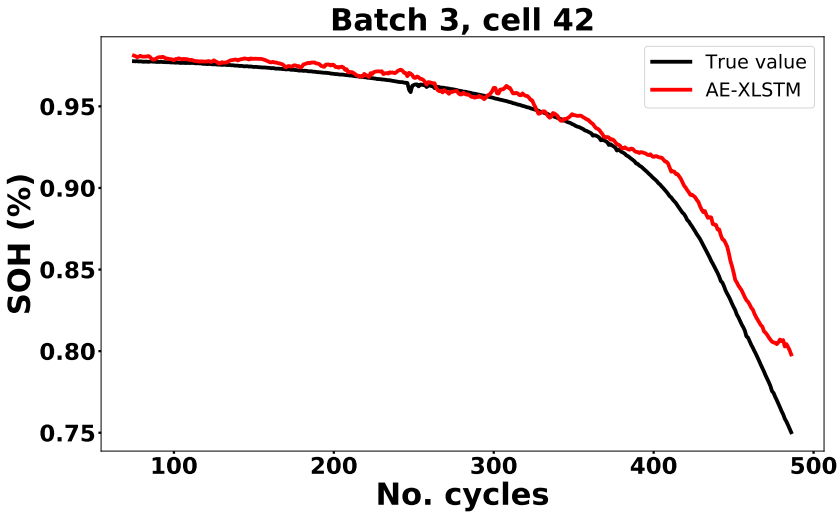

Figure 3.8: Real vs 50-cycles-ahead predicted SOH for battery b3c42 with the AE-XLSTM

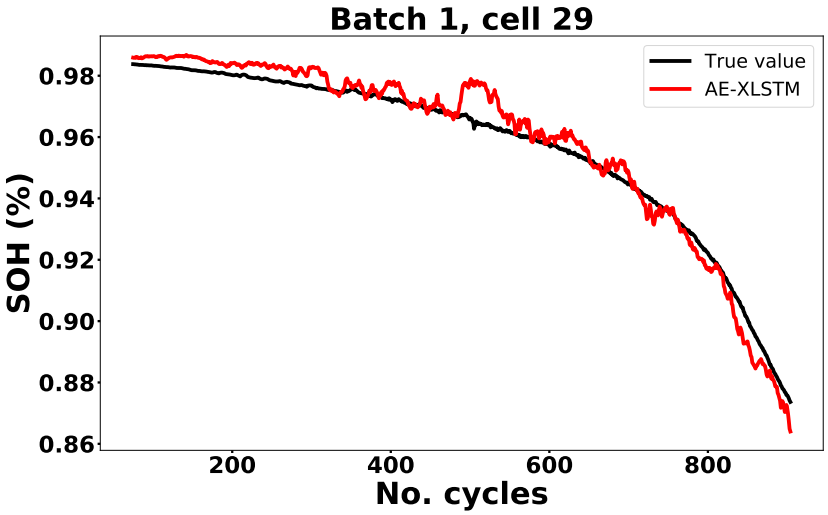

Figure 3.9: Real vs 50-cycles-ahead predicted SOH for battery b1c29 with the AE-XLSTM

3.4.2 TSF-XLSTM

Predicting performances

This section investigates the predicting performances of our different models, for SOH forecasting. Our SOH model has the ability to forecast SOH multiple steps ahead, and observations on the quality of the model are made as a function of the number of steps ahead. The size of the input window stays the same for all tests and was fixed at 25 consecutive cycles. For both models, all error metrics will be shown. For SOH forecasting, the output value is scaled with the maximum-absolute method so it varies between 0 and 1 (all values are positive). MAE and RMSE measurements will then refer to signals that have an amplitude of 1. Different models are trained according to the input data.

TSF-XLSTM Table 3.5 shows the predicting performances of our TSF-XLSTM model, on MIT batteries, in the case of multi-step-ahead predictions. The size of the input window is of 25 cycles, and the SOH prediction can be made from 25 cycles ahead up to 400 cycles ahead. For all cases, two metrics are given: the average prediction error and the minimum prediction error. As explained in Section 3.3.2, different successive trainings are made on different train/validation/test splits, and the average error in computed as the average result of all trainings. The prediction error of the best performing model is also shown for each predicting horizon.

As expected, the best performances are obtained for short term predictions, 25 cycles ahead. As the forecasting horizon grows longer, the predicting performances degrade. The best of our model reaches a 1.14% RMSPE, for a 25 cycles ahead prediction. Nevertheless, with very long term predictions, up to 400 cycles ahead, the RMSPE stays as low as 3.14%. In Figure 3.12, the average and minimum MAE and RMSE of each model, corresponding to each predicting horizon, are plotted. The curves show that the prediction error increases almost linearly according to

the number of cycles ahead. The structure of the model does not vary from one predicting horizon to the other, which means that the architecture is quite robust.

In Figures 3.10 and 3.11, a comparison is made between the real SOH curve and the predicted one, for 25 cycles ahead predictions and 300 cycles ahead predictions. Those predicted curves correspond to predictions that were made with the best performing model, trained to predict 25 or 300 cycles ahead. The batteries chosen to compare real SOH and predicted SOH were picked in the test set of the corresponding model. In both cases, the predicted curves are very close to the real SOH curve.

Given the results presented in Table 3.5, our models stay on average between $1.1.10^{-2}$ (25 cycles ahead) and $2.4.10^{-2}$ (400 cycles ahead) for the MAE, and the standard deviation of the MAE stays below 2.10^{-2} (for 400 cycles ahead). Considering that those measures refer to signals that have a [0,1] range, we can conclude that our TSF-XLSTM models give accurate predictions, at both short term and long term, with a high reliability.

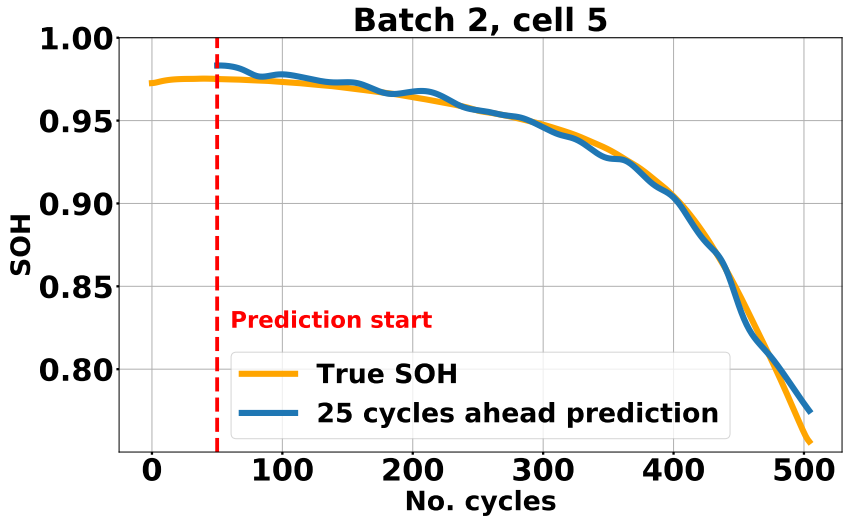

Figure 3.10: Real vs 25-cycles ahead predicted SOH for battery b2c5

TSF-biXLSTM The results obtained with the TSF-biXLSTM are summarised in table 3.6. By comparing tables 3.5 and 3.6, several observations can be made. The performances of the TSF-XLSTM and TSF-biXLSTM are very close. Regarding the MAE of the best models, the TSF-XLSTM has slightly better performances for short term predicting horizons (25 and 50 cycles ahead), and slightly lower performances for long term predicting horizons (350 and 400 cycles ahead). On average however, the MAE TSF-XLSTM has a lower standard deviation.

3.4.3 Comparison and interpretation

There have not been many approaches in the literature dealing with the SOH prediction from the MIT dataset. We compared the predicting performances of the three described models, namely the AE-XLSTM model, the TSF-XLSTM model and the TSF-biXLSTM model.

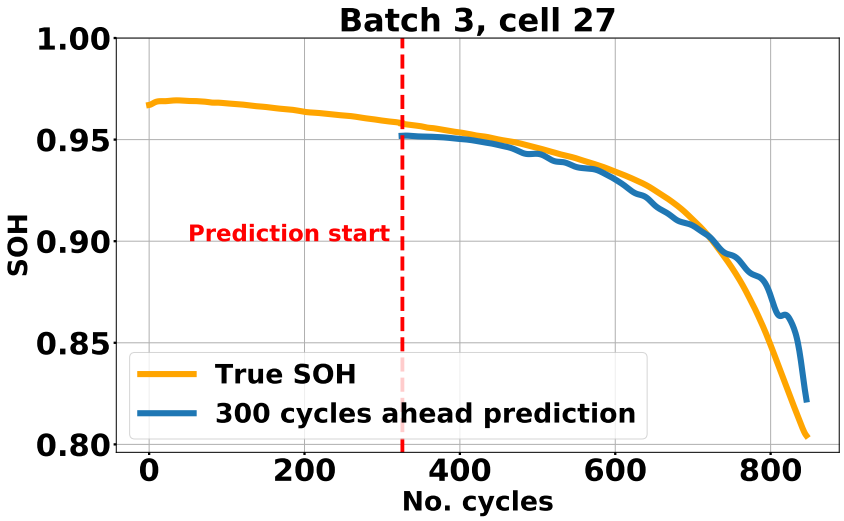

Figure 3.11: Real vs 300-cycles ahead predicted SOH for battery b3c27

Table 3.5: XLSTM performances for SOH prediction on MIT batteries

Metric	Type	Prediction horizon (No. of cycles ahead) 25	50	100	150	200	250	300	350	400
MAE ($*10^{-2}$)	Average	1.1	1.2	1.4	1.3	1.9	1.6	2.0	2.1	2.4
	Best	**0.8**	1.1	1.2	0.9	1.5	1.1	1.5	1.6	2.0
σ_{AE} ($*10^{-2}$)	Average	1.1	1.5	1.6	1.9	2.1	1.9	2.3	2.4	2.8
	Best	**0.7**	1.2	1.1	1.0	1.7	1.5	1.4	1.9	2.0
RMSE ($*10^{-2}$)	Average	1.5	1.9	2.1	2.3	3.0	2.5	3.0	3.2	3.7
	Best	**1.0**	1.6	1.6	1.4	2.2	1.9	2.1	2.5	2.8
RMSPE (%)	Average	1.7	2.2	2.4	2.7	3.3	2.8	3.5	3.7	4.2
	Best	**1.1**	1.8	1.8	1.6	2.6	2.1	2.5	2.9	3.1
NMSE ($*10^{-1}$)	Average	1.2	1.8	2.1	2.5	3.6	2.7	3.9	4.3	5.7
	Best	**0.5**	1.2	1.2	0.8	2.2	1.4	1.7	2.7	3.1

We can see from Table 3.7 that the TSF-XLSTM model outperforms the AE-XLSTM model. For a 50-cycles-ahead SOH prediction, the TSF-XLSTM shows a RMSE of $1.6 * 10^{-2}$ compared to $2.8 * 10^{-2}$ for the AE-XLSTM model.

The TSF-XLSTM is less complex as it only uses LSTM in the model itself. The data preprocessing requires low computational abilities as very simple features are extracted from time series.

3.5 Conclusion on point prediction of SOH

This chapter focuses on the prediction of future SOH values of Li-Ion batteries, based on the study of two major datasets published by the MIT and the Sandia National Laboratory. We propose here several feature extraction strategies coupled with feature selection in order to use time series of current, voltage and temperature

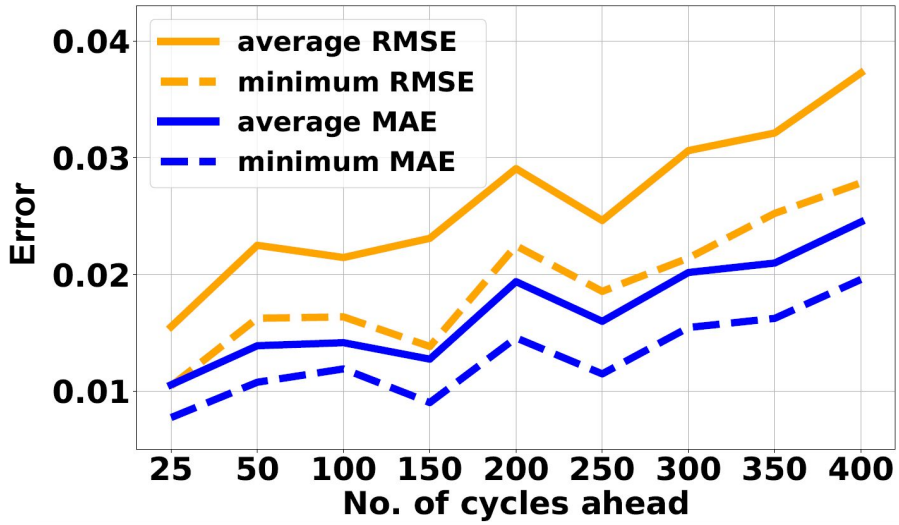

Figure 3.12: Evolution of the average and minimum MAE and RMSE according to the number of cycles ahead

Table 3.6: TSF-biXLSTM performances for SOH prediction on MIT batteries

Metric	Type	Prediction horizon (No. of cycles ahead) 25	50	100	150	200	250	300	350	400
MAE ($*10^{-2}$)	Average	1.0	1.3	1.4	1.2	1.8	1.5	2.0	2.0	2.1
	Best	**0.8**	1.1	1.1	0.9	1.4	1.1	1.5	1.5	1.7
σ_{AE} ($*10^{-2}$)	Average	1.3	1.6	2.0	2.1	2.4	2.1	2.3	2.5	2.5
	Best	**0.7**	1.2	1.0	1.3	1.8	1.4	1.4	1.9	2.1
RMSE ($*10^{-2}$)	Average	1.6	2.1	2.4	2.4	3.1	2.6	3.0	3.2	3.3
	Best	**1.1**	1.7	1.5	1.6	2.3	1.8	2.1	2.4	2.7
RMSPE (%)	Average	1.8	2.3	2.8	2.9	3.6	3.0	3.5	3.7	3.8
	Best	**1.2**	1.8	1.7	1.9	2.7	2.1	2.5	2.8	3.2
NMSE ($*10^{-1}$)	Average	1.3	2.0	3.1	2.9	4.5	3.1	3.9	4.5	4.4
	Best	**0.5**	1.3	1.1	1.2	2.2	1.3	1.7	2.3	3.0

Table 3.7: Comparison of SOH prediction performances, 50 cycles ahead, on MIT batteries

	MAE ($*10^{-2}$)	$\overline{\sigma_{AE}}$ ($*10^{-2}$)	RMSE ($*10^{-2}$)	NMSE ($*10^{-1}$)
TSF-XLSTM	**1.1**	**1.2**	**1.6**	**0.1**
TSF-biXLSTM	1.1	**1.2**	1.7	0.1
AE-XLSTM	2.4	1.2	2.8	8.1

as input to a SOH predicting model. These features, used in combination with LSTMs can lead to accurate and long term prediction of future values of SOH from an input window of 25 cycles.

There are very few approaches in the literature that have based their study on the MIT dataset, and none of them were based on NRX models. Considering that

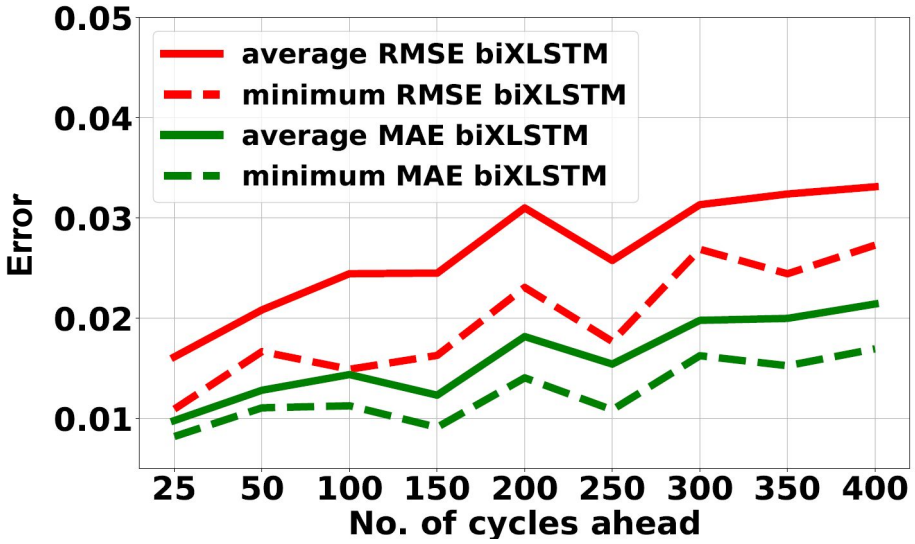

Figure 3.13: Evolution of the average and minimum MAE and RMSE of the bi-directional XLSTM according to the number of cycles ahead

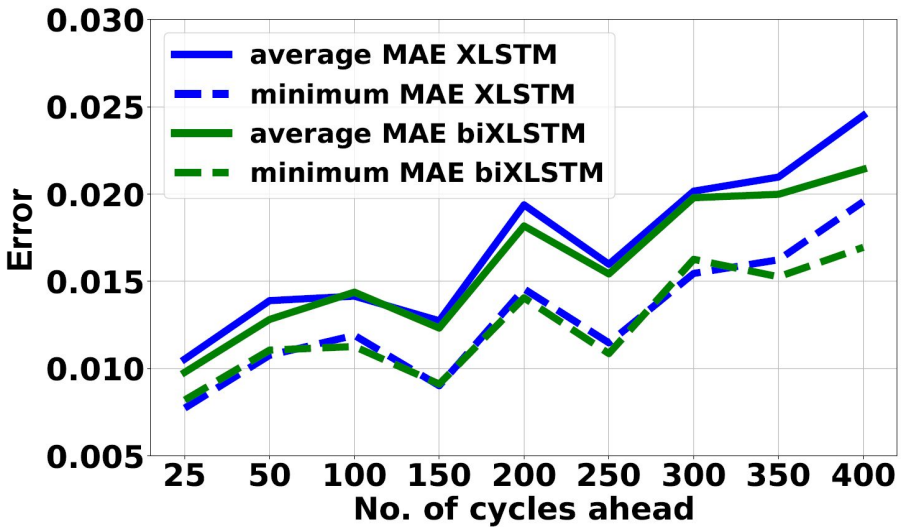

Figure 3.14: Comparison of the MAE of the TSF-XLSTM and the TSF-biXLSTM models according to the number of cycles ahead

the NRX architectures described in this chapter are based on the use of TSF or encoded time series only and not past SOH values, it is hard to compare our TSF-XLSTM or AE-XLSTM models to any NAR models. A generic comparison between our two models and two NAR models developed by Qu *et al.* [QLMF19] and 2021 by Liu *et al.* [LSOW21] is given in table 3.9.

The major difference in the models described in this chapter is that all available data from several batteries are used to train the model. Training data can be considered as offline data, used to learn degradation patterns. Once the model is trained, predictions can be made online from any input window of the test battery. This means that it is not necessary to isolate the first part of the data from a given battery and use it in model learning to predict future SOH values. In [QLMF19], at

least 30% of the data is used for incremental learning, and it can go up to 70% of the SOH curve. That means only the last 50 cycles can be predicted by the model. In [LSOW21], 50% of the SOH data is also used for training. Moreover, in both [QLMF19] and [LSOW21], predictions are made iteratively. We use input windows of 25 cycles, which represents on average around 3% of the lifetime of the batteries that are tested in the MIT dataset.

The very good results obtained by NAR models depend on the nature of the input data. Experimental ageing tests of Li-Ion batteries lead to a steady degradation trend, but one that does not represent the real use of an electric vehicle. By using TSF in a model, the SOH prediction is slightly less accurate, but more flexible and adaptable to different use cases.

Although we do not reach the same accuracy as NAR models, our TSF-XLSTM model has promising performances and could adapt to more realistic situations. It is still complicated to provide quantitative arguments to support this hypothesis, but the principle of NAR models for SOH prediction implicitly requires that the use conditions of a battery remain the same throughout its entire life. By observing operating data, our model could take into account any change in the use environment of the vehicle (through external temperature), or any change in the driving profile of a user (through current and voltage).

Table 3.8: Computed and selected features for the TSF-XLSTMand TSF-biXLSTM

Domain	Feature	Current		Voltage		Temperature	
		Charge	Discharge	Charge	Discharge	Charge	Discharge
Temporal	Total Energy	√	√				
	Area Under the Curve			√	√		
Statistical	Mean				√		
	Root Mean Square						
	Max					√	√
	Min						
Spectral	Fundamental freq.						
	F_{max}					√	
	Power Bandwidth				√		√

Table 3.9: Architecture comparison

	TSF-XLSTM	**AE-XLSTM**	**PA-LSTM** [QLMF19]	**LSTM + GPR + IMF** [LSOW21]
Used features	Time series (V, I, T°)	Time series (V, I, T°)	SOH	SOH
Proposed architecture	-Feature extraction -TSF windows -LSTM	-AE feature extraction -Encoded windows -LSTM	-EMD -Particle Swarm -Attention mechanisms -LSTM	-EMD -GPR -LSTM
Type of model	-NRX -Generic model for all cells	-NRX -Generic model for all cells	-NAR -One model per cell	-NAR -One model per cell
Training data	All available data	All available data	At least 30% of SOH for each cell	50% of SOH for each cell
Type of prediction	-Multi cycles ahead -Online	-Multi cycles ahead -Online	-One cycle ahead -Iterative	-Multi cycles ahead -Iterative

Chapter 4

Seq2Seq for SOH prediction

Contents

4.1 Introduction - From a point prediction to a full sequence prediction

The first two contributions of this thesis take advantage of both historical data and time series. The prediction of RUL through the use of a cycle based ANN makes a powerful use of historical and temperature data, and the prediction of SOH with window based exogenous LSTM proves that time series of current, voltage and temperature give an accurate image of the ageing stage of a battery, both at a short and long term. In order to go further in the use of time series for the prediction of SOH, another type of model is described in this chapter. By structuring data differently than with the previous window-based approach, and by increasing the complexity of the predictive model, a different type of SOH prediction can be made. With the previous TSF-XLSTM, TSF-biXLSTM and AE-XLSTM models, a fixed window of features was used as input to predict a single future point of SOH. The SOH prediction could either be made at short or long term, giving a good estimation of the effect of the use conditions of a battery on its ageing at a precise moment in the future. However, point predictions fail to show when exactly a failure could occur in the life of a battery. What is interesting is to be able to link a very short input feature window with a wider output window of SOH in order to spot the exact moment when the SOH is most going to be affected, and to have a direct and long term view of the ageing process of a battery.

This contribution was inspired by the work of Li *et al.* from the university of Aachen [LSD+21], which is described in detail in chapter 1. The idea is to adapt their NAR model to our NRX approach. Our goal is to be able to predict the SOH of a battery until its EoL by observing a limited window of exogenous input features.

In this chapter, a quick description of the principle of sequence prediction is given, and then the work that was done concerning this contribution is described, with a detailed presentation of the data structure and model architecture, followed by a presentation of the prediction results.

4.2 Seq2Seq for SOH prediction

4.2.1 The principle of sequence prediction

All the sequences that are dealt with in the scope of this research work are time series. With the first two contributions described in the previous chapters, the information contained in time series is exploited to make point predictions, either of the RUL of the battery or of its SOH at different horizons. In the first contribution, a point prediction of the RUL is made from single points of historical data and temperature during one cycle. Although several features are used, the prediction is made from one single time step to one single value. This is referred to as a "one to one" prediction, depicted in figure 4.1. In the second contribution, a point prediction of SOH is made from windows of operating data. Several features are used in one window, which consists in a sequence of 25 consecutive cycles. The model outputs one single value of SOH, therefore a "many to one" prediction is made, as

depicted in figure 4.2. The contribution described in this chapter consists in designing a "many to many" predictive model in order to predict a full SOH sequence from a fixed window of operating data, as shown in figure 4.3. The following sections describe the fundamentals of sequence prediction.

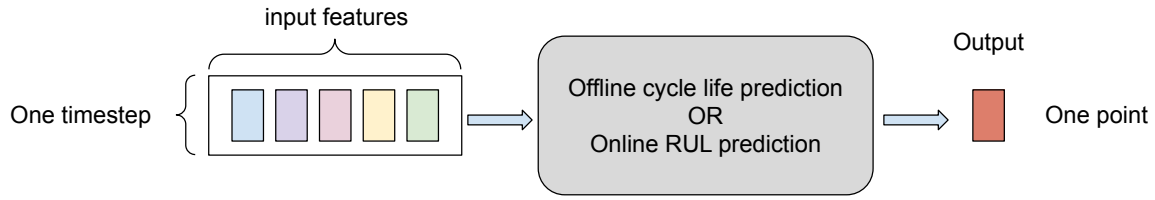

Figure 4.1: One to one prediction

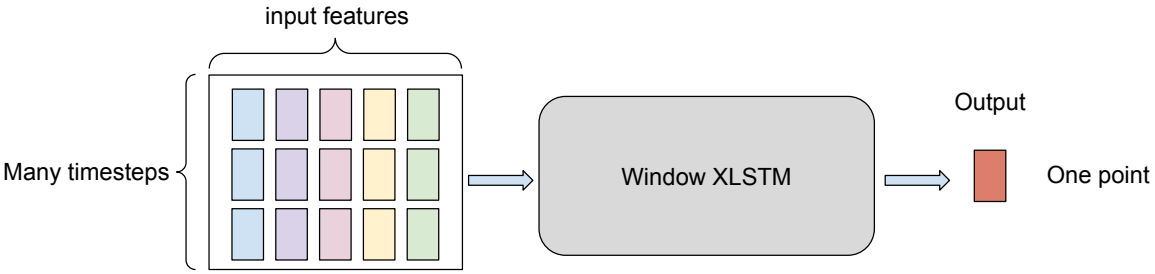

Figure 4.2: Many to one prediction

Figure 4.3: Many to many prediction

Sequence to Sequence learning

Time series are a specific type of sequence data. Throughout the literature, a tremendous amount of research topics concern word or letter sequences, and refer to the field of Natural Language Processing (NLP).

Sutskever *et al.* have described the principle of sequence to sequence learning with ANN. In [SVL14], the principle of the sequence to sequence model is described, and consists in translating an input to an output by overcoming the limitations of traditional DNN (an ANN with multiple hidden layers). Indeed, DNN can only be applied to problems where inputs and targets can sensibly be encoded with vectors of fixed dimensionality. In the case where the length of the sequence is not

known in advance, DNN can't be efficient. Therefore, they describe a novel way of mapping sequences that have different lengths, and lengths that are not linked with any simple monotonic relationship. LSTM are used as encoder and decoder as they have the ability to learn long term dependencies. It means that two different LSTM are used to complete those two functions, and they make use of deep LSTM. Their last contribution consists in reversing the order of the input sequence. This way, the distance between one word and its translation is reduced.

4.3 Data structure for a sequence to sequence approach

4.3.1 Growing window to sequence

The approach described by [LSD+21] is based on an NAR model that uses historical data of SOH to predict the future evolution of SOH. As the battery ages, more and more historical data become available and can therefore be used as input to the predictive model. Here, the goal of the sequence to sequence approach is to be able to predict the entire SOH degradation curve until EoL at once, using all the available historical data at the moment when the prediction is made. In other terms, throughout the life of the battery, the input vector (composed of historical SOH data) grows and the output predicted sequence shrinks.

First predictions should be longer, and are made from very short sequences. As more and more historical data become available, shorter predictions are made from longer input sequences. The accuracy of the model should then be improved over time. Figure 4.4 illustrates the evolution of the input vs output vector of a Seq2Seq model as a function of the moment when the prediction is made. The shorter the RUL of the battery, the longer the input vector and the longer the predicted output. In figure 4.5, a detailed version shows how data can be sampled inside a growing window in order to reduce the amount of processed data.

4.3.2 Sliding window to sequence

The approach described in this chapter consists in adapting the Seq2seq model earlier described and developed by [LSD+21]. In their framework, only historical data of SOH are exploited to predict the future degradation trend of the battery. The aim of this contribution is to shift this NAR Seq2Seq model to an NRX Seq2Seq model that performs well with a fixed amount of data as input. In comparison with the NAR approach, this contribution uses more features as input to the model in order to predict the same signal, which is the entire SOH degradation trend until EoL. In order to reduce the amount of information to be processed by the model, the size of the input window is fixed which means that no matter the moment when the prediction is made, the model will have access to the same amount of data, coming from the last operating cycles. In this way, it is made clearer which part in the life of a battery has the biggest impact on its degradation trend. The principle of sliding windows with a fixed size to predict windows of variable size is depicted in figure 4.6.

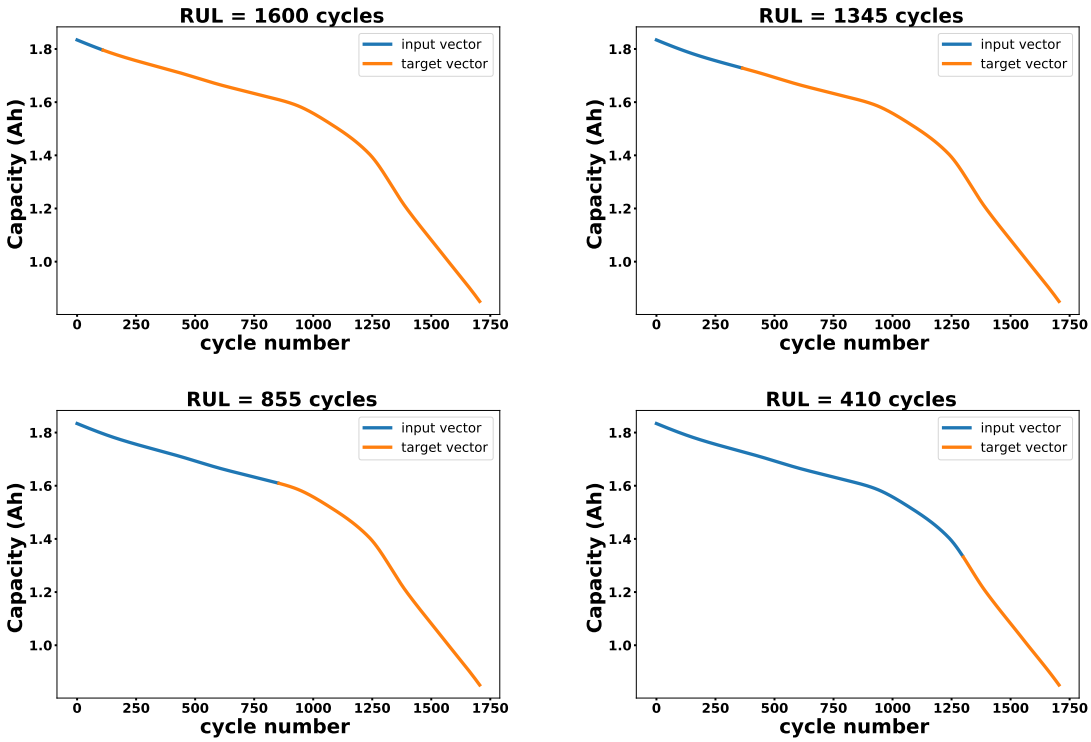

Figure 4.4: Growing input window for sequence prediction

Figure 4.5: Detailed sampling process for growing windows to sequence

The data that was used to train the TSF-XSeq2Seq was built according to this sliding-reducing windows principle, and in order to reduce the amount of processed and predicted data, a specific data sampling method was defined. The input samples correspond to 25 consecutive cycles with no re-sampling. Each time the window moves forward, from one sample to the next, it moves 10 cycles ahead. For the output sequences, one point out of 50 is kept from the original sequence. This sampling process is illustrated more in detail in figure 4.7.

4.4 Seq2seq framework for SOH prediction

4.4.1 Input features

This contribution is a complementary approach to the TSF-XLSTM described in chapter 3. Although it would be interesting to study the impact of the input features on the performances of the SOH sequence prediction model, those first results

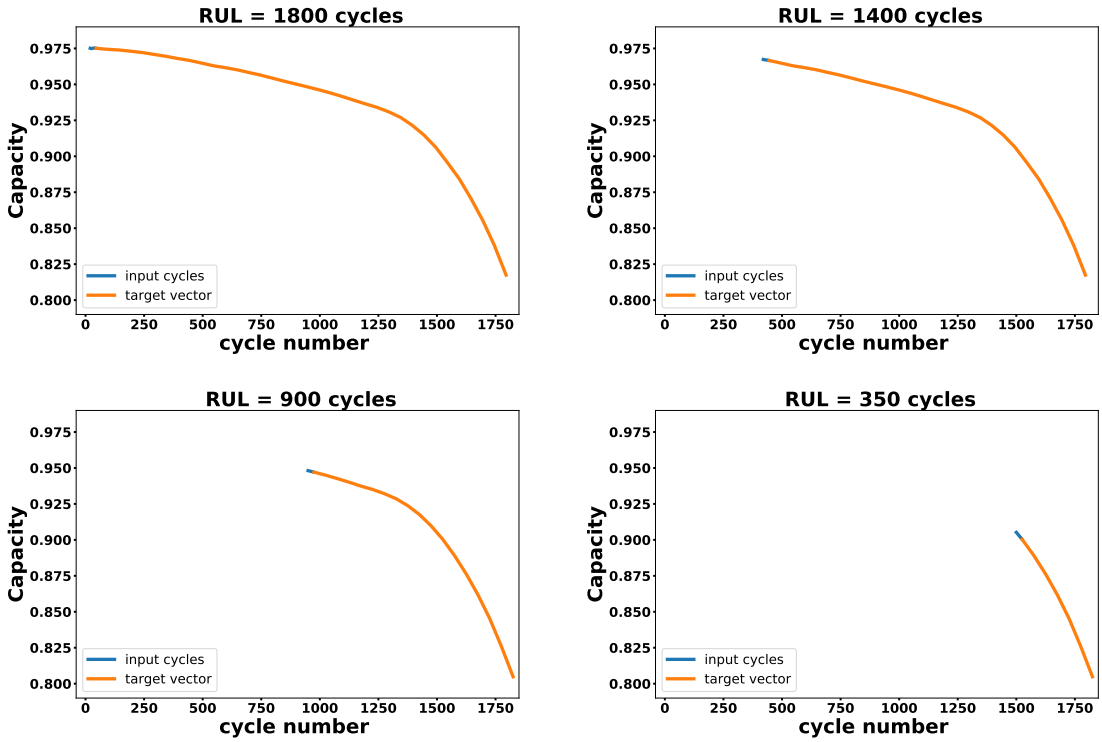

Figure 4.6: Sliding input window for sequence prediction

Figure 4.7: Detailed sampling process for growing windows to sequence

were generated using the same features as in the previous contribution, without further feature extraction or selection process. A detailed description of the feature extraction and selection process is given in section 3.2.4 in the previous chapter.

4.4.2 Data structure

In sections 4.3.1 and 4.3.2, a comparison is made between models that can handle input sequences of a growing length (growing window to sequence) and models that use input sequences of the same length throughout the prediction process (sliding window to sequence). Our contribution is based on a sliding window to sequence approach. Input windows are built in such a way that their shape remains the same, no matter the moment when the prediction is made, but output windows still have a variable length, which implies some adaptations of the model and data structure.

In order for the model to be able to handle sequences of variable length as output, a padding process is applied. All output sequences are made uniform before

the training process, that is to say all sequences are brought to the same size, which corresponds to the length of the longest sequence in the training set. In order to bring all sequences to that length, they are zero padded, which means they are completed from the end with as many zeros as needed to reach the length of the longest output sequence in the training dataset. The shorter the sequence, the more zeros are added in the end. This principle is depicted in figure 4.8.

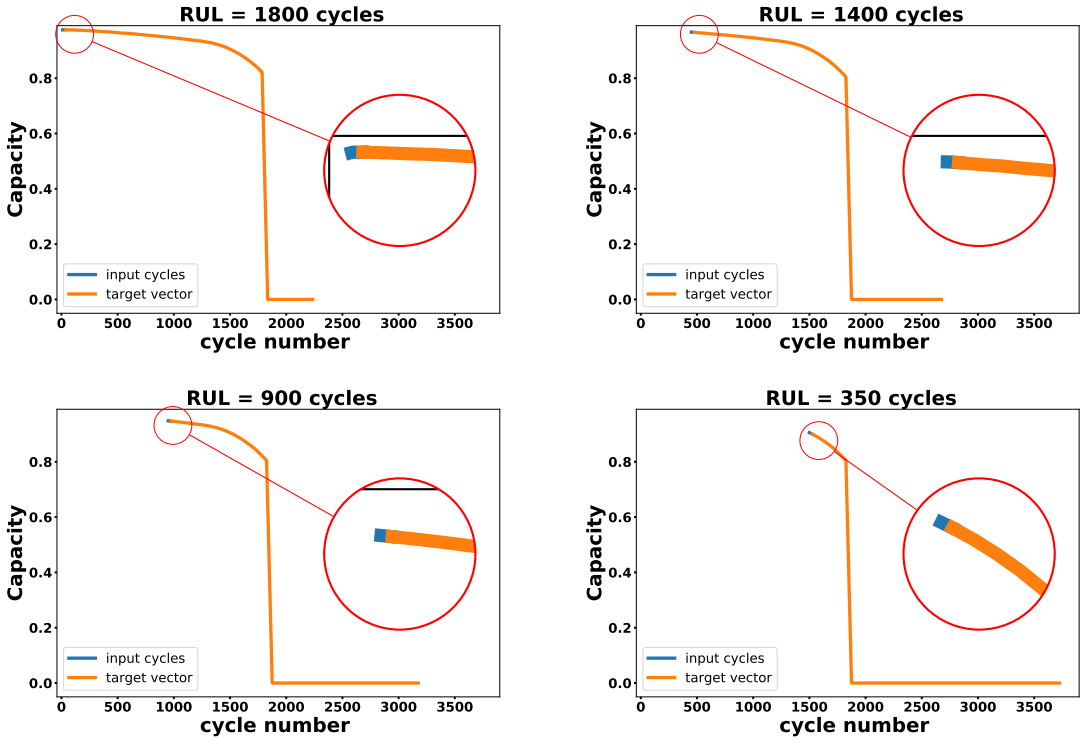

Figure 4.8: Sliding input window for sequence prediction

4.4.3 Architecture

In the previous chapter, a regular LSTM is developed to make a point prediction of SOH from fixed size windows of TSF. The structure of a regular LSTM makes it very easy to process sequences of fixed sizes, but in the scope of this chapter, and as described in section 4.4.2, the targeted output is a window of a variable size corresponding to the evolution of the SOH of a battery until its EoL. Therefore, regular LSTMs are not sufficient to handle the prediction problem and RNN-based Sequence to Sequence models should be used in-stead (Seq2Seq).

Seq2Seq models rely on the same principle as Auto-Encoders, as described in the previous chapter for the AE-XLSTM 3. In the case of a Seq2Seq model, the architecture is the same as an AE, but the input and output vectors are different, and the whole model is kept to make prediction (encoding and decoding parts). This principle could be compared to the translation process as described in section 4.2.1 and in [SVL14]. An input sentence is encoded and then decoded back to another

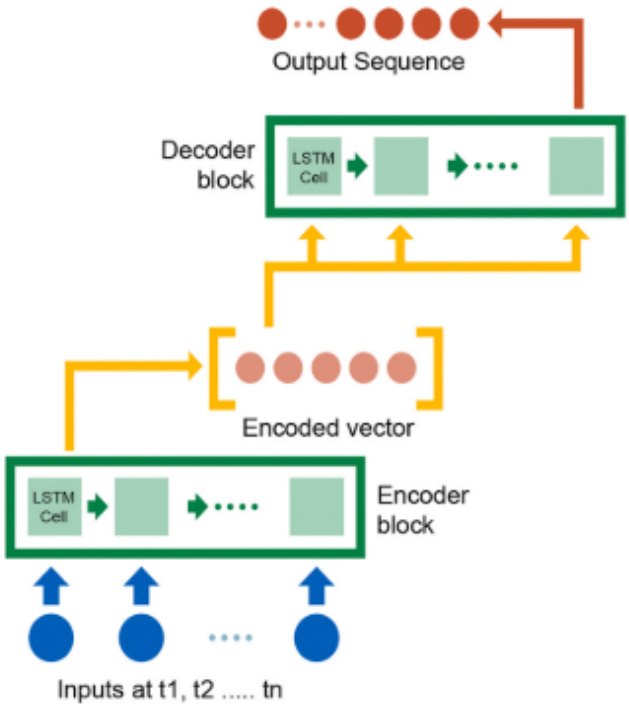

Figure 4.9: Principle of Sequence to Sequence models [LSD+21]

language. Concerning time series, an input window is encoded and decoded back to another time series.

In the case of the NAR Seq2Seq model developed by [LSD+21], input sequences of SOH are padded with zeros. Therefore, for this precise data structure, the first layer in the model is a masking layer in order not to take into account all the zeros in the input signal. The rest of the model corresponds to the encoding-decoding structure, built with LSTM cells that can either be uni-directional or bi-directional. In the scope of this chapter, for the TSF-XSeq2Seq, several sequences of TSF are fed as input to the Seq2Seq model and are decoded back to full sequences of SOH until the EoL of a given battery. As input sequences are not zero-padded, there is no need of a masking layer at the beginning of the model.

All the results presented in the next sections were obtained with the following architecture : the TSF-XSeq2Seq model is composed of four layers in the encoding part and four layers in the decoding part, plus two time-distributed layers after the decoder which makes 10 layers in total. All the layers in the encoding and decoding part of the TSF-XSeq2Seq are identical bi-directional LSTM layers with 100 nodes and a dropout fraction of 0.01. The last time distributed layer has a linear activation function in order to predict any floating value.

4.4.4 Training process

For storage and computation time constraints, tests were only led on one dataset spread into train, validation and test. All the 124 batteries from the three batches of the MIT dataset are shuffled and randomly split between the three ensembles. The

train ensemble contains 79 batteries, the validation ensemble contains 25 batteries and the test ensemble contains the remaining 20 batteries. During training, the Adam optimiser is used (see section 2.5.3 in the previous chapter) with an initial learning rate of 0.0004. The performances of the model on the validation ensemble are continuously observed during training and the training process is stopped thanks to an early stopping method (see 2.5.4). All the prediction results and curves are computed or plotted from different batteries of the test ensemble.

4.4.5 Error metrics

The error metrics that are used in the scope of this work rely on the same score as in the previous models, but they need to be modified in order not to take into account the zero padding.

During the training phase, the MAE is used as the cost function, with a masking step in order to get rid of the zeros at the end of the predicted and true sequence.

4.5 Prediction results

4.5.1 Results

In this section, the predicting performances of the TSF-XSeq2Seq for SOH sequences are investigated. For each input window, composed of several features, the TSF-XSeq2Seq is able to predict a full SOH sequence. Unlike in the previous chapter, several curves are shown for three different batteries belonging to the test ensemble. The size of the input window does not vary from one prediction to another, but the prediction starts later and later as the battery ages, because the input window shifts forward in time. As a consequence, the predicted sequence is shorter and shorter.

Figures 4.10 to 4.12 show the predicting performances of the TSF-XSeq2Seq on batteries b1c17 (that belongs to the first batch of the MIT dataset), b2c27 (that belongs to the second batch) and b3c7 (that belongs to the third batch).

For each battery, four curves are represented. The first one corresponds to the first possible prediction, when the battery has just been through the first 25 cycles that are necessary to build an input window and make a prediction. The three following curves show predictions that are made approximately after one quarter of the life of the battery has passed, then half of the life, and then when only a few cycles remain.

Regarding long term predictions, which is to say when the prediction is made at the very beginning of the life of a battery, the TSF-XSeq2Seq is able to match almost perfectly the SOH degradation curve until the EoL of the three batteries. The second prediction is also very close to the original SOH curve, although a small offset appears at the end of the curve, which induces a difference between the predicted RUL and the real RUL.

For batteries b1c17 and b2c27, predictions stay very close to the original curve until the EoL of the batteries. However, for battery b3c7, a clear gap between the real curve and the predicted one appears from the prediction made after 1000 cycles.

In table 4.1, the errors are computed as follows : for each battery of the test ensemble, predictions are made for each input window, sliding from BoL to EoL. For each prediction the output sequence is compared to the real one, and three types of error scores are represented. The earliest error is the error that is obtained by comparing the first possible prediction for all test batteries, which means the error computed on the prediction that is made after the first 25 cycles in the life of the battery. This early error is computed for all batteries and the average of all earliest error is given as "earliest error" in all tables. Similarly, the latest error is computed from the last sample of each battery. The average error simply consists in averaging all errors of all predictions.

Quite logically, the TSF-XSeq2Seq has lower error rates for late predictions, as the output sequence gets shorter and shorter. However, the error computed for the earliest prediction is in the same order of magnitude as the average error, with a standard deviation of the MAE of 0.02 which shows that the predictions are quite steady and reliable even at a very early degradation stage.

Table 4.1: Performances of the TSF-XSeq2Seq for all test batteries

		TSF-XSeq2Seq
MAPE	Average	2.60
	Earliest	2.95
	Latest	1.46
MAE	Average	0.02
	Earliest	0.03
	Latest	0.01
σ_{AE}	Average	0.01
	Earliest	0.02
	Latest	0.00
RMSE	Average	0.03
	Earliest	0.04
	Latest	0.01
RMSPE	Average	3.24
	Earliest	4.11
	Latest	1.46

4.5.2 Comparison and interpretation

In this section, the prediction results of our TSF-XSeq2Seq model are detailed in comparison with the model developed in [LSD+21] and in comparison with an NAR model developed on the MIT data referred to as NAR-Seq2seq, whose structure is described in the following paragraph.

NAR comparative approach on the MIT dataset

The structure of the NAR-Seq2seq is almost identical as the TSF-XSeq2Seq : the architecture and hyper parameters are the same, but the input features and the shape

of the training data vary. In the NAR-Seq2seq, only one sequence of SOH is used in stead of the previously described combination of TSF sequences used in the TSF-XSeq2Seq. Therefore, the first layer of the NAR-Seq2seq takes as input one single sequence. The aim of this last comparative approach is to study the performances of a model that has the same characteristics as the model developed by [LSD+21] but that would be trained on the MIT dataset, like our TSF-XSeq2Seq. Therefore the structure of the data that was used to train the NAR-Seq2seq is the same as in [LSD+21], growing input windows that are padded with zeros according to their length, and diminishing output windows that are also padded with zeros. Concerning the sampling rate, the input windows take into account one SOH point out of ten. The first window of each battery contains three data points which account for 30 cycles. As for the output sequences, they contain one SOH point out of 40.

Comparison of performances

The comparison between the model developed by [LSD+21] and the TSF-XSeq2Seq should be interpreted carefully considering that those two approaches are very different. First, they apply to different training data. Indeed, the model by [LSD+21] was trained on the dataset that is provided with their study. This dataset is a custom dataset that was built with their own test bench (a complete description of the dataset is provided in chapter 2). And secondly, their approach is based on an NAR model that takes growing windows of SOH as input to predict full sequences of SOH.

The approach described in this chapter is a NRX model with sliding windows as input in stead of growing windows, and was trained on the MIT dataset. The most meaningful comparison is to be made between the TSF-XSeq2Seq and the NAR-Seq2seq because they oppose different strategies but are trained on the same data.

Table 4.2 gathers predicting results from our TSF-XSeq2Seq, the NAR-Seq2seq and the model by [LSD+21]. It appears clearly that our NRX model outperforms both the NAR-Seq2seq and the one trained on Aachen data. For both early prediction and on average, our TSF-XSeq2Seq has lower errors and higher reliability. Both NAR models have very similar performances, although the NAR-Seq2seq seems to have better early performances than average ones when model by [LSD+21] performs better on average than at early stages. Our TSF-XSeq2Seqhas very close performances on average and at an early stage, and a MAE that stays under 0.02.

An interesting comparison to make is with the TSF-XLSTM model described previously in chapter 3. Indeed, this model was the first attempt to predict SOH from TSF. The aim is different, as only point values of SOH are predicted at different horizons, but the input features used in this TSF-XSeq2Seq are exactly the same and the size of the input window is also identical. From table 4.3, it can be seen that the TSF-XLSTM has better performances with predictions under 300 steps ahead. With 350 and 400-steps-ahead predictions, the TSF-XSeq2Seq has better predicting performances. The reliability of both models expressed by the standard deviation of the absolute error stay close (from $1.1 * 10^{-2}$ to $2.8 * 10^{-2}$ for the TSF-XLSTM and $1.0 * 10^{-2}$ for the TSF-XSeq2Seq). The output predicted by the TSF-XSeq2Seq is more complex than a single point which increases the uncertainties. Further tests

should be led in order to improve the architecture of the TSF-XSeq2Seq and also to create an NAR comparative model with a specific architecture that does not only vary from the input features.

Table 4.2: Comparison of performances between [LSD+21], TSF-XSeq2Seq and NAR Seq2Seq on MIT data

		[LSD+21]	NAR Seq2Seq	TSF-XSeq2Seq
MAPE	Average	3.34	7.16	2.60
	Earliest	4.50	4.14	2.95
MAE	Average	0.04	0.06	0.02
	Earliest	0.05	0.04	0.03
σ_{AE}	Average	0.03	0.03	0.01
	Earliest	0.05	0.03	0.02
RMSE	Average	0.05	0.07	0.03
	Earliest	0.08	0.05	0.04
RMSPE	Average	4.37	8.31	3.24
	Earliest	6.78	5.90	4.11

Table 4.3: Average performances of the TSF-XLSTM and TSF-XSeq2Seq for SOH prediction on MIT batteries

Metric	Prediction horizon (No. of cycles ahead)									TSF-XSeq2Seq
	25	50	100	150	200	250	300	350	400	
MAE ($*10^{-2}$)	1.1	1.2	1.4	1.3	1.9	1.6	2.0	2.1	2.4	2.0
σ_{AE} ($*10^{-2}$)	1.1	1.5	1.6	1.9	2.1	1.9	2.3	2.4	2.8	1.0
RMSE ($*10^{-2}$)	1.5	1.9	2.1	2.3	3	2.5	3	3.2	3.7	3.0
RMSPE (%)	1.7	2.2	2.4	2.7	3.3	2.8	3.5	3.7	4.2	3.2

4.6 Conclusion about SOH sequence prediction

This last contribution chapter focuses on the prediction of full SOH sequences of Li-Ion batteries from operating data represented by TSF. The model that was developed for this purpose is built following an approach by Li *et al.* [LSD+21] that aimed at predicting full SOH sequence from growing windows of SOH as the battery ages. Here, the same output is kept, but the input is modified in order to take operating data into consideration rather than SOH only. Input windows are also modified from growing ones to sliding ones, with a fixed size of 25 consecutive cycles. Our study shows that this SOH sequence prediction model, referred to as TSF-XSeq2Seq, has very good predicting performances at all stages in the life of a battery.

As few approaches in the literature are based on the MIT dataset, and even fewer ones on SOH sequence prediction, we compare the results of our TSF-XSeq2Seq with a similar structure but trained on an endogenous feature (SOH only), referred

to as NAR-Seq2seq and with the TSF-XLSTM described in the previous chapter. According to the tests that were led, the TSF-XSeq2Seq that is an exogenous model has better performances than the NAR-Seq2seq, but slightly lower performances than the point prediction exogenous model TSF-XLSTM for predictions under 300 steps ahead. However, the sequence prediction model offers a good complement model and has promising performances and could make it possible to link a specific use mode to a future degradation at any moment.

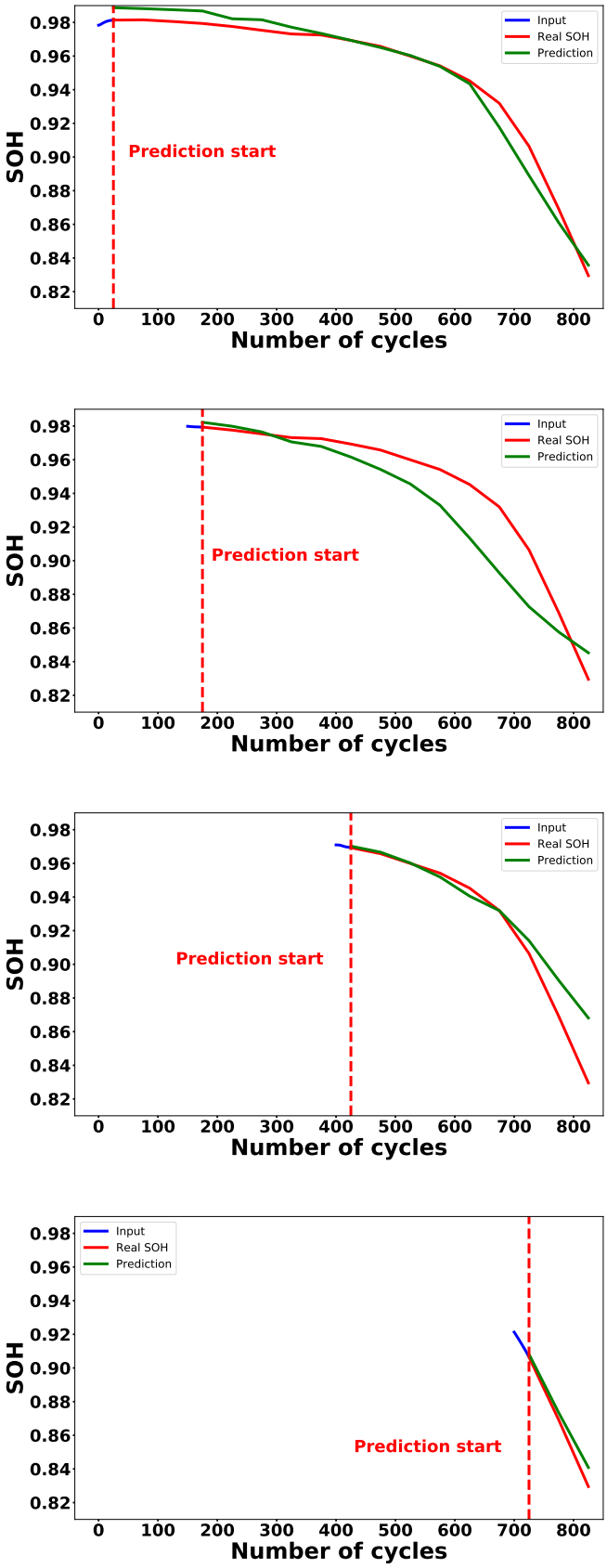

Figure 4.10: Seq2Seq predictions on battery b1c17

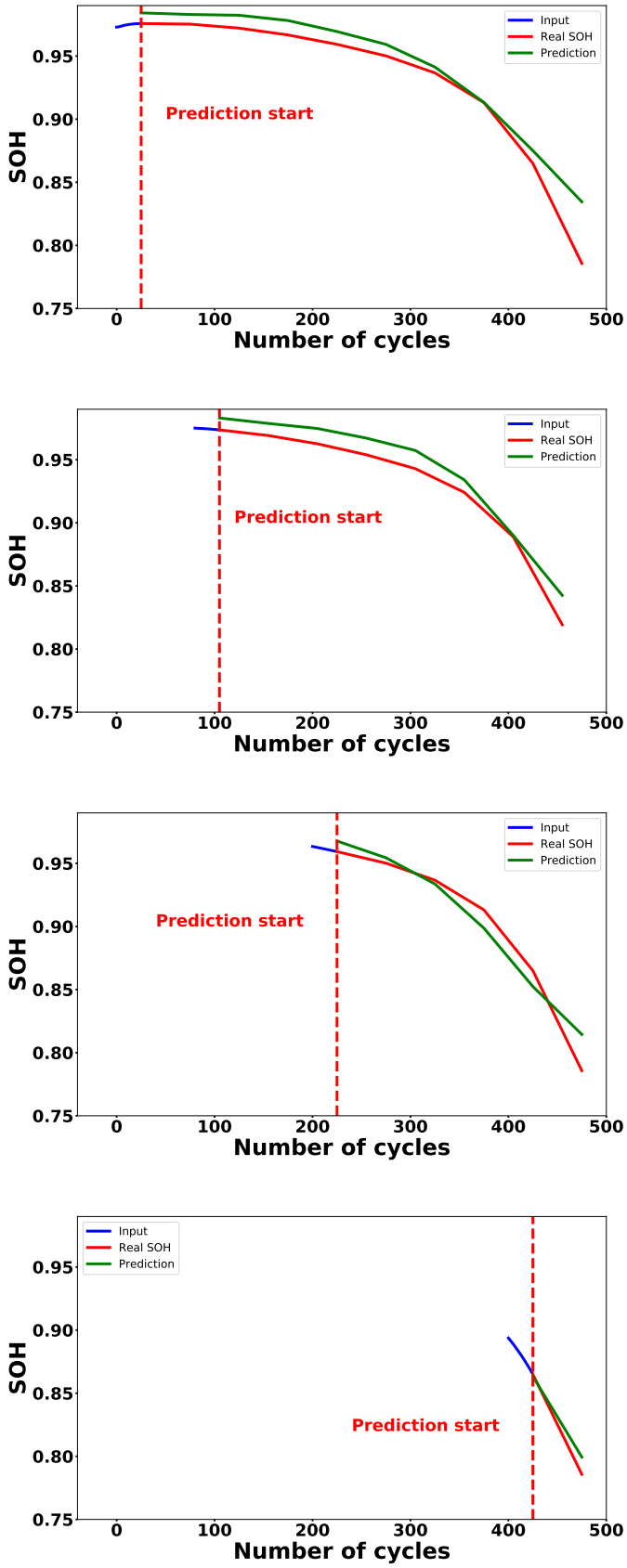

Figure 4.11: Seq2Seq predictions on battery b2c27

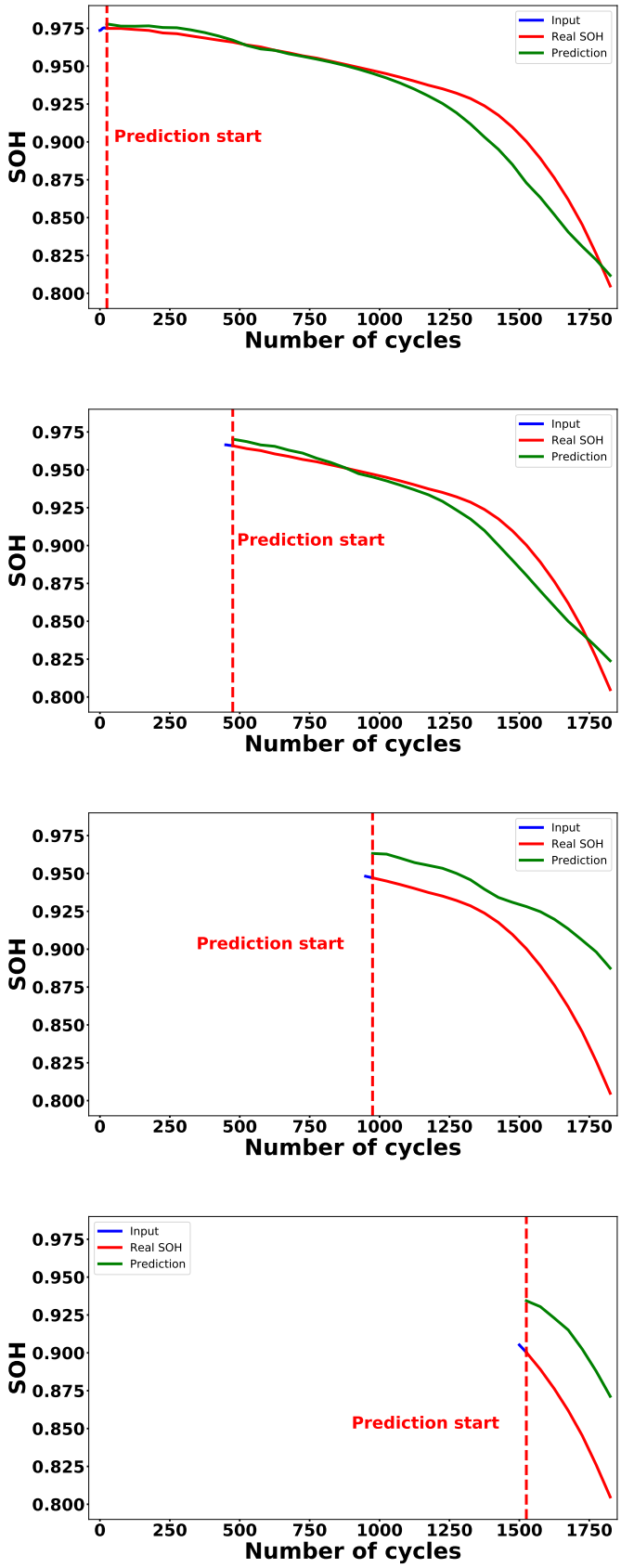

Figure 4.12: Seq2Seq predictions on battery b3c7

Chapter 5

Experimental setup for Li-Ion battery ageing

Contents

5.1 Motivations

In all the models described in the contribution chapters 2, 3 and 4, predictive models are built with public ageing datasets that were built by big research laboratories. All the datasets are presented in chapter 1. In this last chapter, our attempt to build our own ageing dataset is described, with a detailed overview of the test bench, sensors, devices used and test protocols.

The aim of this test bench is to be able to gather ageing data from different Li-Ion batteries with custom conditions and test protocols. This project comes from a simple observation after studying all the publicly available datasets. The aim of all the different predictive models that are built in the scope of this thesis is to be able to predict how a specific use mode will affect the ageing of a battery, represented by its SOH or RUL. Although the developed models are theoretical for now, the ultimate goal of predictive prognostics is to be able to monitor online the functioning of a battery inside a vehicle, with embedded sensors and on-board predictive models (or remote smart devices for prediction, with a data transfer strategy). Therefore, the predictive models should be able to deal with real operating data and provide accurate online predictions. That means models should be trained with data that is as close as possible (or even identical) to real operating data that could be acquired on board a vehicle. The fact is that most dataset, and all the ones that were trained in the scope of the three detailed contributions like the MIT dataset are based on test protocols that are very different to real use conditions. In the MIT dataset for example, each battery is charged and discharged following the same test procedure throughout its whole life. The aim of the dataset as described earlier in chapter 1 is to study the influence of fast charging over the cycle life of LFP battery cells. Therefore, charge protocols with high current rates are implemented to shorten the charge time, and a limited importance is given to the discharge phase during which batteries are discharged with a constant current of 4C. This type of data brings interesting information about the ageing phenomena that can occur in batteries but training a model only from them leads to a partial understanding of what could occur in real life. If training and real data are too different, the predictive model is certain not to perform well on board a vehicle.

This is why we decided to build our own ageing dataset with test protocols that would be closer to real world driving scenarios. We built custom cycling protocols with variable charge and discharge modes for each battery and throughout its life. Batteries are discharged following current profiles that correspond to realistic driving scenarios and that are described in the following sections. Several battery chemistries are tested in order to get the most diverse ageing dataset.

5.2 Data acquisition

All data ageing tests were conducted on a test bench on site, at the INSA Strasbourg. Experimentation started in January 2020 and is still going on as the aim of the test bench is to perpetuate the cycling tests in order to enrich the data that can be used to train predictive models and gather information on the ageing of the batteries. It took a few months to create and optimise the test plans and the setup of the test

bench. The first official cycling tests started in January 2022. The following sections describe the devices that are used to test the batteries, and the test conditions.

5.2.1 Battery cycler

The device used to cycle the batteries is a cycler from Basytec, model XCTS. This cycler has 12 channels and can be used for a great number of applications, including life time testing, cell grading, usability tests, quality insurance, ..., on any kind of electrochemical energy storage systems (Li-Ion batteries, fuel cells, capacitors, ultra capacitors ...). The model that is used does not include a climate chamber, so battery cells are tested at room temperature.

5.2.2 Sensors

Three principal signals are acquired : current, voltage and surface temperature of battery cells. From those signals, other ones are computed in real time such as total capacity (computed from the current integral), capacity per cycle, internal resistance, energy... According to the models that were developed in the scope of this thesis, only current, voltage, temperature and capacity are needed.

5.2.3 Test conditions

All the batteries that are cycled are brand new batteries. The test protocols were designed and improved with specific batteries that were no longer used after that for ageing tests. Batteries are all referenced with specific codes that take into account the chemistry and cell manufacturer (eg. FLP-A123-00, NMC-SAMSUNG-01). As mentioned before, tests are conducted at room temperature inside the lab.

5.2.4 Safety measures

The tests that are conducted should not be too harmful and no extreme use of the battery is made. The purpose of those ageing tests is to study the degradation of batteries under realistic conditions. There should not be any over-heating, under or over voltages, nor positive or negative current peaks over the limits specified by cell manufacturers. Nevertheless, some hardware and software safety measures were implemented in order to get rid of all possible risks.

All the batteries are placed in sealed safety boxes (called Bat-safe) that are meant to contain any battery fire and filter gas emissions. There are maximum two batteries per box. The safety boxes are placed on a lab bench designed for electronic testing, which means they can resist fire. Cables that are connected to the cycler have specific connecting lugs for which we had to design custom and protected small circuits. The connection between the cables on the battery side and the cycle cables is protected by a plastic box as shown in figure 5.2. Battery cells are plugged on a specific circuit (shown in figure 5.3) and no short circuits between power cables is possible.

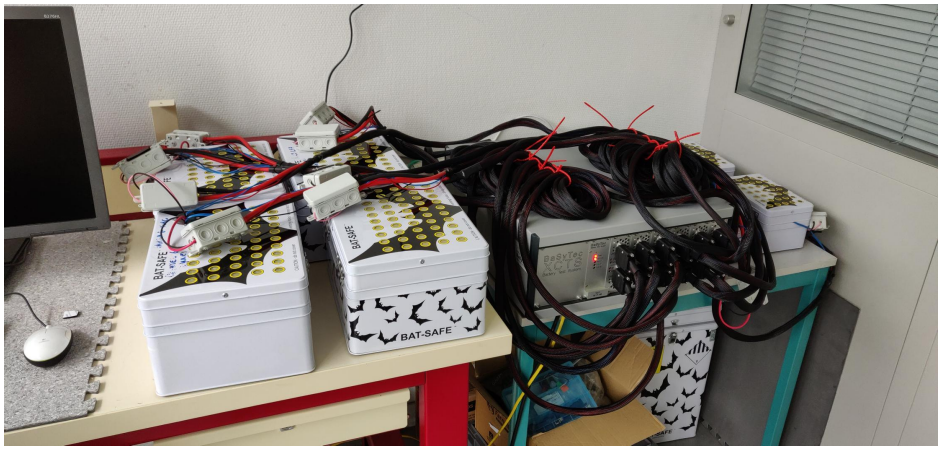

Figure 5.1: Organisation of the test bench

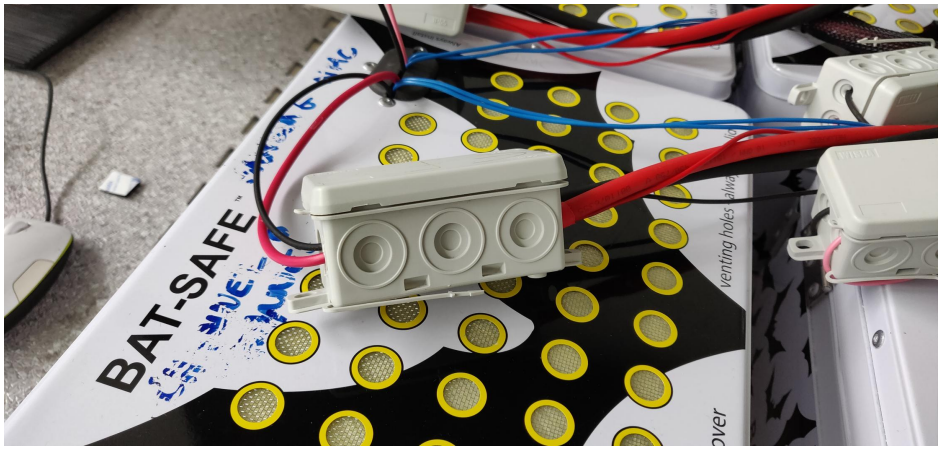

Figure 5.2: Protection boxes for connecting lugs

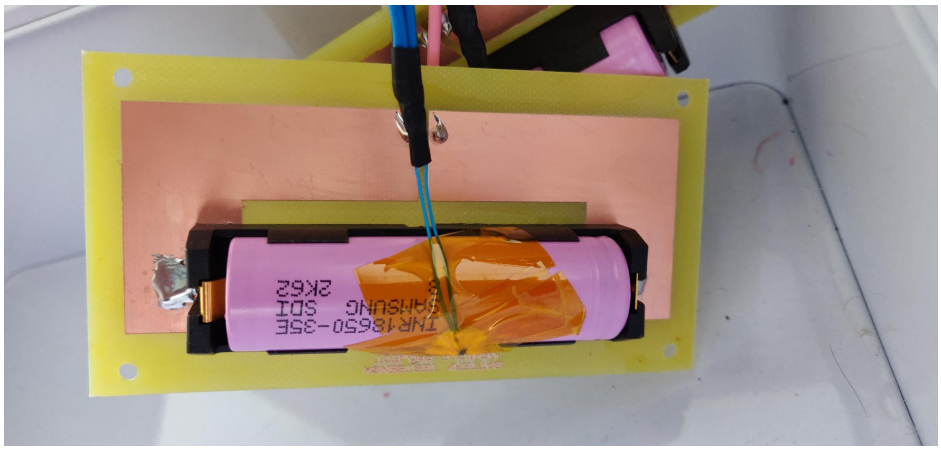

Figure 5.3: Battery connecting circuit inside the bat-safes

The cell voltage, current and temperature are continuously monitored. Stop conditions are defined at the beginning of all test protocols and consist in putting an end to any test if the voltage goes over or under the maximum and minimum recommended values. The same stop conditions are defined for current and temperature.

5.3 Choice of batteries

The aim of the test bench is to get data from different chemistries, as not all car manufacturers use the same technologies in electric vehicles. The two most widespread battery chemistries are LFP and NMC batteries. Our first choice was to use the same cell model as the one tested by the MIT in the dataset that was mainly used to develop the predictive models. Therefore, most of our ageing data comes from LFP cells model APR18650M1A from the manufacturer A123. A123 was then bought by Lithium Werks and we had to switch to model APR18650M1B which has a slightly higher capacity.

Apart from LFP cells, NMC cells were also tested. In the scope of the Vehicle project, a partnership with a French electric motor scooter manufacturer was established. The aim of this partnership was to make use of the data that was collected from their vehicles, that are exclusively used for food delivery. Inside their scooters, NMC cells are used and two manufacturers were tested in their prototypes : Samsung and Panasonic. Some samples coming from their battery cells stocks were tested on our test bench, and we ordered other battery cells from the same manufacturers to increase to amount of data acquired by our test bench.

Chemistry	Manufacturer	C_{nom}	V_{nom}	I_{max}	$T°_{min}$	$T°_{max}$
LFP	A123	1.1 Ah	3.3 V	30 A	- 30°C	+ 60°C
LFP	Lithium Werks	1.2 Ah	3.3 V	50 A (Pulse)	- 30°C	+ 60°C
NMC	Samsung	3.35 Ah	3.6 V	13 A (Pulse)	- 10°C	+ 60°C
NMC	Panasonic	2.25 Ah	3.6 V	1.3 A	-20°C	+ 45°C

Table 5.1: Tested batteries and their characteristics

5.4 Test protocols

The aim is to simulate the cycle ageing of batteries by using them continuously in conditions that are close to the real use of a battery inside an EV. In-stead of discharging the battery cells with a constant current, driving cycles are used to simulate a realistic use of a vehicle, with dynamic currents and pauses while the battery discharges. Different charge protocols are also used, with either fast, standard or slow charging currents. Indeed, an electric vehicle is very unlikely to be charged every time with a fast charger. Most charges are made at night and at home with standard chargers. The only parameter that we couldn't take into account in our test

bench was partial charges and discharges because it is easier to monitor the evolution of SOH with full charges and discharges. Therefore, battery cells are invariably charged and discharged at 100%.

5.4.1 Driving cycles

The battery cycler that is used only allows discharge currents up to 25A per cells which limits the tests range. Moreover, when designing the test protocols, the idea was to create different scenarios that were comparable between them in order to have meaningful ageing results. For some part of the tests, driving cycles were provided by Mob-Ion, and they correspond to an urban use of a motor scooter, which means speed stays under 50 km/h. The driving cycles that were used for the other tests are standardised driving cycles designed to assess performances of thermal vehicles in terms of fuel consumption and greenhouse gas emissions [BLMB09].

WLTC

The Worldwide harmonised Light vehicles Test Cycles (WLTC) is used to assess the performances of light-duty vehicles. The class 3 cycle was used, because it is representative of vehicles driven in Europe and Japan. It is divided into four parts according to the maximum speed : low, medium, high and extra high. Only the urban (low) part of the cycle with speeds under 60km/h was kept [KBW+15].

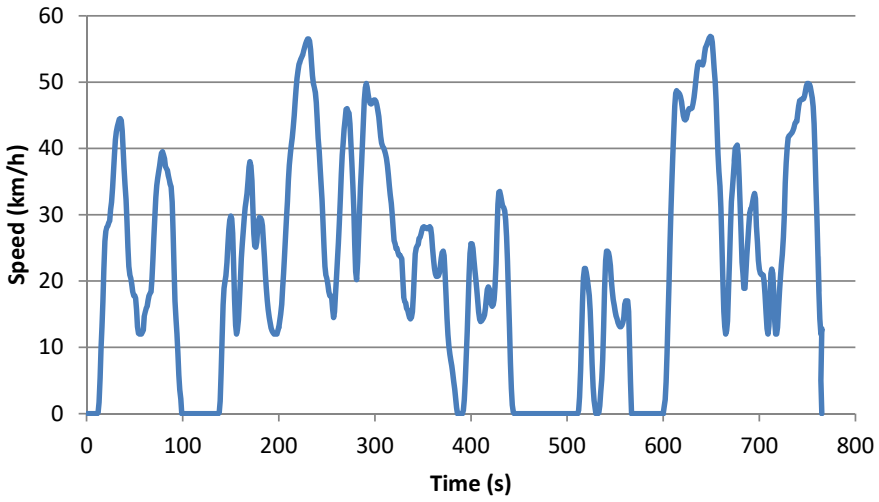

Figure 5.4: Urban WLTC speed profile

ARTEMIS

The ARTEMIS cycle (Assessment and Reliability of Transport Emission Models and Inventory Systems) was designed by the Transport Research Laboratory [PGB07] in order to have a better understanding of emission modelling but also to develop a

harmonised methodology for estimating emissions from all transport modes at the national and international levels. The Urban ARTEMIS cycle ranges from 0 to 58 km/h with an average speed of 17.7 km/h and with several phases of acceleration and breaking.

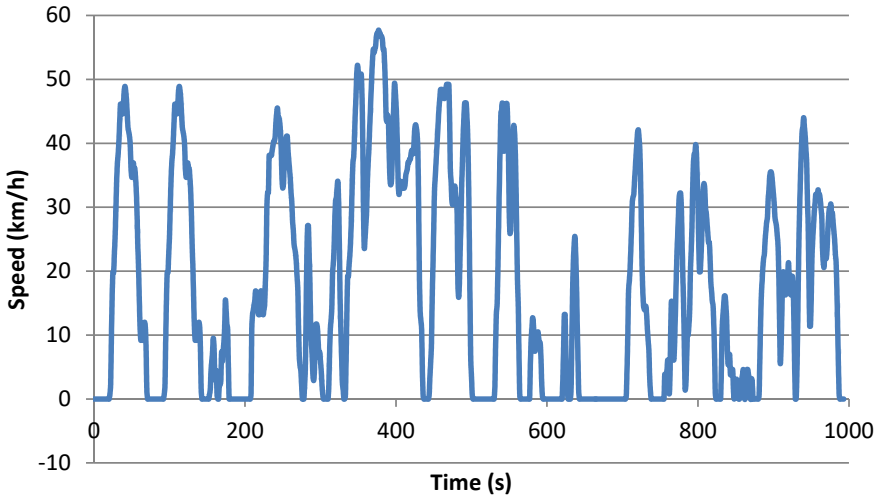

Figure 5.5: Urban ARTEMIS speed profile

Electric scooter driving cycles from Mob-Ion

As mentioned before, a partnership was established with a motor scooter manufacturer. For the tests that were led on the battery cells coming from their stocks, specific driving cycles were used. Those driving cycles come directly from acquired data on one of their scooters. As their scooters are only used in urban environments, the speed stays under 50 km/h and comprises small driving periods punctuated by stops that correspond to red lights or stops for deliveries.

5.4.2 Charging procedures

The charging procedures that were designed for battery tests are regular CC-CV protocols. Three charge profiles are used : a fast one, a standard one and a slow one. The only parameter that varies from one profile to another is the current rate during the CC phase. The standard charge current is recommended by the manufacturer in the cell's datasheet. The slow charge current is half the standard charge current and the fast charge current is between 1.2 and 3.7 times the standard charge current.

Figures 5.6 and 5.7 show two different test protocols, each with a full discharge with a driving cycle. In figure 5.6, the first full driving discharge is followed by a slow charge and then the second one by a fast charge. In figure 5.7, the first full driving discharge is followed by a slow charge and then the second one by a standard charge.

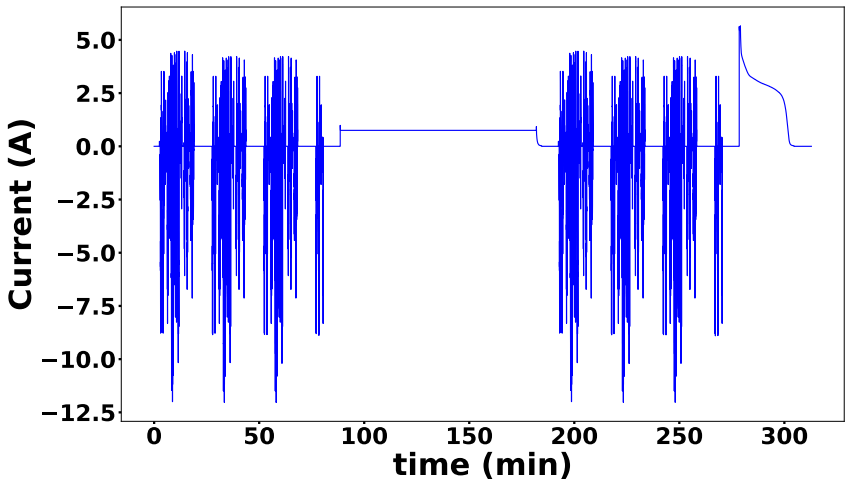

(a) Current

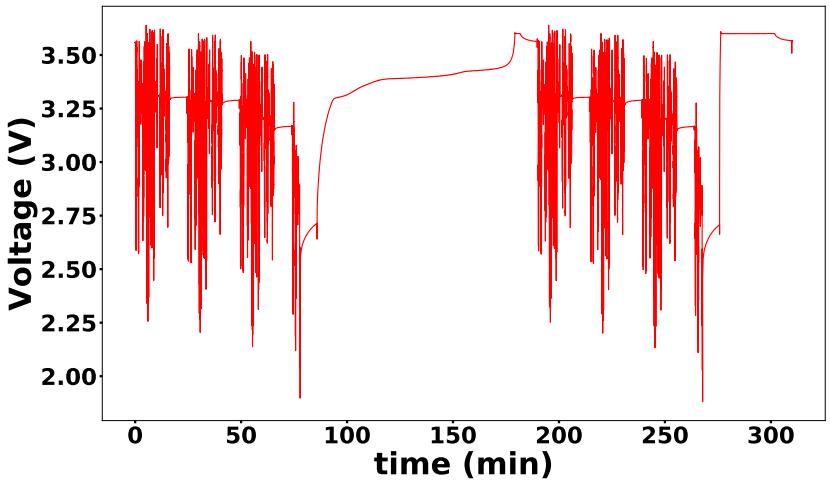

(b) Voltage

Figure 5.6: Slow charge followed by fast charge

5.4.3 Test structures

Figure 5.8 illustrates the global structure of a test protocol, no matter the battery type. The first step in each test protocol is to completely empty the battery, because they usually are delivered at a 50% state of charge. After this first step, a full complete charge with a slow charge current is operated. This is when the first capacity check is done : the battery is fully discharged again at 1C, and this capacity check will be used as a reference for the initial capacity of the battery cell. Another full standard charge follows the capacity check, and then starts the ageing tests that will go on until the battery reaches its EoL (which corresponds to a loss of 20% of its initial capacity).

On figure 5.8, three loops are represented (numbered from 1 to 3) :

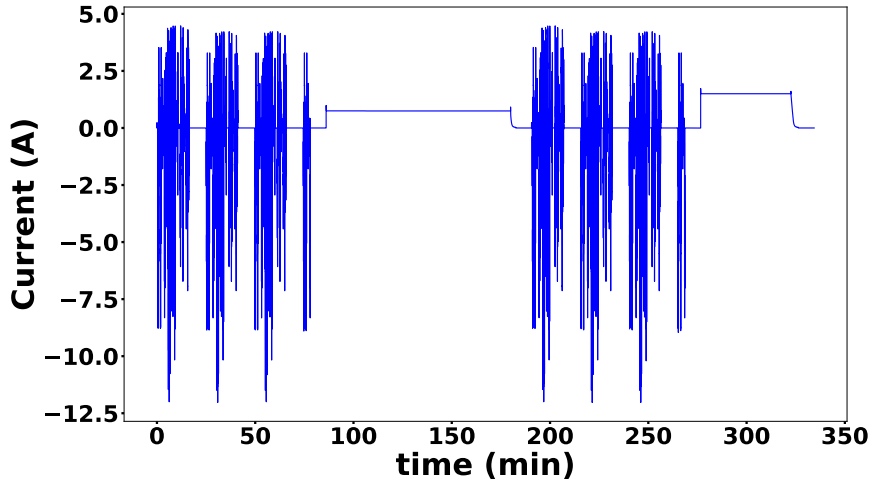

(a) Current

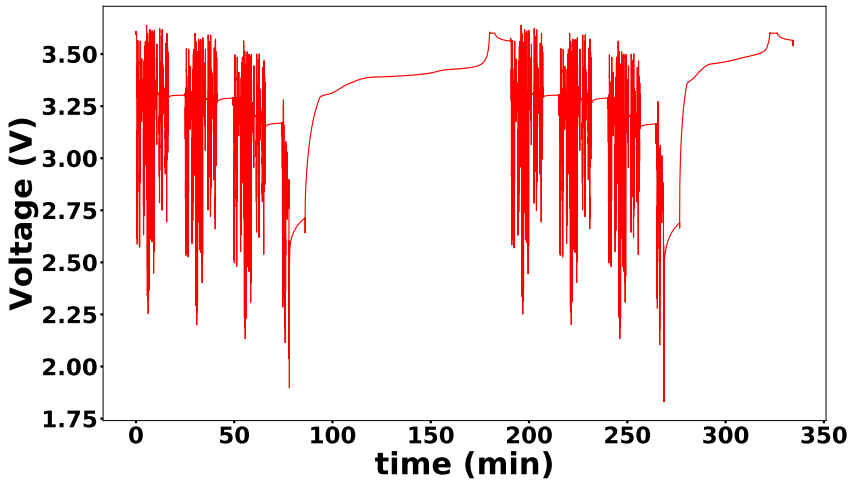

(b) Voltage

Figure 5.7: Slow charge followed by standard charge

1. The first loop is a driving-like full discharge. The driving cycles can be one of the three earlier described one (WLTC, ARTEMIS, or Mob-Ion for the motor scooter cells). This loop can be repeated as many times as needed to completely empty the battery (ie. when the voltage drops below the cut-off voltage).

2. The second loop comprises the first loop. It aims at repeating four times the full driving discharge, and after each of those discharges, a different full charge is operated (either slow, standard or fast).

3. After repeating the full driving discharge combined with a full charge, a capacity check is programmed in order to monitor the ageing of the battery. The capacity check is done by fully discharging the cell at a constant rate of 1C.

This loop, which comprises the first two ones, is repeated as many times as needed to lower the SOH of the battery to 80%.

This structure is a generic structure. For each battery cell manufacturer (except for the one furnished by Mob-Ion), two slightly different kinds of tests were launched. One is referred to as "variable charge/fixed ARTEMIS" and the other one as "fixed standard charge/WLTC ARTEMIS discharge". The global structure of the test is the same, but for the variable charge/fixed ARTEMIS structure, the driving discharge loop only uses ARTEMIS cycles and then the complete charge varies between slow, standard and fast. For the fixed standard charge/WLTC ARTEMIS discharge, the structure reverses and the driving cycles vary between WLTC and ARTEMIS while the full charge always remains a standard charge.

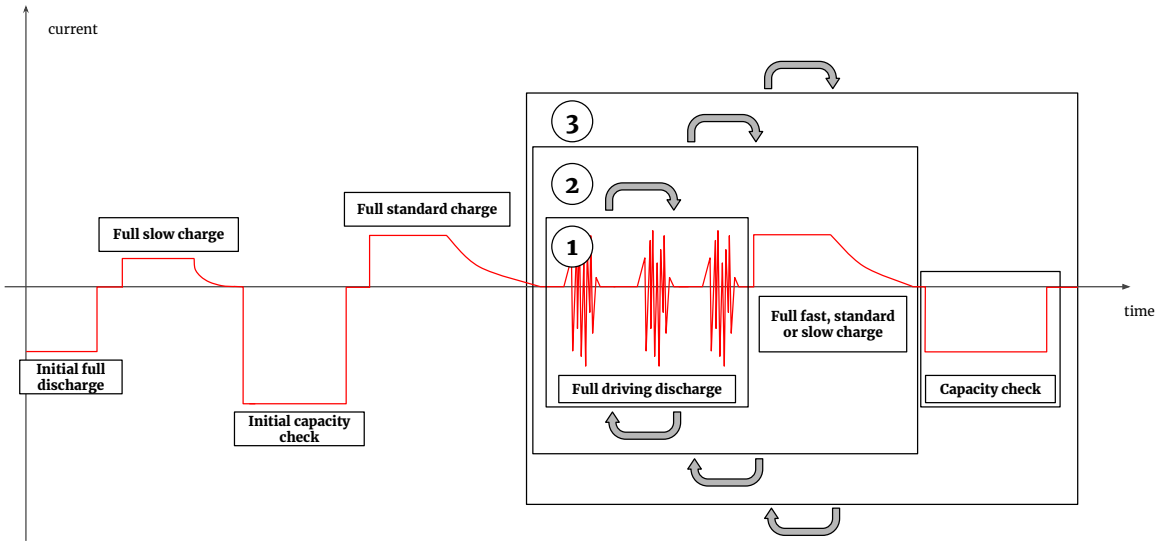

Figure 5.8: Structure of the test protocols

5.4.4 Storage procedures

At some points since the battery cycling was launched, tests had to be stopped for various reasons and some of the batteries that were used to design the tests had to be stored afterwards. Li-Ion batteries need to be put in a specific state of charge before being stored for a long time in order not to degrade. Therefore, we designed a storage procedure that was launched anytime the tests needed to be stopped. This procedure was meant to fully discharge the battery, and then to charge it at 50% with reference to its voltage [KJ17]. The storage voltage is defined as follows :

$$U_{storage} = U_{min} + (U_{charge} - U_{min}) * 0.5 \tag{5.1}$$

where U_{min} is the minimum cell voltage recommended by the manufacturer and U_{charge} is the charge voltage recommended by the manufacturer (U_{charge} is higher than the nominal voltage).

Each time a test has to be stopped, the storage procedure is launched, and then the same full test protocol is started again (comprising the initial discharge, full charge, capacity check and three loops described earlier).

5.5 Ageing results

The current tests have been launched in January 2022. Nine month after, several batteries have seen their SOH drop below 80%, but for most cells, tests are still running.

Samsung cells have all reached their EoL, while the capacity of LFP batteries has barely dropped (1.11Ah for cell LFP-A123-01, 1.07 Ah for cell LFP-A123-02 and 1.04 Ah for cell LFP-A123-03). Panasonic cells are reaching their EoL, but tests will continue until their SOH goes below 80% to see how SOH evolves in late life.

5.6 Conclusion on the experimental setup for Li-Ion battery ageing

This short chapter aimed at presenting the experimental setup that was built all along this PhD to increase the amount of data used to build predictive prognostics models for Li-Ion batteries. Collecting ageing data is quite slow with Li-Ion batteries because they perform very well and take time to degrade. Moreover, the amount of data needs to be very large to train a model and training data must include as many battery cells as possible. The amount of collected data from our test bench up to today is not sufficient to train a SOH predictive model from scratch. However, it could already prove useful for other applications. The prediction of SoC for example does no require that batteries reach their EoL. Only operating data coming from multiple cycles are needed, and our tested batteries have been through several hundreds of full charge and discharge cycles. This test bench is meant to be made permanent, which means that each time a battery cell reaches its EoL, it can be replaced by a new one. Samsung cells for example have already been replaced by new ones. In order to make the best possible use of our ageing data, a database has been created to store and possibly share the information. Ageing data will be made available upon request.

Conclusion and Future Work

Conclusion

Throughout all the chapters of this thesis, the principle and importance of predictive maintenance for Li-Ion batteries were presented. The challenges associated with battery performance are of crucial importance to the development of EVs as part of a truly sustainable development strategy. The transformation of the transport sector will only be truly effective if we take into account the issues surrounding Li-Ion batteries, their production, use and recycling. All the contributions addressed by this thesis focus on the operating mode and environment of Li-Ion batteries. A number of problems have been raised, such as the need for representative data on the use of batteries in vehicles, the need to extract simple features from it, to predict SOH or RUL at any stage of the life of a battery... The use of ANN and RNN makes it possible to model the ageing phenomena that occur inside Li-Ion batteries more efficiently than with physical approaches. Even though the obtained models with ANN and RNN are "black box" models, the facts that they can adapt to any input and be embedded on board a vehicle make them a very powerful tool in the scope of predictive maintenance.

Three major models are built and take advantage of a dataset that was published by the department of chemical engineering of the MIT, in collaboration with Toyota engineering and with the Department of Materials Science and engineering of Stanford university in [SAJ+19].

These models are highly theoretical, suggesting the use of individual battery cells instead of traditional battery packs. However, despite their theoretical nature, these approaches are promising and could be applied to various other situations. It has been shown that even with a minimal amount of input signals consisting of easily obtainable parameters like current, voltage, and temperature, one can gain valuable insights into the battery's environment and usage patterns. The contributions described in the different chapter of this thesis are summarised below.

In chapter 2, a first model for RUL prediction is developed. The advantage and originality of this model lie in the fact that the prediction is based on a single use cycle. An ANN is developed, referred to as cycle-based-ANN. This model takes as input a combination of historical features and features computed from time series of temperature. The obtained predictions are outperforming other approaches of the literature with a MAE of 5.76 cycles.

In chapter 3, time series data of current, voltage, and temperature are exploited to identify the influence of battery usage in the evolution of SOH. Features are extracted from those time series and used as input to a TSF-XLSTM. The prediction is made from a window of 25 consecutive cycles and corresponds to one value of SOH from 25 to 400 cycles ahead.

In chapter 4, a complementary approach to the 2nd contribution is made. In stead of predicting one single value of SOH, the full sequence of SOH until EoL is predicted with a TSF-XSeq2Seq. When comparing the point prediction with the sequence prediction, the TSF-XLSTM model has better performances than the TSF-XSeq2Seq, but the TSF-XSeq2Seq bring a wider view of the impact of a use mode over the global life of a battery.

Finally, in chapter 5, a quick presentation of our battery test bench is given. The aim of this test bench is to gather ageing data form different battery cells, with different test protocols that are close to real operating conditions. Ultimately, this data will be used to train new ML models for the predictive maintenance of Li-Ion batteries.

Future Work

Several perspective can be explored after the different contributions of this thesis.

One of the first goals is to take advantage of the data generated with the test bench in our predictive models. Indeed, there is considerable room for improvement in the usefulness of the contributions if models are trained with realistic data in stead of theoretical data. For now, the amount of collected data is not sufficient to train new models from scratch. However, a first interesting use of the data would be implement transfer learning from pre-trained models. The aim of transfer learning is to improve the performances of a model by transferring information from another domain [WKW16]. In this case, the previously trained TSF-XLSTM or TSF-XSeq2Seq would be the baseline approach, and an upper layer of knowledge could be brought by new data coming from the test bench.

Concerning the test bench, as part of our commitment to open science, some efforts will be put to creating an accessible data base on which ageing data would be uploaded regularly. The idea is to answer the FAIR principles [1].

The ultimate goal of predictive maintenance is to make real-time predictions while a system is being used. This thesis focused on a small part of the development of a predictive maintenance strategy which consists in building predictive models. In order to complete the global approach, the models should be embedded on board a vehicle and make use of instantly acquired data coming from current, voltage and temperature sensors. That way, user could be informed of the impact of their driving habits on the SOH of the battery. Moreover, a real-time internal battery management strategy could be deployed in order to make the best possible use of it. Some protections could be settled such as cell balancing, temperature control, limitation of the current peaks to cite a few... By raising the awareness on the user side about eco-driving and best practices, and by improving the internal management of the battery, the global cycle life and driving range of a battery could be significantly increased. An increased cycle life and better driving range mean a reduced TCO and environmental impact.

[1] https://www.go-fair.org/fair-principles/

Deploying an embedded approach that works with real-time-acquired data requires to study the scalability of the models. Our current theoretical models perform well with a limited amount of data and with (almost) no restriction concerning computation requirements for training and testing. On board a vehicle, it is crucial to make sure that the model will perform equally with potentially less power to run calculation, and more data, or data of a slightly different quality. Cloud computing combined with data transfer could be an option to consider, which is a problem that will be tackled by the European project Energetic [2], hold by INSA Strasbourg.

Finally, a major perspective of this thesis is to improve the understanding of the ageing mechanisms by improving the understanding of the "black box" models that were developed. ANN are complex mathematical functions and it is almost impossible to isolate the contribution of one of the input signals in the prediction of the model. Works on explainability have already started, linked to the prediction of the state of charge of a battery [HSM+23]. The aim of this work is to identify patterns where battery ageing accelerates by analysing temperature data from Li-Ion cells. This approach is based on the use of SHAP, an explanation method first introduced in [LL17].

[2] https://recherche.insa-strasbourg.fr/lancement-projet-horizon-europe-energetic/

Author publications

Peer-reviewed journals

2023 **Jorge I.**, Samet A., Mesbahi T., Boné R., "Time Series Feature extraction for Lithium-Ion batteries State-Of-Health prediction", Journal of Energy Storage, Volume 59, 2023, 106436, ISSN 2352-152X, https://doi.org/10.1016/j.est.2022.106436.

2023 Heitzmann, T., Samet, A., Mesbahi, T., Soufi, C., **Jorge, I.**, Boné, R. (2023). SocHAP: A New Data Driven Explainable Prediction of Battery State of Charge. Computational Science – ICCS 2023. ICCS 2023. Lecture Notes in Computer Science, vol 10477. Springer, Cham. https://doi.org/10.1007/978-3-031-36030-5_37

Conference proceedings

2021 **Jorge I.**, Samet A., Mesbahi T., Boné R.. "Predictive prognostic for Li-Ion batteries in electric vehicles". Upper-Rhine Artificial Intelligence Symposium 2021 (UR-AI 2021), 27 octobre 2021, Kaiserslautern, Germany, Oct 2021, Kaiserslautern, Germany.

2021 Audin P., **Jorge I.**, Mesbahi T., Samet A., De Bertrand De Beuvron F., & Boné R., "Auto-encoder LSTM for Li-ion SOH prediction: A comparative study on various benchmark datasets," Proc. - 20th IEEE Int. Conf. Mach. Learn. Appl. ICMLA 2021, pp. 1529–1536, 2021, doi: 10.1109/ICMLA52953.2021.00246.

2020 **Jorge I.**, Samet A., Mesbahi T., & Boné R., "New ANN results on a major benchmark for the prediction of RUL of Lithium Ion batteries in electric vehicles," Proc. - 19th IEEE Int. Conf. Mach. Learn. Appl. ICMLA 2020, pp. 1246–1253, 2020, doi: 10.1109/ICMLA51294.2020.00196.

2020 **Jorge I.**, Mesbahi T., Paul T., & Samet A., "Study and simulation of an electric scooter based on a dynamic modelling approach," 2020 15th Int. Conf. Ecol. Veh. Renew. Energies, EVER 2020, 2020, doi: 10.1109/EVER48776.2020.9242930

2020 Mesbahi T., Bartholomeus P., & **Jorge I.**, "Hybrid Embedded Power Supply Combining High-Energy Density and Ultra-High Power Lithium-ion Batteries for Electric Vehicle Applications," IEEE Power Energy Soc. Gen. Meet., vol. 2020-August, pp. 0–4, 2020, doi: 10.1109/PESGM41954.2020.9282047.

2019 Mesbahi T., **Jorge I.**, Paul T., & Durand S. (2019). "Design and simulation of lithium-ion battery charger using forward power converter for hybrid energy storage system". 2019 IEEE Vehicle Power and Propulsion Conference, VPPC 2019 - Proceedings. DOI: 10.1109/VPPC46532.2019.8952507.

Interventions in workshops

2020 & 2022 Journée Inter GT SEEDS Diagnostic and prognostic

Dissemination of Research & Awards

2022 Article in the french daily newspaper Liberation, "Raconte-moi ta thèse… sur le vieillissement des batteries dans les véhicules électriques"

2021 First regional prize of the science popularisation competition "Ma thèse en 180 secondes"

Bibliography

[Ade15] Adeptia. The Surprising Things You Don't Know About Big Data. Technical report, 2015.

[AFN19] AFNOR. NF EN 13306 - Terminologie de la maintenance. 2019.

[ASY15] Saeed Aghabozorgi, Ali Seyed Shirkhorshidi, and Teh Ying Wah. Time-series clustering - A decade review. *Information Systems*, 53:16–38, 2015.

[BB12] James Bergstra and Yoshua Bengio. Random search for hyper-parameter optimization. *Journal of Machine Learning Research*, 13:281–305, 2012.

[Bel15] Richard E Bellman. *Adaptive control processes: a guided tour*. Princeton university press, 2015.

[BFCF17] Heather M. Barkholtz, Armando Fresquez, Babu R. Chalamala, and Summer R. Ferreira. A Database for Comparative Electrochemical Performance of Commercial 18650-Format Lithium-Ion Cells. *Journal of The Electrochemical Society*, 164(12):A2697–A2706, 2017.

[BFF+20] Marília Barandas, Duarte Folgado, Letícia Fernandes, Sara Santos, Mariana Abreu, Patrícia Bota, Hui Liu, Tanja Schultz, and Hugo Gamboa. TSFEL: Time Series Feature Extraction Library. *SoftwareX*, 11:100456, 2020.

[Big20] Aurélien Bigo. Les transports face au défi de la transition énergétique. Explorations entre passé et avenir, technologie et sobriété, accélération et ralentissement. page 341, 2020.

[BKD14] Brian Bole, Chetan S. Kulkarni, and Matthew Daigle. Adaptation of an electrochemistry-based Li-ion battery model to account for deterioration observed under randomized use. *PHM 2014 - Proceedings of the Annual Conference of the Prognostics and Health Management Society 2014*, pages 502–510, 2014.

[BLMB09] T. Barlow, S. Latham, I. Mccrae, and P. Boulter. A reference book of driving cycles for use in the measurement of road vehicle emissions. *TRL Published Project Report*, page 280, 2009.

[Bou04] Laurent Bougrain. Practical introduction to artificial neural networks. *IFAC Proceedings Volumes (IFAC-PapersOnline)*, 37(15):347–352, 2004.

[BRM+17] Christoph R. Birkl, Matthew R. Roberts, Euan McTurk, Peter G. Bruce, and David A. Howey. Degradation diagnostics for lithium ion cells. *Journal of Power Sources*, 341:373–386, feb 2017.

[Cho15] F. Chollet. Keras. 2015.

[Chr17a] Christoph Birkl. Diagnosis and prognosis of degradation in lithium-ion batteries. *University of Oxford*, 2017.

[Chr17b] Christoph Birkl. Diagnosis and prognosis of degradation in lithium-ion batteries. *University of Oxford*, 2017.

[CKLF16] Maximilian Christ, Andreas W. Kempa-Liehr, and Michael Feindt. Distributed and parallel time series feature extraction for industrial big data applications. 2016.

[CRPK19] Yohwan Choi, Seunghyoung Ryu, Kyungnam Park, and Hongseok Kim. Machine Learning-Based Lithium-Ion Battery Capacity Estimation Exploiting Multi-Channel Charging Profiles. *IEEE Access*, 7:75143–75152, 2019.

[CTPK09] Haibin Cheng, Pang Ning Tan, Christopher Potter, and Steven Klooster. Detection and characterization of anomalies in multivariate time series. *Society for Industrial and Applied Mathematics - 9th SIAM International Conference on Data Mining 2009, Proceedings in Applied Mathematics*, 1:409–420, 2009.

[DLM18] Yu DIng, Chen Lu, and Jian Ma. Li-ion battery health estimation based on multi-layer characteristic fusion and deep learning. *2017 IEEE Vehicle Power and Propulsion Conference, VPPC 2017 - Proceedings*, 2018-Janua:1–5, 2018.

[Dom21] Domo. Data Never Sleeps 8.0. *Domo*, 21(1):1–9, 2021.

[dRSYL21] Gonçalo dos Reis, Calum Strange, Mohit Yadav, and Shawn Li. Lithium-ion battery data and where to find it. *Energy and AI*, 5, 2021.

[Eur21] European Commission. Regulation of the European Parliament and the Council - amending Regulation (EU) 2019/631 as regards strengthening the CO2 emission performance standards for new passenger cars and new light commercial vehicles in line with the Union's increased climate a. *European Commission*, 0197:1–34, 2021.

[GB16] Xavier Glorot and Yoshua Bengio. Understanding the difficulty of training deep feedforward neural networks. *IEEE Geoscience and Remote Sensing Letters*, 13(8):1074–1078, 2016.

[GBC16] Ian Goodfellow, Yoshua Bengio, and Aaron Courville. *Deep Learning*. MIT Press, 2016. http://www.deeplearningbook.org.

[GBMP13] Jayavardhana Gubbi, Rajkumar Buyya, Slaven Marusic, and Marimuthu Palaniswami. Internet of Things (IoT): A vision, architectural elements, and future directions. *Future Generation Computer Systems*, 29(7):1645–1660, 2013.

[GMK+11] Paul W. Gruber, Pablo A. Medina, Gregory A. Keoleian, Stephen E. Kesler, Mark P. Everson, and Timothy J. Wallington. Global lithium availability: A constraint for electric vehicles? *Journal of Industrial Ecology*, 15(5):760–775, 2011.

[HCR+17] Vanessa Haykal, Hubert Cardot, Nicolas Ragot, Vanessa Haykal, Hubert Cardot, Nicolas Ragot, A Combination, and Variational Mode. A Combination of Variational Mode Decomposition with Neural Networks on Household Electricity Consumption Forecast To cite this version : HAL Id : hal-01588198 A Combination of Variational Mode Decomposition with Neural Networks on Household Electricity C. 2017.

[HHHK19] Dickson N.T. How, M. A. Hannan, M. S. Hossain Lipu, and Pin Jern Ker. State of Charge Estimation for Lithium-Ion Batteries Using Model-Based and Data-Driven Methods: A Review. *IEEE Access*, 7:136116–136136, 2019.

[HK19] W. Chang H. Knobloch, A. Frenk. Predicting Battery Lifetime with CNNs. 2019.

[HSM+23] Théo Heitzmann, Ahmed Samet, Tedjani Mesbahi, Cyrine Soufi, Inès Jorge, and Romuald Boné. Sochap: A new data driven explainable prediction of battery state of charge. pages 463–475, 2023.

[HTL+17] Shyh Chin Huang, Kuo Hsin Tseng, Jin Wei Liang, Chung Liang Chang, and Michael G. Pecht. An online SOC and SOH estimation model for lithium-ion batteries. *Energies*, 10(4), 2017.

[HXGL12] Hongwen He, Rui Xiong, Hongqiang Guo, and Shuchun Li. Comparison study on the battery models used for the energy management of batteries in electric vehicles. *Energy Conversion and Management*, 64:113–121, 2012.

[HXLP20] Xiaosong Hu, Le Xu, Xianke Lin, and Michael Pecht. Battery Lifetime Prognostics. *Joule*, 4(2):310–346, 2020.

[IFW+19] Hassan Ismail Fawaz, Germain Forestier, Jonathan Weber, Lhassane Idoumghar, and Pierre Alain Muller. Deep learning for time series classification: a review. *Data Mining and Knowledge Discovery*, 33(4):917–963, 2019.

[JHS+21] Mohd Javaid, Abid Haleem, Ravi Pratap Singh, Shanay Rab, and Rajiv Suman. Significance of sensors for industry 4.0: Roles, capabilities, and applications. *Sensors International*, 2(June):100110, 2021.

[JW98] Bradley A. Johnson and Ralph E. White. Characterization of commercially available lithium-ion batteries. *Journal of Power Sources*, 70(1):48–54, 1998.

[KB15] Diederik P. Kingma and Jimmy Lei Ba. Adam: A method for stochastic optimization. *3rd International Conference on Learning Representations, ICLR 2015 - Conference Track Proceedings*, pages 1–15, 2015.

[KBW+15] Dennis G. Kooijman, Andreea E. Balau, Steven Wilkins, Norbert Ligterink, and Rob Cuelenaere. WLTP Random Cycle Generator. *2015 IEEE Vehicle Power and Propulsion Conference, VPPC 2015 - Proceedings*, (October), 2015.

[Kel19] John D. Kelleher. *Deep Learning*. The MIT Press, 09 2019.

[KH13] Ron Kohavi and George H.John. Wrappers for feature subset selection. *Lecture Notes in Computer Science (including subseries Lecture Notes in Artificial Intelligence and Lecture Notes in Bioinformatics)*, 7920 LNCS(97):654–678, 2013.

[KJ17] Peter Keil and Andreas Jossen. Aging of lithium-ion batteries in electric vehicles:. *Dissertation*, 7(1):41–51, 2017.

[KKN14] Samina Khalid, Tehmina Khalil, and Shamila Nasreen. A survey of feature selection and feature extraction techniques in machine learning. *Proceedings of 2014 Science and Information Conference, SAI 2014*, pages 372–378, 2014.

[KP11] Jonghoon Kang and Ashlie K. Patterson. Principal component analysis of mRNA levels of genes related to inflammation and fibrosis in rats treated with TNBS or glutamine, 2011.

[KY19] Phattara Khumprom and Nita Yodo. A data-driven predictive prognostic model for lithium-ion batteries based on a deep learning algorithm. *Energies*, 12(4), 2019.

[LB98] Yann LeCun and Yoshua Bengio. *Convolutional Networks for Images, Speech, and Time Series*, page 255–258. MIT Press, Cambridge, MA, USA, 1998.

[LBH15] Yann Lecun, Yoshua Bengio, and Geoffrey Hinton. Deep learning. *Nature*, 521(7553):436–444, 2015.

[LDS18] Xiang Li, Qian Ding, and Jian Qiao Sun. Remaining useful life estimation in prognostics using deep convolution neural networks. *Reliability Engineering and System Safety*, 172, 2018.

[LKRH15] Sara Landset, Taghi M. Khoshgoftaar, Aaron N. Richter, and Tawfiq Hasanin. A survey of open source tools for machine learning with big data in the Hadoop ecosystem. *Journal of Big Data*, 2(1):1–36, 2015.

[LL17] Scott M. Lundberg and Su In Lee. A unified approach to interpreting model predictions, 2017.

[LSD+21] Weihan Li, Neil Sengupta, Philipp Dechent, David Howey, Anuradha Annaswamy, and Dirk Uwe Sauer. One-shot battery degradation trajectory prediction with deep learning. *Journal of Power Sources*, 506:230024, 2021.

[LSOW21] Kailong Liu, Yunlong Shang, Quan Ouyang, and Widanalage Dhammika Widanage. A Data-Driven Approach with Uncertainty Quantification for Predicting Future Capacities and Remaining Useful Life of Lithium-ion Battery. *IEEE Transactions on Industrial Electronics*, 68(4):3170–3180, 2021.

[LTZ12] Fei Tony Liu, Kai Ming Ting, and Zhi Hua Zhou. Isolation-based anomaly detection. *ACM Transactions on Knowledge Discovery from Data*, 6(1):1–44, 2012.

[LXJL13] Bing Long, Weiming Xian, Lin Jiang, and Zhen Liu. An improved autoregressive model by particle swarm optimization for prognostics of lithium-ion batteries. *Microelectronics Reliability*, 53(6):821–831, 2013.

[LZP19] Yuefeng Liu, Guangquan Zhao, and Xiyuan Peng. Deep learning prognostics for lithium-ion battery based on ensembled long short-term memory networks. *IEEE Access*, 7(Mcmc):155130–155142, 2019.

[LZWD19] Xiaoyu Li, Lei Zhang, Zhenpo Wang, and Peng Dong. Remaining useful life prediction for lithium-ion batteries based on a hybrid model combining the long short-term memory and Elman neural networks. *Journal of Energy Storage*, 21(December 2018):510–518, 2019.

[Mas09] Hideyuki Noguchi Masaki Yoshio. *Lithium-Ion Batteries, Chapter 2*. 2009.

[MK19] Michael G. Pecht and Myeongsu Kang. *Prognostics and Health Management of Electronics*. John wiley edition, 2019.

[MSV+20] Juan José Montero Jimenez, Sébastien Schwartz, Rob Vingerhoeds, Bernard Grabot, and Michel Salaün. Towards multi-model approaches to predictive maintenance: A systematic literature survey on diagnostics and prognostics. *Journal of Manufacturing Systems*, 56(March):539–557, 2020.

[OHL+08] John D. Owens, Mike Houston, David Luebke, Simon Green, John E. Stone, and James C. Phillips. GPU computing. *Proceedings of the IEEE*, 96(5):879–899, 2008.

[PBF+20] Yuliya Preger, Heather M. Barkholtz, Armando Fresquez, Daniel L. Campbell, Benjamin W. Juba, Jessica Romàn-Kustas, Summer R. Ferreira, and Babu Chalamala. Degradation of Commercial Lithium-Ion Cells as a Function of Chemistry and Cycling Conditions. *Journal of The Electrochemical Society*, 167(12):120532, 2020.

[PGB07] I S McCrae P G Boulter. Artemis: Assessment and reliability of transport emission models and inventory systems – final report. *TRL Limited*, October 2007.

[PS16] Ieee Power and Energy Society. *IEEE Standard Glossary of Stationary Battery Terminology*. 2016.

[Puy01] Liu Puyin. Approximation capabilities of multilayer feedforward regular fuzzy neural networks. *Appl. Math.- J. Chin. Univ.*, 16(1):45–57, 2001.

[QLMF19] Jiantao Qu, Feng Liu, Yuxiang Ma, and Jiaming Fan. A Neural-Network-Based Method for RUL Prediction and SOH Monitoring of Lithium-Ion Battery. *IEEE Access*, 7:87178–87191, 2019.

[RDW+20] Lei Ren, Jiabao Dong, Xiaokang Wang, Zihao Meng, Li Zhao, and Jamal Deen. A Data-driven Auto-CNN-LSTM Prediction Model for Lithium-ion Battery Remaining Useful Life. *IEEE Transactions on Industrial Informatics*, 17(5):1–1, 2020.

[RDW+21] Lei Ren, Jiabao Dong, Xiaokang Wang, Zihao Meng, Li Zhao, and M. Jamal Deen. A Data-Driven Auto-CNN-LSTM Prediction Model for Lithium-Ion Battery Remaining Useful Life. *IEEE Transactions on Industrial Informatics*, 17(5):3478–3487, 2021.

[RFCS+18] Roozbeh Razavi-Far, Shiladitya Chakrabarti, Mehrdad Saif, Enrico Zio, and Vasile Palade. Extreme Learning Machine Based Prognostics of Battery Life. *International Journal on Artificial Intelligence Tools*, 27(8), 2018.

[ROC+18] Alvin Rajkomar, Eyal Oren, Kai Chen, Andrew M. Dai, Nissan Hajaj, Michaela Hardt, Peter J. Liu, Xiaobing Liu, Jake Marcus, Mimi Sun, Patrik Sundberg, Hector Yee, Kun Zhang, Yi Zhang, Gerardo Flores, Gavin E. Duggan, Jamie Irvine, Quoc Le, Kurt Litsch, Alexander Mossin, Justin Tansuwan, De Wang, James Wexler, Jimbo Wilson, Dana Ludwig, Samuel L. Volchenboum, Katherine Chou, Michael Pearson, Srinivasan Madabushi, Nigam H. Shah, Atul J. Butte, Michael D. Howell, Claire Cui, Greg S. Corrado, and Jeffrey Dean. Scalable and accurate deep learning with electronic health records. *npj Digital Medicine*, 1(1):1–10, 2018.

[RZH+18] Lei Ren, Li Zhao, Sheng Hong, Shiqiang Zhao, Hao Wang, and Lin Zhang. Remaining Useful Life Prediction for Lithium-Ion Battery: A Deep Learning Approach. *IEEE Access*, 6:50587–50598, 2018.

[SAJ+] K. A. Severson, Peter .M Attia, Norman Jin, Zi Yang, Nicholas Perkins, Michael H. Chen, M. Aykol, P.K. Herring, Dimitrios Fraggedakis, Martin Z. Bazant, Stephen J. Harris, William C. Chueh, and Richard D. Braatz. *(Supplementary information)Data-driven prediction of battery cycle life before capacity degradation*.

[SAJ+19] Kristen A. Severson, Peter M. Attia, Norman Jin, Nicholas Perkins, Benben Jiang, Zi Yang, Michael H. Chen, Muratahan Aykol, Patrick K. Herring, Dimitrios Fraggedakis, Martin Z. Bazant, Stephen J. Harris, William C. Chueh, and Richard D. Braatz. Data-driven prediction of battery cycle life before capacity degradation. *Nature Energy*, 4(5):383–391, 2019.

[Sam00] A. L. Samuel. Some studies in machine learning using the game of checkers. *IBM Journal of Research and Development*, 44(1-2):207–219, 2000.

[SAS17] Robert Schröder, Muhammed Aydemir, and Günther Seliger. Comparatively Assessing different Shapes of Lithium-ion Battery Cells. *Procedia Manufacturing*, 8(October 2016):104–111, 2017.

[Sch06] Arthur Schuster. On the Periodicities of sunspots. *Philosophical Transactions of the Royal Society of London*, 206(Series A, Containing Papers of a Mathematical or Physical Character):69–100, 1906.

[Sch15] Jürgen Schmidhuber. Deep Learning in neural networks: An overview. *Neural Networks*, 61:85–117, 2015.

[SGC09] Bhaskar Saha, Kai Goebel, and Jon Christophersen. Comparison of prognostic algorithms for estimating remaining useful life of batteries. *Transactions of the Institute of Measurement and Control*, 31(3-4):293–308, 2009.

[SHK+14] Nitish Srivastava, Geoffrey Hinton, Alex Krizhevsky, Ilya Sutskever, and Ruslan Salakhutdinov. Dropout: A simple way to prevent neural networks from overfitting. *Journal of Machine Learning Research*, 15:1929–1958, 2014.

[SLA12] Jasper Snoek, Hugo Larochelle, and Ryan P. Adams. Practical Bayesian optimization of machine learning algorithms. *Advances in Neural Information Processing Systems*, 4:2951–2959, 2012.

[SSL+20] Sheng Shen, Mohammadkazem Sadoughi, Meng Li, Zhengdao Wang, and Chao Hu. Deep convolutional neural networks with ensemble learning and transfer learning for capacity estimation of lithium-ion batteries. *Applied Energy*, 260(December 2019):114296, 2020.

[SVL14] Ilya Sutskever, Oriol Vinyals, and Quoc V. Le. Sequence to sequence learning with neural networks. *Advances in Neural Information Processing Systems*, 4(January):3104–3112, 2014.

[TF95] G Thimm and E Fiesler. Neural network initialization. In José Mira and Francisco Sandoval, editors, *From Natural to Artificial Neural Computation*, pages 535–542, Berlin, Heidelberg, 1995. Springer Berlin Heidelberg.

[TH12] Tijmen Tieleman and Geoffrey Hinton. Lecture 6.5 - RMSProp, COURSERA: Neural Networks for Machine Learning. Technical report, 2012.

[The10] The Boston Consulting group. Focus Batteries for Electric Cars, Challenges, Opportunities, and the Outlook to 2020. 2010.

[TNN+19] Khawla Tadist, Said Najah, Nikola S. Nikolov, Fatiha Mrabti, and Azeddine Zahi. Feature selection methods and genomic big data: a systematic review. *Journal of Big Data*, 6(1), 2019.

[TR15] Tanvir R. Tanim and Christopher D. Rahn. Aging formula for lithium ion batteries with solid electrolyte interphase layer growth. *Journal of Power Sources*, 294:239–247, 2015.

[VABA18] Amirthalakshmi Veeraraghavan, Viswa Adithya, Ajinkya Bhave, and Shankar Akella. Battery aging estimation with deep learning. *2017 IEEE Transportation Electrification Conference, ITEC-India 2017*, 2018-Janua:1–4, 2018.

[VR16] Claudio Vitari and Elisabetta Raguseo. *Digital data, dynamic capability and financial performance: an empirical investigation in the era of Big Data*, volume Volume 21. 2016.

[VSP+17] Ashish Vaswani, Noam Shazeer, Niki Parmar, Jakob Uszkoreit, Llion Jones, Aidan N. Gomez, Łukasz Kaiser, and Illia Polosukhin. Attention is all you need. *Advances in Neural Information Processing Systems*, 2017-Decem(Nips):5999–6009, 2017.

[WCZ+19] Jia Wu, Xiu Yun Chen, Hao Zhang, Li Dong Xiong, Hang Lei, and Si Hao Deng. Hyperparameter optimization for machine learning models based on Bayesian optimization. *Journal of Electronic Science and Technology*, 17(1):26–40, 2019.

[WFG16] Lifeng Wu, Xiaohui Fu, and Yong Guan. Review of the remaining useful life prognostics of vehicle lithium-ion batteries using data-driven methodologies. *Applied Sciences (Switzerland)*, 6(6), 2016.

[WKW16] Karl Weiss, Taghi M. Khoshgoftaar, and Ding Ding Wang. *A survey of transfer learning*, volume 3. Springer International Publishing, 2016.

[wYPO16] Gae won You, Sangdo Park, and Dukjin Oh. Real-time state-of-health estimation for electric vehicle batteries: A data-driven approach. *Applied Energy*, 176:92–103, 2016.

[YPO17] Gae Won You, Sangdo Park, and Dukjin Oh. Diagnosis of Electric Vehicle Batteries Using Recurrent Neural Networks. *IEEE Transactions on Industrial Electronics*, 64(6):4885–4893, 2017.

[ZdCd+20] Tiago Zonta, Cristiano André da Costa, Rodrigo da Rosa Righi, Miromar José de Lima, Eduardo Silveira da Trindade, and Guann Pyng Li.

Predictive maintenance in the Industry 4.0: A systematic literature review. *Computers and Industrial Engineering*, 150(October):106889, 2020.

[zKYZ+21] Jin zhen Kong, Fangfang Yang, Xi Zhang, Ershun Pan, Zhike Peng, and Dong Wang. Voltage-temperature health feature extraction to improve prognostics and health management of lithium-ion batteries. *Energy*, 223:120114, 2021.

[ZRFG17] Shuai Zheng, Kosta Ristovski, Ahmed Farahat, and Chetan Gupta. Long Short-Term Memory Network for Remaining Useful Life estimation. In *2017 IEEE International Conference on Prognostics and Health Management, ICPHM 2017*, pages 88–95. Institute of Electrical and Electronics Engineers Inc., jul 2017.

[ZTZ+20] Yunwei Zhang, Qiaochu Tang, Yao Zhang, Jiabin Wang, Ulrich Stimming, and Alpha A. Lee. Identifying degradation patterns of lithium ion batteries from impedance spectroscopy using machine learning. *Nature*, (April), 2020.

[ZXHL17] Yongzhi Zhang, Rui Xiong, Hongwen He, and Zhiru Liu. A LSTM-RNN method for the lithuim-ion battery remaining useful life prediction. *2017 Prognostics and System Health Management Conference, PHM-Harbin 2017 - Proceedings*, (20150098), 2017.

Résumé en français de la thèse de doctorat

1 Introduction

1.1 Contexte

En France comme dans beaucoup d'autres pays du monde, la grande majorité des déplacements se fait en véhicules individuels motorisés, qu'il s'agisse de voitures ou de deux-roues. Le secteur des transports est responsable de 15 % des émissions de gaz à effet de serre dans le monde, et de 30 % en France. Le Parlement européen a réaffirmé sa position concernant l'objectif de zéro émission pour le secteur des transports d'ici 2035 [Eur21]. Parmi d'autres mesures, un texte a été adopté pour interdire la commercialisation de véhicules thermiques neufs d'ici à cette date. À ce jour, les véhicules électriques (VE) constituent la seule alternative sérieuse aux véhicules thermiques. Les batteries les plus répandues dans les VE sont les batteries lithium-ion (Li-Ion), qui sont récemment devenues un sujet d'intérêt et de préoccupation. Les ressources nécessaires à la construction des VE, et plus particulièrement des batteries Li-Ion, ont fait l'objet d'une prise de conscience collective.

L'utilisation de ces batteries est l'une des principales raisons pour lesquelles la diffusion des VE est ralentie. Elles comptent pour la majeure partie du prix d'un VE, et bien que la recherche dans le domaine des transports ait porté les performances des VE au même niveau que celles des véhicules thermiques, l'un des arguments le plus souvent cité à l'encontre des VE réside dans leur manque d'autonomie.

L'électrification des transports ne sera efficace dans le contexte global de la transition écologique que sous certaines conditions. Dans cette optique, les VE pourraient devenir un maillon essentiel dans la chaîne des mobilités durables.

L'une des façons d'améliorer les VE est de travailler sur la structure des véhicules eux-mêmes et sur la gestion de l'énergie à la fois à l'intérieur des véhicules et du point de vue de l'utilisateur. L'un des meilleurs moyens d'atténuer la tension sur les matières premières est de développer des véhicules de taille optimale pour répondre aux besoins réels des utilisateur·ice·s et de réduire autant que possible les émissions de carbone liées à la conception des véhicules et des batteries. Les modes de mobilités sobres doivent être explorés davantage, avec des véhicules plus petits et plus légers et des batteries plus petites. Récemment, la société CATL a travaillé sur des batteries condensées[1], qui pourraient permettre à des batteries deux fois plus petites que les modèles actuels de transporter la même quantité d'énergie. Du côté français, la société Tiamat a travaillé sur des batteries sodium-ion pour la mobilité et le stockage stationnaire de l'énergie [2]. Cette technologie de batteries offre une densité de puissance plus élevée que les batteries Li-Ion (de 1 à 5 kW/kg pour les batteries sodium-ion contre 0,5 à 1 kW/kg pour les batteries Li-Ion) et une durée de vie plus longue (jusqu'à 8000 cycles pour les batteries sodium-ion).

Des véhicules et des batteries conçus pour être réparables et recyclables, avec une autonomie raisonnable pour les trajets quotidiens, et un système de gestion de l'énergie efficace sont les points clés pour que les véhicules électriques soient vraiment propres.

[1] "CATL launches condensed battery with an energy density of up to 500 Wh/kg, enables electrification of passenger aircrafts", 19 Apr 2023.

[2] " Nous voulons créer en France un Tesla de la batterie sodium-ion ", affirme Laurent Hubard, directeur de Tiamat Energy (Consulté en septembre 2023)

La gestion de l'énergie, quant à elle, consiste à faire le meilleur usage possible de la batterie. Du côté du véhicule, il peut s'agir d'équilibrer les cellules d'un pack de batteries, de limiter les pics de courant, de réchauffer la batterie avant la charge, de la refroidir pendant la conduite... Du côté des usagers, il est très important d'identifier les comportements les plus dommageables pour la batterie. De cette manière, un retour d'information pourrait être effectué afin d'éviter les situations dangereuses et d'aider les utilisateur·ice·s à développer une conduite écologique et responsable.

1.2 Structure de la thèse et contributions

Dans le cadre de cette thèse, l'amélioration des performances des batteries a été étudiée en se concentrant sur la recherche de données brutes de fonctionnement des batteries Li-Ion, en les rendant utilisables dans un algorithme d'apprentissage automatique et en construisant des modèles prédictifs. Dans les chapitres de contributions théoriques, plusieurs modèles seront présentés, en mettant l'accent sur les données. Des informations sont données sur le type de données utilisées et sur ce qui est extrait des données brutes afin d'entraîner des modèles d'apprentissage automatique. L'objectif des trois contributions théoriques qui seront détaillées est de trouver un moyen de lier la façon dont une batterie est utilisée à son stade de vieillissement et d'identifier à l'avance l'impact d'une certaine utilisation sur la capacité de stockage.

Dans le premier chapitre, les outils théoriques nécessaires à la compréhension des contributions sont décrits, ainsi que les principes fondamentaux du fonctionnement des batteries Li-Ion et les approches existantes concernant la maintenance prévisionnelle des batteries Li-Ion. Dans le chapitre 2, la première contribution est détaillée. Cette première contribution est liée à la prédiction de la durée de vie restante (RUL) des cellules Li-Ion testées par le MIT dans un jeu de données décrit de manière étendue. Dans le troisième chapitre, un modèle de prédiction du SOH en fonction des données d'utilisation (courant tension et température) est décrit. La prédiction est faite à partir de données provenant d'une fenêtre de plusieurs cycles d'utilisation consécutifs et consiste en une seule valeur future de SOH (de 25 à 400 cycles en avance). Dans le chapitre 4, la même fenêtre d'utilisation est reprise en entrée d'un modèle plus complexe, de type Sequence to Sequence (Seq2Seq). Ce modèle permet de prédire une séquence complète de SOH jusqu'à la fin de vie d'une batterie. Enfin, dans le cinquième et dernier chapitre, le dispositif expérimental conçu pour faire cycler des batteries selon des sollicitations sur mesure et récolter des données de fonctionnement est présenté.

2 État de l'art (Chapitre 1)

2.1 Outils théoriques

2.1.1 Type de données exploitées

Cette thèse porte sur l'exploitation de séries temporelles relevées lors de l'utilisation des batteries Li-Ion (majoritairement des données de courant, tension et température). Ces séries temporelles sont discrètes, multi-variées et synchrones. Les modèles développés prennent en entrée plusieurs variables pour prédire un seul signal à la fois (soit le RUL soit le SOH). Les variables d'entrées et de sortie sont systématiquement distinctes

(aucun signal en entrée du modèle ne se retrouve dans le résultat de prédiction), donc les modèles sont dits exogènes. Tous les modèles développés sont des modèles régressifs, qui permettent de prédire une ou plusieurs valeurs futures d'un seul signal à partir de plusieurs séries temporelles multi-variées.

Avant d'être exploitées dans les modèles d'apprentissages, les données brutes font l'objet d'un pré-traitement en plusieurs étapes. Le but du pré-traitement de données est d'extraire des paramètres représentatifs du phénomène de vieillissement des batteries en lien avec leur mode d'utilisation, puis de sélectionner les paramètres les plus pertinents afin de réduire la quantité de données à prendre en compte lors de la phase d'apprentissage.

2.1.2 Modèles d'apprentissage

Les modèles développés dans cette thèse sont des modèles d'apprentissage automatique, qui est une branche de l'intelligence artificielle. L'apprentissage automatique permet de tirer de la connaissance à partir de données réelles grâce à un processus d'apprentissage. L'objectif de ce processus est de trouver une fonction mathématique capable d'associer les données d'entrée à une sortie correspondante. La fonction mathématique qui résulte du processus d'apprentissage est ce que l'on appelle le modèle, qui sera utilisé pour prendre des décisions. Les modèles décrits dans les trois chapitres de contributions théoriques sont des modèles d'apprentissage supervisés, basés sur des réseaux de neurones de différents types selon les données traitées et la prédiction faite. Ces réseaux peuvent être à propagation directe (figure 2) ou récurrents (Recurrent Neural Networks, RNN), de type Long Short Term Memory (LSTM) (figure 3).

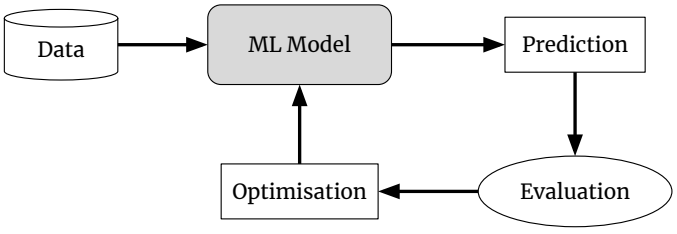

Figure 1: Principe du processus d'apprentissage

2.2 Les batteries Li-Ion

Les batteries Lithium-Ion (Li-Ion) connaissent un véritable essor depuis les années 1990, de fait de la popularisation massive des véhicules électriques.

Les batteries Li-Ion, et les batteries en général, sont des dispositifs de stockage de l'énergie électrique. Ce sont des dispositifs électrochimiques qui convertissent l'énergie chimique en électricité dans les deux sens. Toutes les batteries, quelle que soit leur composition chimique, sont composées d'une *anode* (électrode négative) et d'une *cathode* (électrode positive). Les deux électrodes flottent dans un *électrolyte* et sont séparées par une membrane appelée *séparateur*. Dans les batteries Li-Ion, la cathode est protégée du contact direct avec l'électrolyte par un filtre appelé *interface électrolyte solide* (SEI). Le principe de fonctionnement d'une batterie Li-Ion est résumé dans la figure 4.

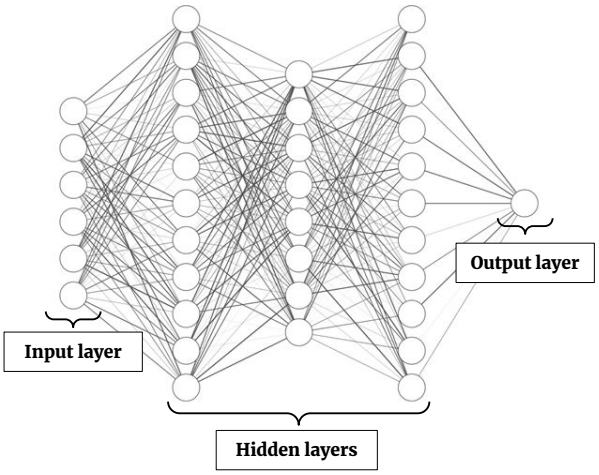

Figure 2: Structure d'un réseau de neurone artificiel à propagation directe

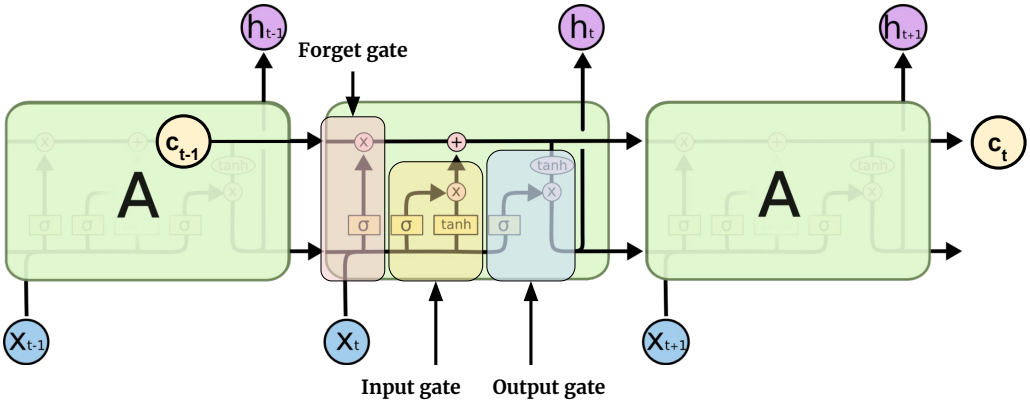

Figure 3: Structure d'un RNN de type Long Short Term Memory (LSTM)

Le phénomène de vieillissement d'une batterie Li-Ion peut provenir de nombreux facteurs externes et internes. Les mécanismes physiques tels que le stress thermique ou mécanique peuvent influencer la dégradation (par exemple avec une température externe élevée, des vibrations dues à l'état de la route, etc.) Les mécanismes chimiques se produisent à l'intérieur de la batterie et peuvent être divisés en deux modes de dégradation principaux : La perte lithium, qui est causée par la consommation d'ions lithium par le biais de réactions secondaires et la perte de matière active, qui entraîne une perte de capacité de stockage. Les mécanismes de dégradation d'une batterie sont résumés dans la figure 5.

2.3 Données de vieillissement de batteries

Les modèles développés étant des modèles d'apprentissage, les données de vieillissement jouent un rôle essentiel.

Les données de fonctionnement des batteries Li-Ion à l'intérieur des véhicules sont très difficiles à obtenir en raison des défis liés aux performances des batteries. Il est très fréquent que les constructeurs automobiles gardent confidentielles toutes les informations relatives aux batteries et à leur gestion afin d'être compétitifs et de gagner des parts de marché dans le secteur de l'automobile. Par conséquent, la plupart des

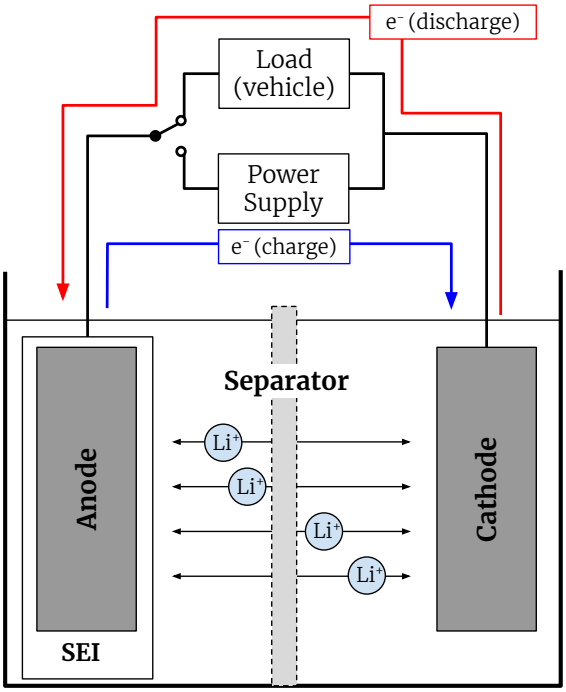

Figure 4: Schéma de fonctionnement d'une batterie Li-Ion

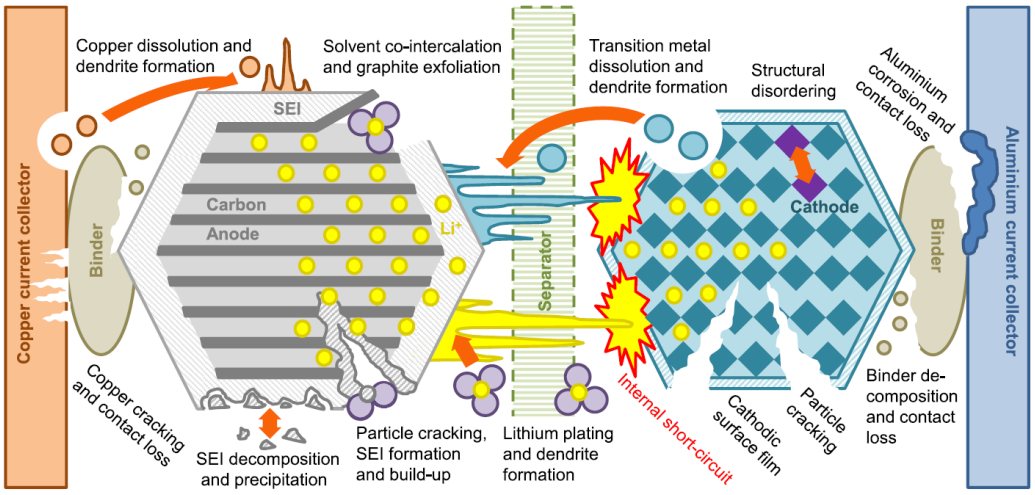

Figure 5: Mécanismes de dégradation dans les batteries Li-Ion [BRM+17]

données accessibles au public proviennent de laboratoires qui ont mené des recherches sur les performances des batteries Li-ion dans différents contextes et avec différents objectifs. L'acquisition de données sur le vieillissement des batteries Li-Ion peut prendre beaucoup de temps et nécessiter beaucoup de ressources, car elles sont si performantes qu'un grand nombre de cycles est nécessaire pour observer une détérioration. En outre, les dispositifs d'essai sont très coûteux, d'autant plus dans des conditions d'essai extrêmes (telles que des températures contrôlées élevées ou basses dans des chambres climatiques). Afin de réduire les coûts et la puissance nécessaire pour tester les batteries, il est presque systématique d'utiliser des cellules et non des packs batteries complets. En effet, la puissance requise pour charger ou décharger complètement des batteries de véhicules est beaucoup plus élevée qu'avec des cellules isolées. Les princi-

Table 1: Principaux jeux de données publics sur le vieillissement de cellules Li-Ion

Nom du jeu de données	**Organisme**	**# Cellules**	**Année**	**Remarques**
PCoE Battery Dataset	NASA Ames	34	2008-2010	
Cycle Life Prediction Dataset	MIT - Stanford University	124	2017-2018	
Short-Term Cycling Performance Dataset	Sandia National Laboratories	24	2017	Chimies et températures différentes
Long-Term Degradation Dataset	Sandia National Laboratories	86	2018-2020	Chimies, températures et profondeurs de décharge différentes
Oxford Battery Degradation Dataset	Oxford University	8	2015	Profils de conduite

paux jeux de données disponibles dans la littérature et exploités dans cette thèse sont résumés dans le tableau 2

2.4 Approches existantes pour la maintenance prévisionnelle des batteries Li-Ion

En ce qui concerne les batteries, la maintenance prévisionnelle vise à déterminer comment et quand une défaillance se produira en fonction des données de fonctionnement antérieures acquises par divers capteurs, mais vise également à donner une image à long terme de l'état de santé de la batterie [WWYL19]. Dans une grande majorité d'articles, la maintenance prévisionnelle des batteries Li-Ion consiste à déterminer leur durée de vie utile restante. Une batterie est considérée comme hors d'usage pour un véhicule électrique lorsqu'elle a atteint 80% de son état de santé initial (fig 6).

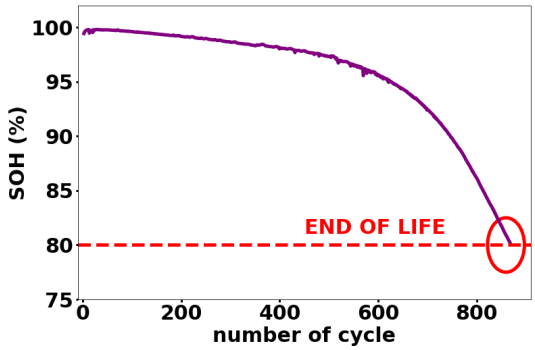

Figure 6: Evolution of SOH, from 100% to 80%

La plupart des approches traitent de la prédiction de la RUL en termes de cycles. Cela peut se faire soit en prévoyant l'évolution temporelle du SOH de la batterie, soit

en effectuant une régression directe sur le RUL.

Dans les deux cas (prédiction SOH ou RUL), on trouve une grande variété d'approches dans la littérature. Les approches basées sur les données pour la maintenance prévisionnelle des batteries peuvent être classées en trois catégories : **Modèles autorégressifs non linéaires** (NAR), **Modèles autorégressifs non linéaires avec variables exogènes** (NARX), et **Modèles régressifs non linéaires avec variables exogènes** (NRX).

2.5 Modèles autorégressifs non linéaires

L'approche NAR consiste à observer une fenêtre de valeurs passées du SOH pour prédire la tendance future du SOH. Dans la plupart des approches NAR, les réseaux de neurones récurrents (RNN) sont utilisés en raison de leur capacité à apprendre des représentations à partir de séquences de données. Dans [LZWD19], Li *et al.* ont combiné la décomposition en mode empirique des courbes de SOH avec les réseaux de neurones d'Elmann et des LSTM. Zhang *et al.* dans [**?**] et Liu dans [LZP19] ont également divisé les courbes SOH en fenêtres successives afin de les prendre comme entrée de plusieurs réseaux LSTM.

2.6 Modèles autorégressifs non linéaires avec variables exogènes

Les approches NARX diffèrent des approches NAR par l'inclusion d'autres variables d'entrée dans les modèles prédictifs. Le SOH est combiné à d'autres paramètres représentatifs du phénomène de vieillissement afin de prédire la tendance future du SOH avec plus de précision. Dans [KY19], Khumprom et Yodo ont utilisé des paramètres extraits des courbes de courant et de tension pour prédire le futur SOH avec un réseau de neurones à propagation directe.

2.7 Modèles régressifs non linéaires avec variables exogènes

Avec les approches NRX, seules les variables exogènes sont utilisées pour prédire le SOH ou le RUL. Pour la prédiction du SOH avec les approches NRX, seules les caractéristiques extraites des séries temporelles telles que le courant et la tension sont utilisées comme entrée du modèle. Pour la prédiction du RUL, seul le SOH ou une combinaison du SOH et d'autres caractéristiques peuvent être utilisés. Dans [YPO17], You, Park et Oh ont isolé des fenêtres de courant et de tension comme entrée d'un modèle LSTM multiple. Ren *et al.* dans [RZH$^+$18] ont extrait des caractéristiques des courbes temporelles avec des auto-encodeurs, combinés avec des réseaux de neurones à convolutions et des LSTM pour la prédiction du RUL.

3 Contributions de cette thèse

3.1 Prédiction de la durée de vie restante (RUL) à partir de paramètres historiques (Chapitre 2)

Ce chapitre décrit les travaux réalisés concernant une estimation précoce et hors ligne de la durée de vie globale des batteries Li-Ion et une prédiction en ligne de la durée de vie utile d'une batterie. Une analyse des données fournies par le MIT

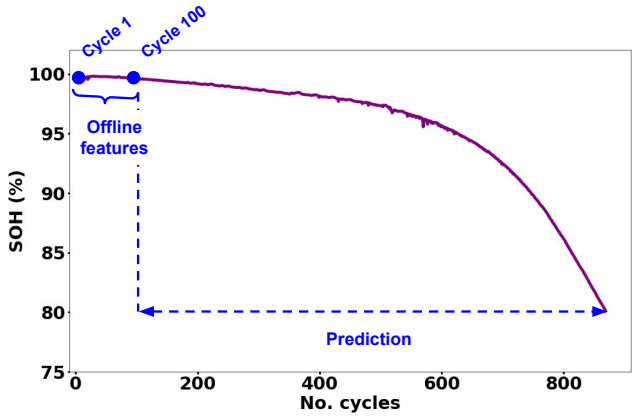

Figure 7: Stratégie de prédiction de la durée de vie globale hors ligne

est tout d'abord effectuée. Plusieurs indicateurs de santé sont extraits des données d'exploitation brutes. Selon le type de prédiction (prédiction de la durée de vie du cycle *hors ligne* ou prédiction de la durée de vie utile *en ligne*), deux modèles sont conçus et évalués, sur la base de structures de données et d'indicateurs de santé différents. Cette approche établit un lien direct entre les données de fonctionnement de la batterie et sa durée de vie.

La stratégie *hors ligne* pour l'estimation de la durée de vie globale décrite dans ce chapitre consiste à comparer l'état d'une batterie neuve qui n'a subi aucune phase de charge ou de décharge avec l'état de la même batterie après 100 cycles de fonctionnement complets (charges et décharges complètes successives), comme cela a été fait dans l'étude de [SAJ+]. Les batteries Li-Ion étant très efficaces et l'utilisation des batteries étant identique du début à la fin de vie dans l'ensemble des données du MIT, des dommages minimes sont observés entre le cycle 0 et le cycle 100. Néanmoins, le moindre changement dans les performances de la batterie après 100 cycles d'utilisation peut être exploité pour estimer sa durée de vie globale. La stratégie de prédiction hors ligne est décrite dans la figure 7. Plusieurs paramètres sont extraits de la comparaison entre les courbes de capacité et de résistance interne aux cycles 1 et 100, aux cycles 4 et 5 et directement au cycle 2.

La stratégie *en ligne* pour la prédiction de la durée de vie utile décrite dans ce chapitre consiste à observer chaque cycle de fonctionnement d'une batterie et à en extraire des indicateurs de santé. Ces indicateurs de santé sont utilisés comme données d'entrée dans un modèle d'estimation qui permet une prédiction en ligne de l'autonomie d'une batterie. Cela signifie que pour chaque batterie, chaque cycle d'utilisation peut être utilisé comme entrée du modèle d'estimation, et qu'il peut y avoir autant de prédictions que le nombre de cycles dans la vie d'une batterie (voir figure 8). Pour chaque cycle d'utilisation, plusieurs paramètres sont extraits des données historiques (le SOH, la résistance interne (IR), le temps de charge, ...), ainsi que des courbes de température (T_{moy}, T_{min}, T_{max}, ...) et sont ensuite exploités en entrée d'un réseau de neurones à propagation directe pour prédire le RUL (voir fig 11).

La figure 11 montre les performances de prédiction du modèle en ligne pour la prédiction RUL. Le tableau 2 compare les performances du modèle de prédiction de la durée de vie globale hors ligne et de la prédiction du RUL en ligne avec d'autres approches de la littérature, basées sur le même ensemble de données et d'autres modèles de prédiction du RUL. Le modèle en ligne atteint une erreur absolue de 9,25 cycles en

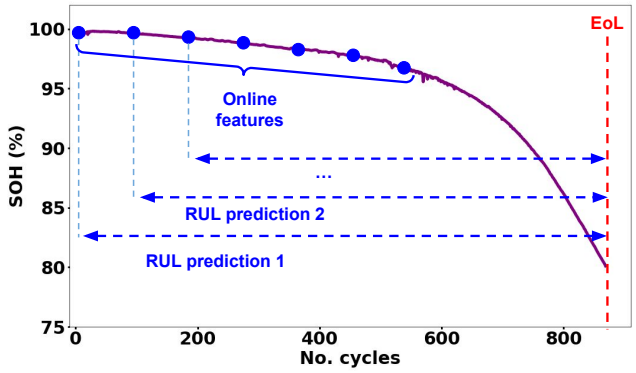

Figure 8: Stratégie de prédiction de la durée de vie globale en ligne

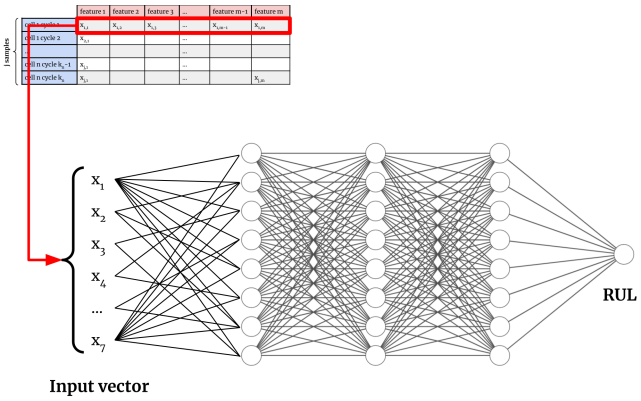

Figure 9: Structure du réseau de neurones pour la prédiction en ligne de la RUL

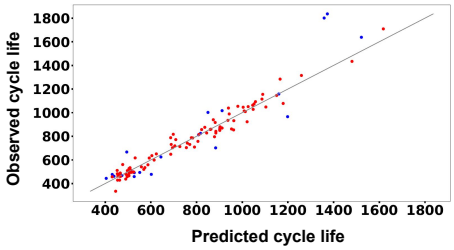

Figure 10: Performances de prédiction de la durée de vie globale hors ligne

moyenne et surpasse les deux autres approches décrites dans [SAJ+] et [HK19].

Bien que cette approche donne des résultats très précis pour la prédiction de la durée de vie utile des cellules, elle présente certaines lacunes. La méthode en ligne ne prend en compte que les caractéristiques historiques et certains paramètre extraits de courbes de température, ce qui signifie que les séries temporelles de la tension et de la température ne sont pas prises en compte. En outre, chaque cycle de la vie d'une cellule est considéré comme un échantillon d'entrée du modèle d'apprentissage, ce qui signifie que tous les cycles sont considérés comme indépendants. Afin d'étudier l'impact des conditions de fonctionnement d'une batterie sur son SOH, les séries temporelles du courant, tension et température doivent être prises en compte.

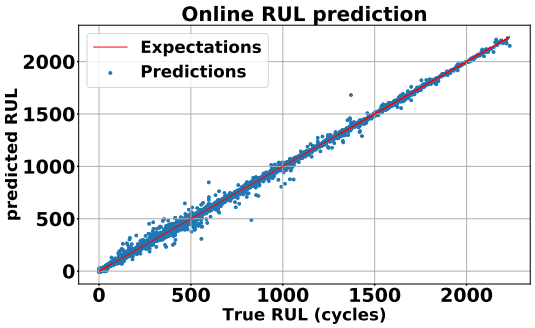

Figure 11: Performance de prédiction en ligne du RUL

Table 2: Comparaison des performances de prédiction du modèle en ligne avec la littérature

	RMSE	MAE	MAPE
Prédiction hors ligne de la durée de vie globale	115,95	81,91	10,09
Prédiction en ligne du RUL	**12.25**	**5.76**	**4.26 %**
LR from [SAJ+]	173	N/A	8.6 %
CNN from [HK19]	N/A	115	N/A

3.2 Prédiction de l'état de santé (SOH) à partir de séries temporelles (Chapitre 3)

La deuxième contribution de cette thèse consiste à compléter le modèle de prédiction en ligne du RUL basé sur les cycles par un modèle capable de prédire le SOH d'une batterie en fonction de ses conditions d'utilisation. Ce modèle de prédiction du SOH est basé sur l'utilisation de modèles non linéaires régressifs avec des variables exogènes, utilisant uniquement des caractéristiques externes extraites des données de conduite pour prédire les valeurs futures du SOH (courbes de courant, de tension et de température).

Dans ce chapitre, deux modèles sont décrits. Ces deux modèles permettent d'extraire des paramètres des séries temporelles de courant, tension et température deux deux manière différentes : grâce à un modèle d'apprentissage d'une part (Auto-encodeur) et par des méthodes calculatoires d'autre part (TFS). Ces paramètres extraits sont utilisés en entrée de deux modèles différents, respectivement référencés sous les termes **AE-XLSTM** et **TSF-XLSTM**. Ces deux modèles sont basés sur l'utilisation de réseaux de neurones récurrents de types LSTM.

Avec les deux modèles, les prédictions de SOH peuvent être faites à très court terme ou à plus long terme. L'ensemble de données d'entraînement pour la prédiction du SOH dans cette approche est construit de manière à ce que plusieurs horizons de prédiction soient possibles. Les valeurs futures du SOH sont prédites de 25 à 400 cycles à l'avance.

Dans les figures 12 et 13, une comparaison est faite entre la courbe réelle du SOH et la courbe prédite, pour des prédictions à 50 cycles d'avance avec l'AE-XLSTM et des prédictions à 25 cycles d'avance avec le TSF-XLSTM.

Le tableau 3 montre que le modèle TSF-XLSTM est plus performant que le modèle AE-XLSTM. Pour une prédiction du SOH à 50 cycles d'avance, le TSF-XLSTM

Table 3: Comparaison des performances de prédiction du SOH, 50 cycles à l'avance, sur les cellules du MIT

	MAE ($*10^{-2}$)	$\overline{\sigma_{AE}}$ ($*10^{-2}$)	RMSE ($*10^{-2}$)	NMSE ($*10^{-1}$)
TSF-XLSTM	**1.1**	**1.2**	**1.6**	**0.1**
AE-XLSTM	2.4	1.2	2.8	8.1

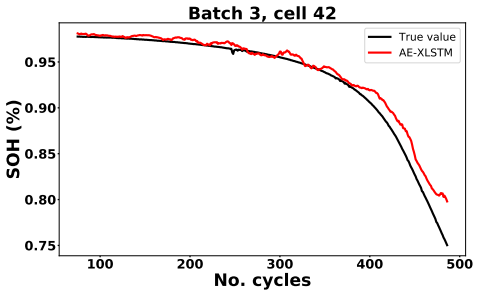

Figure 12: AE-XLSTM
Prédiction du SOH 50 cycles en avance

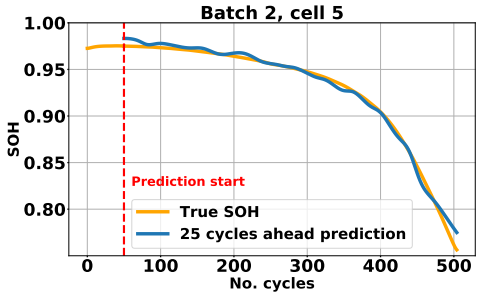

Figure 13: TSF-XLSTM
Prédiction du SOH 25 cycles en avance

présente une RMSE de $1,6 * 10^{-2}$ contre $2,8 * 10^{-2}$ pour l'AE-XLSTM.

Le modèle TSF-XLSTM est moins complexe car il n'utilise que des LSTM dans le modèle lui-même, contrairement au modèle AE-XLSTM qui fait entrer en jeu un Auto-encodeur en amont du LSTM. Le pré-traitement des données nécessite de faibles capacités de calcul car des caractéristiques très simples sont extraites des séries temporelles.

Bien que ces modèles aient de très bonnes performances, ils ne prédisent qu'une seule valeur de SOH dans le futur. En prédisant une séquence complète de SOH à partir d'une fenêtre de plusieurs cycles consécutifs, l'impact d'une utilisation donnée sur le SOH d'une batterie pourrait être étudié plus précisément.

3.3 Utilisation d'un modèle de type Seq2Seq pour la prédiction de séquences d'état de santé (SOH) (Chapitre 4)

La dernière contribution de cette thèse consiste à améliorer la méthode précédente de prédiction du SOH en produisant une séquence complète de SOH plutôt qu'un point unique. Le problème passe d'une régression sur le SOH à une approche de prédiction de séquence à séquence. Une telle approche a été mise en œuvre dans [LSD+21]. Dans cet article, des chercheur·euse·s de l'université allemande d'Aix-la-Chapelle décrivent un nouvel ensemble de données sur le vieillissement des batteries Li-Ion, qui a servi à construire un modèle de type séquence à séquence (Seq2Seq) permettant de prédire la dégradation de la capacité.

Le principe de la prédiction Seq2Seq repose sur l'utilisation de cellules LSTM construites comme un Encodeur-Décodeur. Le modèle décrit dans [LSD+21] est un modèle NAR, ce qui signifie que seules les valeurs passées de SOH sont utilisées pour prédire les valeurs futures. Nous avons adapté cette approche pour transformer le modèle de prédiction de séquences de SOH en un modèle NRX, qui prenne en entrée une fenêtre fixe de 25 cycles consécutifs d'utilisation d'une cellule (représentés par des paramètres extraits des séries temporelles de courant, tension et température) et qui

prédise l'évolution du SOH de cette cellule jusqu'à la fin de sa vie. De plus, le modèle a été adapté pour pouvoir l'entraîner sur les données issues du MIT et non plus celles fournies par l'université d'Aix-la-Chappelle.

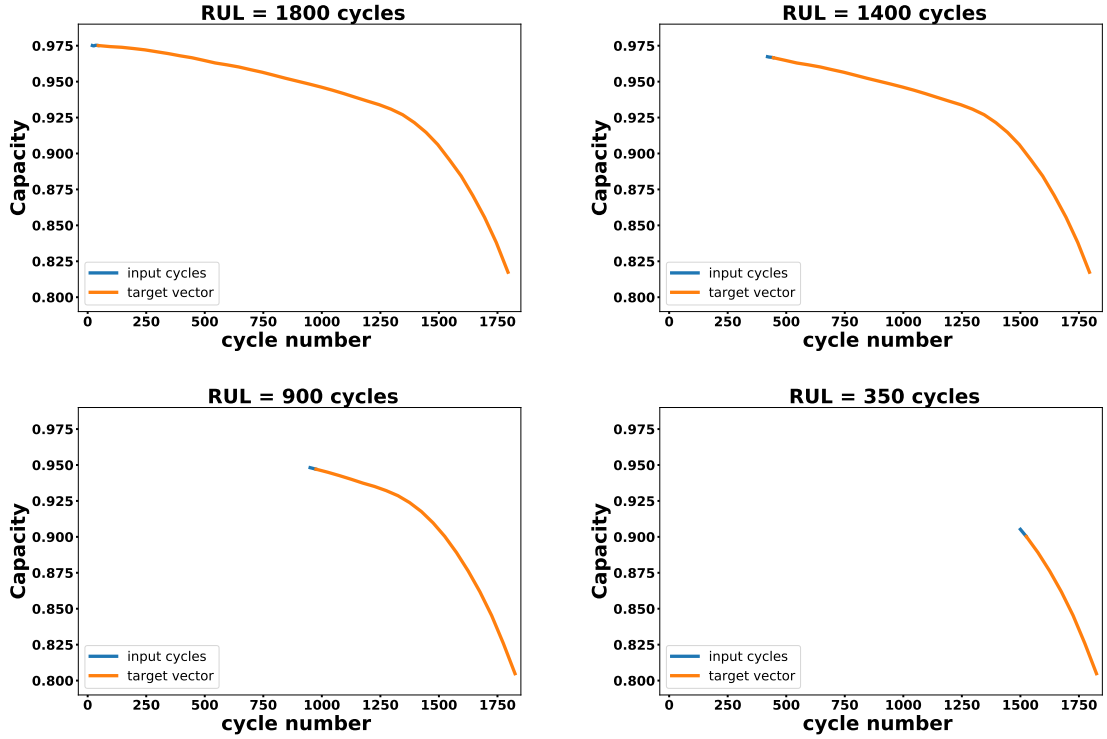

Figure 14: Principe des fenêtres glissantes pour la prédiction de séquences de SOH

La figure 15 montre les performances de prédiction de notre TSF-XSeq2Seq pour la prédiction du SOH à partir d'une seule fenêtre de 25 cycles consécutifs sur la cellule b1c17 du jeu de donnée du MIT et à deux moments différent dans la vie de la cellule. Dans le tableau 4, une comparaison est faite entre les performances du modèle de [LSD+21] et notre TSF-XSeq2Seq. Pour chaque métrique d'erreur, deux mesures sont fournies : l'erreur obtenue lors de la première prédiction possible à partir de la première fenêtre d'entrée extraite des séries temporelles de courant, tension et température de chaque cellule de l'ensemble de test, et l'erreur moyenne obtenue sur l'ensemble des fenêtres d'entrée de toutes les cellules de test.

Il apparaît clairement que notre modèle NRX est plus performant que le modèle endogène basé sur les données d'Aix-la-Chapelle. Tant pour la prédiction précoce que sur la moyenne de toutes les prédictions possibles, notre TSF-XSeq2Seq a des erreurs plus faibles et une meilleure réplicabilité des résultats.

3.4 Dispositif expérimental (Chapitre 5)

Le dernier chapitre de cette thèse décrit le travail effectué pour construire notre propre ensemble de données sur le vieillissement de cellules de batteries Li-Ion, avec une présentation détaillée du banc d'essai, des capteurs, des dispositifs utilisés et des protocoles d'essai.

L'objectif est de construire un banc d'essai complet pour différents types de cellules de batterie et d'obtenir des données de vieillissement à partir d'un dispositif de cyclage

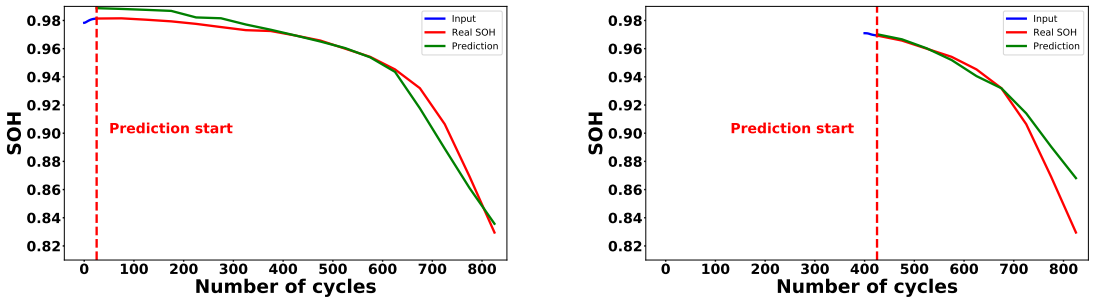

(a) Prédiction en début de vie

(b) Prédiction en milieu de vie

Figure 15: Prédiction de séquences complètes de SOH sur la cellule b1c17

Table 4: Comparaison des performances de prédiction entre la méthode [LSD$^+$21] sur les données d'Aix-la-Chapelle et le TSF-XSeq2Seq sur les données MIT

		[LSD$^+$21]	TSF-XSeq2Seq
MAPE	En moyenne	3.34	2.60
	1$^{\text{ère}}$ prédiction	4.50	2.95
MAE	En moyenne	0.04	0.02
	1$^{\text{ère}}$ prédiction	0.05	0.03
σ_{AE}	En moyenne	0.03	0.01
	1$^{\text{ère}}$ prédiction	0.05	0.02
RMSE	En moyenne	0.05	0.03
	1$^{\text{ère}}$ prédiction	0.08	0.04
RMSPE	En moyenne	4.37	3.24
	1$^{\text{ère}}$ prédiction	6.78	4.11

de batterie.

Plusieurs protocoles d'essai ont été établis et différentes cellules de batterie peuvent être testées en même temps en suivant des cycles de charge et de décharge prédéfinis. Notre objectif est de constituer un ensemble de données complet avec une très large gamme de tests représentatifs de l'utilisation réelle des batteries dans les VE. Par exemple, les tests qui ont été définis avec le cycleur correspondent à des phases de charge rapide, standard ou lente et à des conditions de décharge qui sont définies d'après plusieurs cycles de conduite normalisés.

Les tests actuels ont été lancés en janvier 2022. Neuf mois plus tard, plusieurs batteries ont vu leur SOH passer sous la barre des 80%, mais pour la plupart des cellules, les tests se poursuivent.

Certaines cellules NMC ont atteint leur fin de vie, tandis que la capacité des batteries LFP a à peine baissé. Certains tests seront poursuivis au-delà des 80% de dégradation pour observer l'évolution du SOH.

4 Conclusion et travaux futurs

Dans cette thèse, trois modèles majeurs sont construits et tirent parti d'un jeu de données publié par le département d'ingénierie chimique du MIT, en collaboration avec

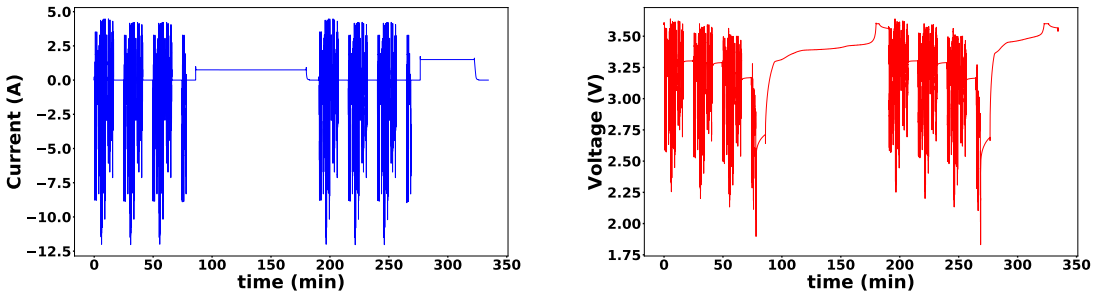

(a) Courant (b) Tension

Figure 16: Charge lente suivie d'une charge rapide

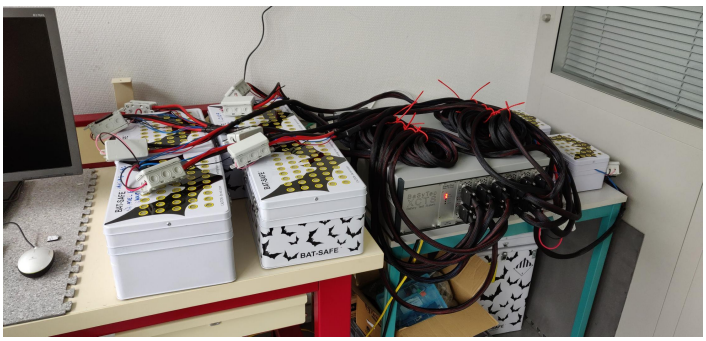

Figure 17: Installation du banc de test

Toyota engineering et avec le département de science des matériaux et d'ingénierie de l'université de Stanford [SAJ+19].

Ces modèles sont très théoriques et suggèrent l'utilisation de cellules de batterie individuelles au lieu de packs batterie complets. Cependant, malgré leur caractère théorique, ces approches sont prometteuses et pourraient être appliquées à diverses autres situations. Il a été démontré que même avec une quantité minimale de signaux d'entrée extraits des courbes de courant, tension et température, il est possible d'obtenir des informations précieuses sur l'environnement de la batterie et ses modes d'utilisation. Les différentes contributions décrites permettent de prédire avec fiabilité la durée de vie restante et l'évolution de l'état de santé de cellules Li-Ion, en fonction de leur mode d'utilisation et à tout moment de leur vie.

Les perspectives d'évolution de ces travaux sont nombreuses. La quantité de données générées par le banc d'essai décrit dans le chapitre 5 n'était pas suffisante au moment de la publication des travaux pour pouvoir entraîner un modèle complet. Une première amélioration consisterait en l'emploi de ces données au sein des algorithmes d'apprentissage, suivi de la publication des données dans une démarche de science ouverte.

Le but de la maintenance prévisionnelle est de prendre en compte l'évolution d'un système dans son environnement d'utilisation pour prédire de potentielles défaillances. Le fait d'embarquer les modèles développés dans des systèmes de gestion de la batterie embarqués permettrait d'en exploiter tout le potentiel.

Université de Strasbourg

Inès JORGE

Machine-learning-based predictive maintenance for Lithium-Ion batteries in electric vehicles

École doctorale Mathématiques, sciences de l'information et de l'ingénieur | ED 269 Université de Strasbourg

Résumé

La batterie est un élément central des véhicules électriques, soumis à de nombreux enjeux en termes de performances, sécurité et coût. La durée de vie des batteries en particulier fait l'objet d'une grande attention, car elle doit s'aligner avec la durée de vie d'un véhicule. Dans ce contexte, la maintenance prévisionnelle vise à prédire de manière fiable la durée de vie utile restante (RUL) et l'évolution de l'état de santé (SOH) d'une batterie Lithium-Ion (Li-Ion) en utilisant les données d'utilisation passées et présentes, de manière à anticiper les opérations de maintenance. L'objectif de cette thèse est de tirer profit de l'information contenue dans les séries temporelles de courant, tension et température via des algorithmes d'apprentissage automatique. Plusieurs modèles prédictifs ont étés développés à partir de jeux de données publics, afin de prédire le RUL d'une batterie ou l'évolution de son SOH à plus ou moins long terme.

Mots clefs : Batteries lithium-ion, Véhicules Électriques, Maintenance Prévisionnelle, Apprentissage Automatique, Séries Temporelles, SOH, RUL

Résumé en anglais

The battery is a central component of electric vehicles, and is subject to numerous challenges in terms of performance, safety and cost. The life of batteries in particular is the subject of a great deal of attention, as it needs to be aligned with the life of a vehicle. In this context, predictive maintenance aims to reliably predict the remaining useful life (RUL) and the evolution of the state of health (SOH) of a Lithium-Ion (Li-Ion) battery using past and present operating data, so as to anticipate maintenance operations. The objective of this thesis is to take advantage of the information contained in the time series of current, voltage and temperature via machine learning algorithms. Several predictive models have been developed from public datasets, in order to predict the RUL of a battery or the evolution of its SOH in the more or less long term.

Keywords: Lithium-Ion batteries, Electric Vehicles, Predictive Maintenance, Machine Learning, Time Series, SOH, RUL